Investigation of Novel Sensing and Human-Robot Collaboration for Enhanced Quality Inspections

Uqba Othman

DEPARTMENT OF DESIGN, MANUFACTURING AND ENGINEERING MANAGEMENT

University of Strathclyde, Glasgow, UK

A thesis presented in partial fulfilment of the requirements for the degree of Doctor of Philosophy

February,2026

Declaration

This thesis is the outcome of the author's original research. It has been independently composed and has not been previously submitted for any degree-awarding examination.

Generative AI-based tools were used in a limited, transparent, and non-substantive manner during the preparation of this thesis. Specifically, **ChatGPT (OpenAI, various 2024–2025 versions)** was used to support **language refinement, clarity improvement, structural suggestions, and editorial feedback** during drafting and revision. The AI tool was used interactively as a writing aid and discussion partner, similar to editorial or proofreading assistance.

No AI tools were used to generate original scientific ideas, research questions, hypotheses, experimental designs, methodologies, data, results, analyses, interpretations, or conclusions. All technical content, scientific contributions, analytical decisions, and interpretations presented in this thesis are entirely the author's own. The author takes full responsibility for the accuracy, integrity, and originality of the work.

Signed: Uqba Othman

Date: 23/02/2026

Acknowledgement

I extend my deepest gratitude to my academic supervisors, Dr. Erfu Yang and Prof. Xichun Luo, for their invaluable guidance and unwavering support throughout my PhD journey. Their mentorship has been instrumental in shaping this research.

I sincerely thank Dr. Ophelie Torres (Unilever) as my industrial supervisor for her collaboration and insights, which greatly enriched my work. I also acknowledge Unilever and TrainFX Limited for their financial support and my university for providing the resources necessary for this research.

My heartfelt appreciation goes to my colleagues and friends, Andrew Loeliger, Charles Walker, Mohamed Adlan Ait Ameur, and Dino Bertolaccini, whose technical assistance and encouragement made this journey smoother.

On a personal level, I dedicate this work to my father, Shaikh Zeid, whose unwavering support and wisdom have shaped me, and to my late mother, Zubiada—may Allah grant her Jannah. Though absent, her love and dreams remain deeply rooted in my heart. This achievement is as much hers as it is mine.

I am also deeply grateful to Prof. David Butler and Dr. Dorothy Evans for their unlimited support and belief in my potential. Their invaluable guidance, encouragement, and insightful discussions have played a significant role in shaping my academic growth. Their unwavering support has not only refined my research skills but has also instilled in me a deep sense of resilience and curiosity. Through their support, I have gained the confidence to navigate challenges and push the

boundaries of knowledge. I will always cherish their wisdom, patience, and the lasting impact they have had on my academic journey and personal development.

To my brother, Mohammed Salim, your constant support has been my refuge, and I am forever thankful.

Finally, I draw strength from the resilience of Palestine, where perseverance is a way of life. As Ghassan Kanafani said, “The human being is a cause.” This PhD is not just an academic milestone but a testament to resilience, sacrifice, and the unwavering pursuit of knowledge.

I am profoundly grateful to everyone who has shaped this journey.

Abstract

The integration of collaborative robots (Cobots) and automated inspection stages in industrial manufacturing remains challenging due to the complexity of quality control processes, particularly in liquid spreading, painting, and coating applications. Existing quality control methods suffer from significant inconsistencies and operational inefficiencies, with manual inspection typically exhibiting error rates of 30–50 percent and throughput losses that can reduce effective productivity by up to 40 percent. Fully automated systems, while faster, often lack the adaptability and flexibility required to assess both surface defects and thickness variations in real time. This thesis investigates the development of Human-Robot Collaboration (HRC), sensing, and vision system to enhance real-time quality control inspection of liquid spreading or coating applications in manufacturing environments. Specifically, it presents a ResNet-101–based CNN vision system and a capacitive sensing approach, with a UR10e Cobot employed to assist in sensor deployment and spatial scanning, tested on a case study focused on liquid spreading and coating uniformity assessment.

The thesis presents several key contributions. It introduces a novel sensor fusion approach that integrates capacitive sensing for thickness consistency inspection, validated through a main case study performed in collaboration with Unilever and another case study performed to inspect coating mocking real industrial inspection which can be in automotive or aerospace industrial field. In this contribution, an adaptive regression model for thickness estimation is proposed, achieving a Mean Squared Error (MSE) of 0.00699 and an R-squared (R^2) value of 0.915. Both metrics demonstrate the robustness and predictive capability of the model in non-destructive thickness measurement beyond existing techniques.

Additionally, a customized ResNet-101 model is developed and optimized for liquid spreading defect classification using a dataset comprising 6,900 images. The model achieved a training accuracy of 97.99% and a validation accuracy of 100%. While such performance is unusually high for real-world image classification tasks, this outcome is attributed to the controlled nature of the dataset, the clear visual distinctions between the Full, Fault, and Empty classes, and the relatively limited size and variability of the validation set. These factors reduce dataset complexity and increase the likelihood of achieving near-perfect accuracy. Nonetheless, this also indicates that further testing on larger and more diverse datasets is required to fully validate the model's robustness and rule out the possibility of dataset bias or inadvertent information leakage. The sensing and vision systems are utilized to inspect the liquid spreading on a mimic substrate, where the capacitive sensor checks the thickness consistency and the vision system classifies the spreading based on surface images into three categories: full, empty, and fault. Furthermore, for the sensing component specifically, the approach was extended to test coating over a metal plate, mimicking coating processes in the automotive industry and other industrial coating applications. The results demonstrated that the approach could be adopted for coating classification, successfully categorizing coatings into four distinct classes: no coating, full coating, excessive coating, and defective coating.

To ensure seamless integration with industrial workflows, the system is deployed on a collaborative robot (UR10e), leveraging automated motion planning and real-time data synchronization for defect detection and thickness assessment. Furthermore, as the research is HRC-based, a human operator with significant responsibilities collaborates in the inspection process, paving the way for full in-

process quality control inspection cell adoption in industrial settings. The human operator is responsible for monitoring the inspection process and taking action based on obtained results.

Finally, these contributions are applied to the inspection of liquid spreading and coating processes in industrial settings, demonstrating HRC-based quality control inspection system that autonomously detects defects, assesses thickness variations, and provides real-time feedback to the operator for process optimization. The system can be easily adapted to various manufacturing applications, providing scalable, and flexible solutions for industries such as automotive, aerospace, and healthcare. These advancements collectively address the limitations of traditional quality control methods, paving the way for broader adoption of AI-driven, HRC-based inspection systems in modern manufacturing.

Contents

List of Figures

List of Tables

Publications from Thesis

Published

Journals

[1] U. Othman and E. Yang, "Human–robot collaborations in smart manufacturing environments: Review and outlook," *Sensors*, vol. 23, no. 12, p. 5663, Jun. 2023, doi: 10.3390/s23125663.

- This paper presents a detailed survey on human robot collaboration in manufatruring as summarised in Chapter 1 and 2. My contributions as the first author are as follows: I conducted all literature review activities and prepared the manuscript drafts.

Conferences

[2] U. Othman and E. Yang, "An overview of human–robot collaboration in smart manufacturing," in *2022 27th International Conference on Automation and Computing (ICAC)*, Bristol, United Kingdom, 2022, pp. 1–6, doi: 10.1109/ICAC55051.2022.9911168.

- This paper presents an overview of human robot collaboration systems in manufacturing, as discussed in Chapters 1 and 2. This paper is a reduced version of the journal publication [1] . My contributions as the first author are as follows: I conducted all literature review activities and prepared the manuscript drafts.

[3] U. Othman, M. A. Ait Ameur, E. Yang, and O. Torres, "CNN-based ResNet-101: A high-accuracy quality control inspection approach for industrial applications in liquid spreading on skin-mimic substrates," in *2025 International Conference on Software, Knowledge, Information Management & Applications (SKIMA)*, Paisley, United Kingdom, 2025, pp. 1–6, doi: 10.1109/SKIMA66621.2025.11155456..

- This paper presents the technical work conducted in Chapter 3. The paper covers the vision-robotic system designed for performing the defect detection while liquid is being spread on the mimic substrate. My contributions as the first author are as follows: I developed the presented system, performed all experiments and prepared the manuscript drafts.

Submitted

Journals

U. Othman, M. Ameur, E. Yang, C. Walker, and O. Torres, "Cobot-Assisted Capacitive Sensing for Real-Time, Micrometre-Scale Thickness Measurement of Liquid Films ," *submitted to Measurement Dec*. 2025.

- This paper presents the technical work conducted in Chapter 4. The paper covers the capacitive sensing and cobot-assisted system designed for performing the defect detection while liquid is being spread on the mimic substrate. My contributions as the first author are as follows: I developed the presented system, performed all experiments and prepared the manuscript drafts.

Chapter 1. Introduction

1.1 Research Background and Motivation

Industrial automation for quality control inspection is undergoing a transformative evolution, driven by advanced technologies such as Human-Robot Collaboration (HRC), machine vision powered by Convolutional Neural Networks (CNNs), and high-precision sensing systems [4]. These innovations are pivotal in shaping smart manufacturing systems by enhancing flexibility, precision, scalability, and adaptability. This research focuses on integrating cutting-edge technologies into a unified system designed to optimize production processes and address critical quality control challenges, such as defect detection and in-process inspection. Aligning with the principles of Industry 4.0, this study emphasizes the development of adaptive, efficient manufacturing workflows that leverage advanced automation.

The proposed system is designed to exploit the capabilities of Collaborative robots (cobots) in precision and task repeatability, CNN-powered vision systems for rapid surface inspection and defect identification, and capacitive sensing technology, which proved an outperformance in thickness measurements at the micron scale. Together, these technologies form a robust framework for achieving reliable and scalable quality control inspection in complex working environment. By combining automated vision, sensing, and robotic systems with human expertise, this research delivers a data-driven, flexible, and efficient solution tailored to the increasing demand for high-quality and customized products.

One persistent challenge in manufacturing lies in achieving uniformity and precision in production processes such as liquid spreading, coating, and painting [5,

6]. These processes are critical in industries such as automotive, aerospace, and healthcare, where surface coating quality directly affects both aesthetic and functional performance [7]. Current quality control methods often prioritize surface defect detection but fail to measure critical parameters such as coating thickness, leading to inefficiencies, material waste, and costly rework [8]. This research addresses these gaps by integrating capacitive sensing into quality control workflows, enabling comprehensive inspections that assess both surface uniformity and thickness [6].

Conventional quality control approaches face inherent limitations. Manual inspections, though prevalent, are error-prone and unsuitable for high-volume production due to scalability constraints [9]. Fully automated systems, while efficient, often lack the adaptability required for complex decision-making scenarios, necessitating human intervention. Existing sensing technologies, such as ultrasonic or laser sensors, are frequently hindered by environmental factors and material-specific constraints, compromising their reliability. Vision systems, while effective for surface defect detection, are insufficient for assessing thickness [10]. To address these shortcomings, this research proposes a novel framework that integrates the positional precision of the UR10e cobot (repeatability of ±0.05 mm), human operator expertise, the imaging capabilities of a ResNet-101 CNN trained on high-resolution images (1920×1080 px), and the quantitative film-thickness measurements provided by the capacitive sensor, which offers a sensitivity in the micrometre range and enables regression-based estimation with an average prediction error of 0.00699 mm^2 MSE.

This combination enables a comprehensive and adaptive quality control process

capable of resolving surface-defect features and thickness variations with millimetre-to-micrometre-level precision, tailored to the dynamic requirements of advanced manufacturing systems.

The motivation for this research is further reinforced by challenges identified during a collaborative project with Unilever, where non-uniform liquid spreading during tack tests was observed to compromise product quality. This highlighted the necessity for precise, real-time inspections of both surface coverage and thickness. By integrating HRC, 2D and 3D scanning technologies, and capacitive sensing, this research aims to set new benchmarks for in-process quality control. The proposed system is poised to significantly benefit industries such as automotive, aerospace, and healthcare by improving production efficiency, reducing material waste, and enhancing customer confidence through superior product quality.

1.2 Aims and Objectives

The rapid advancements in Human-Robot Collaboration (HRC), machine vision, and sensing technologies have introduced transformative potential in industrial quality control, particularly in addressing challenges such as liquid spreading, coating, and painting processes. Despite these advancements, conventional methods for quality control face critical limitations. Manual inspection processes are prone to human error and inefficiency, while fully automated systems often lack adaptability and fail to provide comprehensive assessments, such as simultaneous surface defect detection and thickness measurement. Moreover, existing sensing technologies, including ultrasonic and laser-based approaches, are frequently hindered by environmental factors and material-specific constraints.

To overcome these limitations, this research aims to develop high-precision, adaptive quality control system leveraging HRC, capacitive sensing, and machine vision technologies. The proposed system is designed to address the critical requirements of flexibility, scalability, real-time feedback, and reliability in smart manufacturing processes, with a particular focus on liquid spreading and coating applications in industries such as automotive, aerospace, and healthcare.

The overarching aim of this research is to develop a high precision, adaptive quality control system capable of reliably assessing both surface condition and micron scale thickness uniformity in liquid spreading and coating processes.

The objectives of this research are as follows:

- To review the state of the art in HRC, machine vision, and capacitive sensing to identify the limitations of existing in-process quality control methods.
- To develop and calibrate a capacitive sensing approach capable of providing reliable, non-destructive thickness estimation for liquid spreading and coating applications.
- To design and train a CNN based vision system that supports robust surface state classification for real time inspection.
- To integrate these sensing, vision, and robotic components into a structured human robot collaborative workflow suitable for in-process quality control in liquid spreading and coating applications.

1.3 Methodology Overview

This research methodology is designed to develop quality control approach that combines Human-Robot Collaboration (HRC), CNN-based vision, and capacitive

sensing technologies to enhance real-time inspection in industrial manufacturing. The approach aligns with the overall aim and objectives of this thesis by enabling scalable, flexible, and automated quality control inspection, addressing challenges in accuracy, adaptability, and efficiency of production processes. Traditional manual inspection methods are inconsistent and labour-intensive, while existing automated quality control solutions struggle with real-time adaptability and multi-sensor integration. To overcome these limitations, this methodology integrates a vision-based defect detection system, a capacitive sensing system for non-destructive thickness measurement, and HRC, vison and sensing system for an adaptive quality control inspection framework.

The CNN-based vision system automates defect detection in liquid spreading applications by classifying surface conditions into categories such as Full, Fault, or Empty. ResNet-101 was selected for its high accuracy and deep feature extraction capabilities, making it highly suitable for industrial image classification. The model was trained and validated using a dataset comprising 6,900 images collected under varying lighting conditions to ensure robustness. To further enhance the model's adaptability, data augmentation techniques such as rotation, scaling, and contrast adjustments were applied. The vision system operates in real-time, processing images from a high-resolution camera and generating classification results that contribute to the overall quality control assessment.

In parallel, a capacitive sensing system is deployed to perform non-destructive thickness measurement, addressing limitations in defect identification that vision-based systems alone cannot overcome. The CS1 capacitive sensor, calibrated for micron-level accuracy, is mounted on a UR10e collaborative robot, which

autonomously moves the sensor to predefined inspection points. By automating sensor positioning, the system ensures repeatable, precise, and adaptive quality control measurements.

Sensor data is integrated with the CNN-based vision system to provide a comprehensive defect assessment, leveraging a sensor fusion strategy that combines spatial and material property information. The fusion mechanism considers real-time sensor outputs and CNN classification probabilities, enhancing decision-making accuracy in industrial inspection scenarios.

To ensure reliability and flexibility, human oversight is incorporated into the system, allowing operators to monitor, verify, and handle exceptions when necessary. The inspection outputs from the vision and sensing systems are visualized on the laptop screen after arranged analysis is performed, enabling real-time analysis of detected defects and their underlying causes. The generated insights contribute to a structured quality control assessment form, which documents findings and provides recommendations for process optimization and defect mitigation. This approach ensures that the system is adaptable to production variability, reinforcing the reliability of industrial quality inspection.

Simulation and experimental validation played a critical role in assessing the integration of HRC, CNN-based vision, and capacitive sensing for real-time quality control inspection. RoboDK was utilized to simulate robotic motion accuracy, trajectory optimization, and collision avoidance, ensuring smooth and precise robotic movements before real-world deployment. Python was employed for real-time data synchronization between the UR10e robot, CS1 capacitive sensor, and camera, with communication established via Ethernet (TCP/IP) and USB protocols to maintain

seamless integration. The ResNet-101 CNN model performed defect classification, while camera and sensor calibration techniques were applied to optimize lighting conditions, correct distortions, and achieve high-precision thickness measurements. Experimental evaluation included a series of defect detection trials, thickness measurement accuracy tests, and repeatability assessments to confirm system reliability. A real-world case study, conducted in collaboration with Unilever, demonstrated the system's effectiveness in addressing liquid spreading consistency challenges. The findings highlighted the system's high detection accuracy, adaptability to variations in production conditions, and significant improvements in inspection efficiency compared to conventional methods. To achieve these aims, the research develops a unified inspection framework that integrates collaborative robots for precise and repeatable sensor and camera positioning, a CNN based vision system for surface classification, and capacitive sensing for micron scale thickness estimation. This methodological combination provides the basis for a high precision inspection workflow capable of supporting real time quality control in liquid spreading and coating applications.

1.4 Thesis Organization

Chapter 1 introduces the research problem, motivation, and significance of integrating Human-Robot Collaboration (HRC), CNN-based vision, and capacitive sensing for real-time quality control in industrial manufacturing. It outlines the research objectives, contributions, and structure of the thesis.

Chapter 2 provides a comprehensive literature review, beginning with an in-depth discussion of Human-Robot Interaction (HRI), including its definitions, classifications, and levels of interaction between humans and robots. It then explores

classifications of Human-Robot Collaboration (HRC), phases of system design, and strategies for achieving various collaboration levels in industrial settings. This is followed by an in-depth analysis of smart manufacturing technologies that facilitate the implementation of HRC within manufacturing systems. Finally, the chapter outlines key findings from the literature and highlights specific research gaps and challenges that this thesis aims to address.

Chapter 3 presents the CNN-based vision system for the detection of defect , detailing the selection of ResNet-101, dataset preparation, and model training. The chapter demonstrates the the vision system classification of surface conditions and integrates the robotic system to automate quality inspections of surface defect detection task.

Chapter 4 focuses on the capacitive sensing system for thickness measurement, describing sensor selection, calibration methods, and integration with the robotic platform. It demonstrates how capacitive sensing complements vision-based inspections by providing micron-level thickness assessment for more comprehensive defect detection.

Chapter 5 describes the full system integration and validation, covering both simulation and real-world testing. It details the use of RoboDK for motion simulation, Python for system integration, and real-world implementation in a Unilever case study. Experimental findings, including accuracy assessments and performance evaluations, are analysed to demonstrate the effectiveness of the system in industrial settings.

Chapter 6 concludes the thesis by summarising key findings, discussing the contributions and implications of this research, and outlining potential future

directions. It highlights areas of improvement, such as expanding compatibility with diverse liquid types and enhancing real-time adaptability, ensuring the system broader applicability in smart manufacturing environments.

Chapter 2. Research Methodology

2.1 Introduction

This chapter presents the methodological framework that guided the development, integration, and evaluation of the human–robot collaborative inspection system combining machine vision, capacitive sensing, and robotic automation. The research adopts a mixed-methods experimental approach, integrating quantitative analysis of sensor and vision performance with qualitative evaluation of human supervisory roles and system workflow behaviour. The methodology is structured to support the overarching research aim of developing an in-process quality control system capable of assessing liquid spreading uniformity with high precision, reliability, and operational robustness.

The chapter outlines the research philosophy, system-level methodological design, the rationale for method selection, experimental strategies applied across the two case studies, and the triangulation of quantitative and qualitative findings. This structure ensures that the methodology connects directly to the research objectives while providing a coherent foundation for the technical developments presented in subsequent chapters.

2.2 Research Philosophy and Methodological Positioning

The research follows a mixed-methods experimental methodology, combining quantitative empirical testing with qualitative assessment of human–robot interaction components. Quantitative methods were essential for evaluating the predictive accuracy of the CNN-based vision system, analysing the voltage–thickness relationships captured by the capacitive sensor, and assessing the repeatability of robot positioning. These experiments provided numerical evidence supporting the

system's capability to detect defects and estimate liquid thickness across a predefined range.

Complementing this, qualitative elements were incorporated to evaluate the human role within the inspection loop, including supervisory decision-making, interpretation of borderline cases, and the operational fit of the workflow within a real manufacturing scenario. This dual methodological orientation reflects the nature of smart manufacturing systems, where automation and human oversight must coexist to ensure reliability and adaptability.

2.3 Overall Research Approach

The research approach is grounded in system development and iterative experimental validation. The methodology involves four interconnected stages:

1. System Design and Integration

   Development of an inspection system combining capacitive sensing, robotic positioning, and CNN-based surface classification, with human operators responsible for calibration supervision and final decision-making.

2. Experimental Evaluation of Subsystems

   Quantitative testing of the machine vision model, capacitive sensor performance, and robot-assisted positional repeatability.

3. Cross-Modality System Validation

   Assessment of how the sensing and vision components complement each other in detecting defects and thickness deviations.

4. Real-World Case Study Implementation

   Validation of the system within an industrial context in collaboration with

Unilever, followed by a second case study evaluating coating inspection using the integrated robotic–capacitive sensing methodology.

This staged methodology ensures that subsystem performance is rigorously evaluated before integration, enabling clear attribution of strengths and limitations.

2.4 Method Selection and Justification

The methods adopted in this research were selected based on suitability for in-process inspection of liquid spreading and coating uniformity. The rationale for each methodological component is summarised below.

2.4.1 Machine Vision for Defect Classification

A deep Convolutional Neural Network, specifically ResNet-101, was selected due to its strong performance in image classification tasks and its robustness in handling variable lighting and texture conditions. The model was pre-trained on ImageNet and fine-tuned on a custom dataset representing three surface states: Full, Fault, and Empty. This supervised learning approach enables reliable detection of surface anomalies, complementing the quantitative information obtained from the capacitive sensor.

2.4.2 Capacitive Sensing for Liquid Thickness Estimation

Capacitive sensing was chosen for its ability to detect micrometre-scale variations in the thickness of dielectric materials. The Micro-Epsilon CS1 sensor, operating across a 0–1 mm range, demonstrated stable behaviour and a near-linear voltage response within the narrower thickness window of 15–90 μm. A linear regression model was adopted due to the consistent monotonic voltage–thickness

relationship observed experimentally, enabling predictive estimation of liquid spread thickness.

2.4.3 Robotic Automation

A UR10e collaborative robot was used to ensure repeatable sensor positioning at nine predefined inspection waypoints. The robot's ±0.05 mm repeatability supports consistent measurement conditions across repeated trials. Python-based control scripts ensured synchronised execution of robot motions, sensor sampling, and image capture, providing a deterministic experimental workflow.

2.4.4 Human-Robot Collaboration

Human involvement was incorporated where interpretive judgment or calibration confirmation was required. The methodology emphasises supervised autonomy, where the robot and sensing system handle repetitive and deterministic tasks, while the operator addresses ambiguous or out-of-range cases. This division of labour informs the qualitative dimension of the methodology.

2.5 Experimental Methodology

2.5.1 Data Collection Strategy

Experimental data were collected through structured procedures involving both pre-spreading and post-spreading inspection phases. Nine waypoints were defined on the substrate to ensure spatial coverage. For each waypoint, the robot positioned the sensor and camera for simultaneous voltage sampling and image capture. This coordinated acquisition supports cross-modality validation between the vision and sensing systems.

The dataset for the machine vision model included images classified into Full, Fault, and Empty spreading outcomes. A 70/20/10 split was used for training, validation, and testing, ensuring that the model was evaluated using unseen samples.

2.5.2 Case Study Methodology

Two case studies were conducted:

1. Unilever Liquid Spreading Case Study

   The system was tested on a skin-mimic substrate with defined thickness levels of 15, 30, 60, and 90 μm. This real-world scenario enabled assessment of the system's performance in an industrial quality control environment.

2. Coating Inspection Case Study

   To generalise the methodology beyond liquid spreading, the integrated robotic–capacitive sensing system was evaluated for coating inspection tasks relevant to automotive and aerospace applications. This case study demonstrated that the sensing and robotic components can be adapted to different industrial requirements.

Both case studies followed controlled experimental protocols with repeated trials to evaluate reliability.

2.5.3 Cross-Modality Validation

Validation involved comparing sensor-based thickness estimates with CNN-based classifications. Samples flagged by either method were subjected to human review, enabling identification of mismatches and deeper examination of system behaviour. This cross-validation process strengthens the methodological integrity of the system.

2.6 Qualitative Methodology

The qualitative component focuses on the role of the human operator within the inspection loop. Observations were collected during experimental execution regarding:

- Frequency and nature of operator intervention
- Interpretation of borderline cases
- Calibration confirmation behaviour
- Interaction with system feedback and error messages

These observations informed the evaluation of the Human-Robot Collaboration model, providing insights into practical system deployment and operational constraints.

2.7 Reliability, Validity and Limitations

The methodology incorporates strategies to ensure reliability and validity, including:

- Repeated trials across all thickness levels
- Use of robot-assisted positioning to minimise human-induced measurement variation
- Consistent environmental conditions during experiments
- Calibration checks at the beginning of each session
- Cross-modality confirmation between sensor and vision outputs

Limitations acknowledged in the methodology include environmental sensitivity of capacitive sensing, the robot's ±0.05 mm repeatability, and dependence on human judgment for ambiguous cases. These constraints are addressed in later chapters through analysis and discussion.

2.8 Ethical and Safety Considerations

The methodology adheres to safety standards for collaborative robotics. The UR10e was operated within its certified safety zones, and human involvement in calibration and review stages was conducted with appropriate handling protocols. No personal or sensitive data were collected.

2.9 Summary

This chapter has presented the research methodology underpinning the development and evaluation of the proposed multimodal inspection system. By combining quantitative experimentation with qualitative assessment within a mixed-methods framework, the methodology provides a coherent foundation for the technical implementations and results described in subsequent chapters.

Chapter 3. Literature Review on Human-Robot Collaboration for Smart Manufacturing

3.1 Introduction

This chapter provides a comprehensive review of existing research on human-robot collaboration (HRC) in the context of smart manufacturing. It systematically defines and categorizes human-robot interactions based on work tasks, direct contact, and both simultaneous and sequential processes. Furthermore, it classifies human-robot collaboration according to collaboration levels, work roles, safety control mechanisms, and communication interfaces.

In addition, this chapter examines advanced technologies such as collaborative robots (cobots), vision and sensing systems, and artificial intelligence (AI) tools to assess their impact on enhancing productivity within manufacturing industries. The benefits and limitations of these technologies in industrial applications are critically analyzed to identify current bottlenecks in real-world implementations.

A key focus of this research is the quality control inspection stage, a critical process for ensuring business competitiveness and enhancing customer satisfaction. Consequently, this study aims to improve quality control inspection in industrial settings. The research scope has been determined through a critical analysis aligned with the project's aims and objectives, leading to the identification of knowledge gaps in this domain.

3.2 Human-Robot Interaction Classification

Industrial robots have become a fundamental element in the competitive pursuit of enhanced production efficiency among manufacturing companies [11]. The International Federation of Robotics (IFR) projected a 13% growth rate for the robot production industry worldwide in 2019 [12]. Recently, the IFR has reported significant growth in the industrial robotics sector in recent years. According to the IFR's World Robotics 2024 report, the global average robot density reached a record 162 units per 10,000 employees in 2023, more than doubling from 74 units seven years prior. Furthermore, many corporations are increasingly prioritizing the integration of advanced capabilities into the robotic systems they develop. These enhancements often encompass improved user-friendliness, greater flexibility, and enhanced safety mechanisms. Consequently, there is a growing demand for robots that can collaborate with humans while ensuring safety and adapting to a diverse range of tasks and dynamic industrial environments [13]. As collaborative robots (cobots) continue to gain traction, businesses of all sizes are finding it increasingly viable to incorporate robotic systems into their production processes. The accessibility and adaptability of cobots enable industries to enhance efficiency, streamline workflows, and optimize manufacturing operations, thereby fostering greater automation across various sectors. This, in turn, can lead to improved efficiency and flexibility within industrial environments. The integration of human-robot interaction phases plays a crucial role in this process, as it allows for more seamless collaboration between the robot and the human operator. For instance, cobots can be programmed to perform highly accurate, repetitive or physically demanding tasks, freeing up human operators to focus on more complex and creative

aspects of the production process. Ultimately, the successful integration of cobots can result in a safer, more productive, and more adaptable industrial ecosystem [14]. The nature of human-robot interaction is heavily influenced by various factors, including the specific task that needs to be performed, the shared workspace, the degree of direct contact between the human and the robot, as well as the sequencing and timing of the different processes involved. Consequently, interactions between humans and robots can be broadly categorized into four primary types [15, 16]:

3.2.1 Coexistence interaction

refers to a scenario where a human operator and a robot are working on different tasks in different workspaces without the need for physical barriers[17, 18]. For example, robots may be responsible for heavy lifting and assembly while human operators oversee quality control and oversight. The limited connection between the human and the robot in this type of interaction allows for greater flexibility and efficiency in the production process [17]. In [19], the coexistence interaction is demonstrated in real world case study where the robots conduct surface quality measurements on metallic parts while operators simultaneously perform manual inspections in the same workspace without direct collaboration

3.2.2 Synchronization Interaction

this type of interaction between the human and the robot involves a scenario where a human operator and a robot share the same workspace but work at different times in sequential manner. Both the human and the robot are responsible for performing specific tasks, and they communicate with each other by providing

instructions and feedback. This type of interaction requires a high degree of coordination and synchronization between the human and the robot. In this scenario, the human operator and the robot are looking at the same target and working in sequential order to achieve the desired outcome. So, the human operator might be assigned for loading a machine with raw materials, while the robot is performing the actual manufacturing process. The human operator and the robot would need to work together in sync to ensure that the machine is loaded correctly and that the manufacturing process is carried out without interruption [15].

3.2.3 Cooperation Interaction

cooperation relation refers to where a human operator and a robot work at the same time towards a shared objective but have separate interests[20]. They both have access to the same technological resources to obtain information about the work task, but there is no direct connection between them[21]. Even though their workspaces may overlap, the human operator and the robot do not interfere with each other's work. The focus is on achieving a common goal while pursuing individual interests. For instance, in a warehouse, a human operator might be responsible for managing inventory and order fulfilment, while a robot is responsible for material handling and transportation. Both the human operator and the robot can access the same information about inventory and order status but work independently to achieve their respective objectives[22]. This type of interaction promotes efficient resource allocation and coordination between the human and the robot.

3.2.4 Collaboration Interaction

Collaboration interaction involves a scenario where a human operator and a robot work in synergy towards a common goal in the same workspace at the same time. This type of interaction is more advanced than cooperation interaction and requires a high level of coordination and communication between the human operator and the robot [23]. In collaborative interactions, the human operator and the robot work closely together, forming an united system. Direct contact between these system agents is facilitated and regulated through advanced sensing technologies, ensuring safe and efficient interaction within the shared workspace. Since the actions of one agent directly impact the other, human-robot collaboration requires a seamless integration of roles. For instance, in the assembly of a complex component, the human operator may handle intricate aspects of the task, such as placing and aligning components and making critical decisions [24], while the robot is responsible for tasks requiring strength and precision, such as heavy lifting and accurate positioning. This division of labor leverages the complementary strengths of both agents, enhancing efficiency and overall production quality. The effectiveness of collaborative interactions is contingent upon the seamless and efficient cooperation between the human operator and the robotic system. The interaction between these agents can be established through both physical and contactless moods, each necessitating specific information to facilitate optimal functionality within the collaborative framework. In physical interactions, the measurement of forces and torques enables the robotic system to infer human intent and dynamically adjust its actions accordingly. This real-time sensory feedback mechanism enhances the robot's capacity for adaptive and intuitive responses, thereby improving the

efficiency, safety, and overall efficacy of human-robot collaboration in complex industrial tasks. [25]. At the same time, a contactless connection between the human and the robot is implemented through appropriate communication techniques to ease the working relationship between the human and the robot. Direct (speech, gestures, force) and indirect (intention recognition, eye blinking) communications between the human and the robot, can be detected and analyzed using advanced sensing technologies such as machine vision and haptic feedback, so the robot will be able to understand the human's intentions and respond regarding the task needs [26].

Table 3.1 summarizes human-robot interaction features considering the shared contents of work tasks, direct contact, and simultaneous and sequential processes [27].

Table 3.1 Classification of Interaction Types Based on Shared Content, Work Tasks, and Process Characteristics.

	Interaction			
Shared Content	**Coexistence**	**Synchronization**	**Cooperation**	**Collaboration**
Work Task		×		×
Direct Contact		×		×
Simultaneous process	×		×	×
Workspace		×	×	×
Sequential process		×	×	

In the first part of this chapter, the classification of human-robot interaction (HRI) in industrial settings is explored considering definition and classification. The increase of utilizing and integrating collaborative robots (cobots) is enhancing productivity, flexibility, and safety. Four primary interaction types are identified: coexistence, where humans and robots operate separately; synchronization, involving

sequential task execution in a shared workspace; cooperation, where both work towards a common goal with minimal direct interaction; and collaboration, the most integrated form, requiring real-time coordination and direct interaction.

The discussion highlights the role of advanced sensing and communication technologies, such as machine vision, haptic feedback, and intent recognition, in enabling adaptive and safe collaboration. Table 1 systematically summarizes these interaction types based on workspace sharing, task execution, physical contact, and process synchronization

3.3 Definition and Classification of Human-Robot Collaboration (HRC)

Human -Robot Collaboration (HRC) systems are designed to harness the complementary strengths of human operators and robotic systems to achieve a shared operational objective[28, 29]. Human operators will be able to contribute their cognitive abilities—such as experience-driven decision-making, adaptive problem-solving, and contextual judgment—while robots enhance productivity through their computational efficiency, precision, and repeatability[30]. However, in the design phase, it is critical to ensure the seamless and safe interaction between humans and robots within shared workspaces[31]. Collaborative robots (cobots) incorporate advanced safety features, including force-limiting actuators, real-time motion tracking, and predictive control algorithms, facilitating direct human-robot interaction[32]. In contrast, traditional industrial robots typically require physical separation due to their high-speed and high-force operations. Therefore, the implementation of safety measures must be context-dependent, balancing task efficiency with risk mitigation strategies, including the use of adaptive safety zones, dynamic speed adjustments, and predictive hazard detection systems[33]. In the

meanwhile, designing an effective integration of HRC system requires a multidisciplinary approach, encompassing robotics, human factors engineering, machine vision, sensing technologies, and occupational safety. Therefore, the demand on adapting cutting edge models and algorithms is rising specially in advanced manufacturing environments leading intelligent collaboration[34].

The collaboration relation is a significant success sign in industrial automation, redefining human-robot synergy by facilitating direct interaction, seamless communication, and dynamic task coordination. Unlike conventional automation where robotic systems are mostly isolated, collaborative workspaces leverage the complementary strengths of human cognition and robotic precision. This integration enhances operational efficiency, adaptability, and real-time decision-making. However, the effectiveness of such systems hinges on addressing key challenges, including trust in automation, cognitive load on operators, and ensuring safety without compromising productivity. The increasing emphasis on collaborative environments underscores both the transformative potential and the complexities of HRC implementation, necessitating further research into optimization strategies, regulatory frameworks, and long-term workforce implications.

In major industrial sectors such as automotive and aerospace, companies are increasingly investing in flexible and intuitive solutions to enhance production efficiency and sustainability. Flexible solutions can boost productivity and enhance workplace safety, as robots support human operators in high-risk or physically demanding activities [35]. The integration of HRC systems thus fosters a more adaptive and efficient collaboration between humans and robots. [36].

HRC systems operate intelligently to achieve production objectives feasibly. The incorporation of advanced technologies such as AI, augmented reality, and machine vision-based convolutional neural networks (CNNs) in smart manufacturing environments enables human operators to work more competently [37]. The adoption of these technologies within HRC systems fosters efficient and flexible workspaces, empowering human operators to make crucial decisions that impact the entire production line. For instance, collaborative robots, equipped with intuitive interfaces and sensory systems, assist human operators with repetitive and hazardous tasks, thereby reducing the risk of workplace injuries. This synergy leverages the strengths of both humans and robots to improve productivity and efficiency in the manufacturing industry [38]. Notably, studies have quantified these improvements, reporting up to a 30% increase in productivity with the implementation of HRC systems , significant enhancements in manufacturing flexibility and efficiency , and increased efficiency in U-shaped production lines through cobot integration[39]

As mentioned, in the age of the Fourth Industrial Revolution “Industry 4.0” significant changes to conventional programming approaches have been delivered. So, workers with less technical expertise can effectively operate and communicate with robots. Utilizing simple gestures, voice commands, and eye blinking, the interaction with robots during tasks without the need for traditional tools is achieved. This shift towards more intuitive and natural means of communication has transformed the nature of work from reactive to proactive, driving progress and innovation in various industries [40].

Therefore, designing Human-robot collaboration HRC system is crucial. The design phase is determined by the agent's effort dynamics, the nature of work concerns, human operator satisfaction, and the ease of critical information transferring between operators and cobots [41]. Accordingly, the HRC system can be classified into four main aspects that are outlined in Figure 3.1.

Figure 3.1 Structural components of HRC system.

3.3.1 Collaboration Levels

The HRC system is initiated on the principle of teamwork and cooperation between humans and robots. To facilitate effective collaboration in shared environments, researchers have been working to establish standardized approaches. In [41, 42], the levels of collaboration in the HRC system have been categorized as follows:

- **Independent Collaboration:** in the context of HRC, the "Independent" level refers to scenarios where humans and robots perform separate tasks without direct interaction. The robot autonomously executes its designated functions, while the human operator focuses on distinct responsibilities. Despite the lack of direct cooperation, the integration of robots in such settings can enhance overall productivity and efficiency. This approach is particularly suitable for workflows that do not require close coordination between human and robotic agents [43].
- **Sequential Collaboration:** This level of collaboration involves alternating task execution between robots and human operators, requiring precise coordination to optimize workflow efficiency. This approach is widely used in manufacturing, where robots handle precision tasks such as welding, followed by human inspection for quality control. The primary benefits include enhanced productivity, reduced errors, and improved worker safety by delegating hazardous or repetitive tasks to robots [13]. In industries like automotive manufacturing, sequential HRC balances automation with human adaptability, ensuring high-quality production while leveraging the strengths of both entities [44]
- **Simultaneous Collaboration:** in simultaneous level, both HRC system entities engage in distinct processes on a shared task without direct interaction. For example, in manufacturing, a robot might perform welding while a human operator conducts quality inspections concurrently. This approach enhances productivity and efficiency by reducing task completion time and minimizing errors. It is optimal for tasks that do not require close

coordination or communication between humans and robots. By enabling both parties to work on the same task simultaneously, it increases productivity and efficiency, thereby reducing the overall time required to complete the task.

- **Supportive Collaboration:** Both human operators and robots engage concurrently on a shared task, necessitating precise synchronization and communication. This collaboration leverages the human's adaptability and the robot's precision to enhance task performance. For example, in manufacturing, a human operator might perform intricate tasks such as welding or painting, while a robot stabilizes the workpiece, adjusting its position to align with the operator's movements, thereby ensuring high precision. This collaborative approach is particularly effective for tasks requiring meticulous coordination, as it combines human dexterity with robotic accuracy, leading to increased efficiency and productivity.

3.3.2 Work Roles

In industrial world, human operators and robots are assigned different roles depending on the task at hand [45]. Completing a task in the HRC system requires the human operator and the robot to finish their individual and shared responsibilities. Even if they work independently, their tasks are interdependent, and both are crucial to the overall task's success. The pace of the task can be set individually or mutually agreed upon by both parties. Figure 3.2 illustrates a representative HRC workflow in concrete assembly, where the human positions reinforcement and formwork, while the robot performs concrete pouring and vibration. A feedback loop enables human intervention when tolerance deviations are detected, ensuring process continuity.

This example highlights the structured coordination and interactivity fundamental to industrial HRC systems.

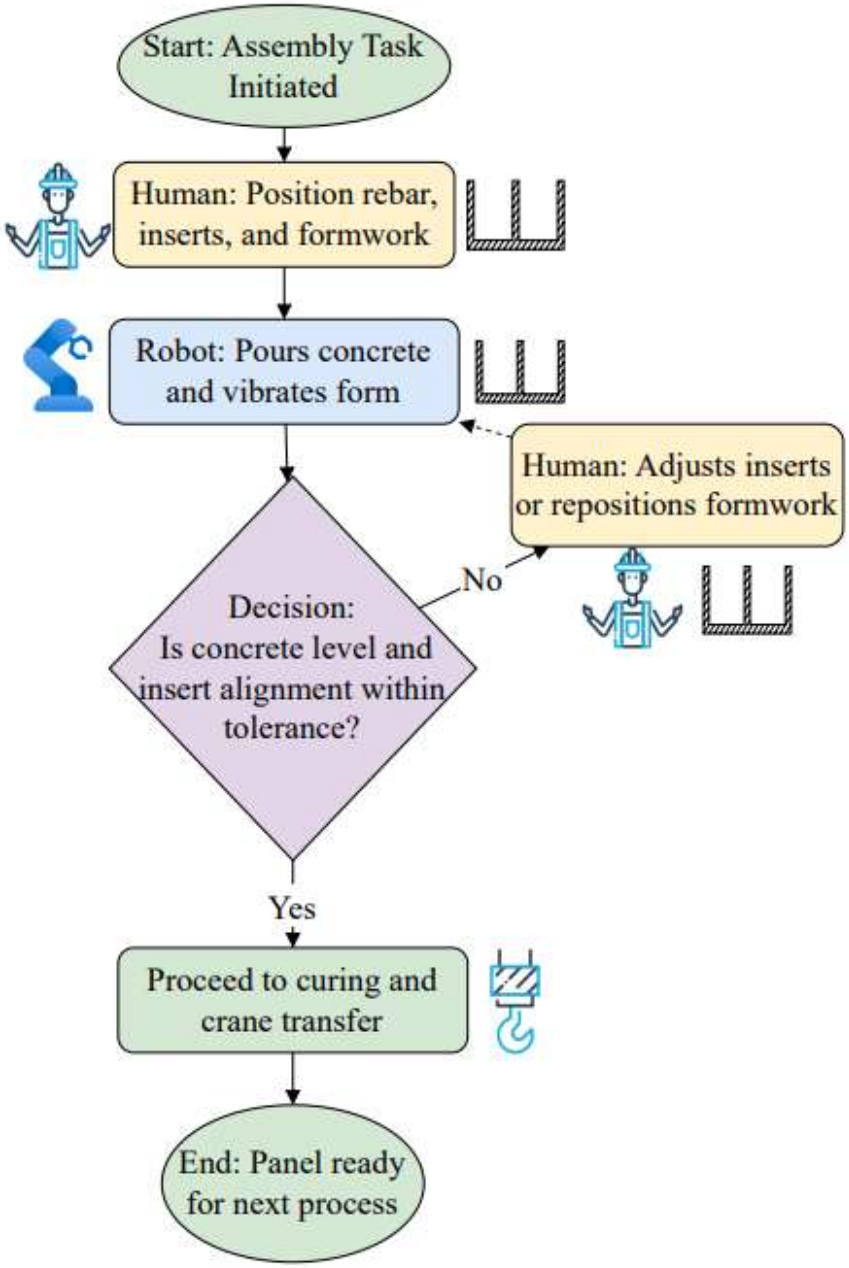

Figure 3.2 HRC workflow in concrete assembly illustrating task allocation, decision-making, and a feedback loop for human intervention based on alignment tolerance.

There are two types of relationships between the human operator and the robot: master-slave or peer-based. In a master-slave relationship, the master sets the pace, and the slave follows. In a peer-based relationship, both have equal decision-making power and can collaborate to set the pace. When designing and implementing HRC systems, these relationships are essential to consider as they can impact the system's effectiveness[46]. According to the classification in [41], The HRC system has three distinct types of roles that can be assigned to either human operators or robots for examination.

- **Supervision:** Collaboration between a human operator and a robot at the supervision level is characterized by a master-slave relationship, in which the human operator takes on the role of the master. The human operator is responsible for supervising and directing the actions of the robot, which functions as the slave. This level of collaboration is best suited for tasks that demand a high degree of precision and accuracy, where the human operator must closely monitor the robot's actions. For example, in a manufacturing process, the human operator may use a joystick or other controls to direct the robot's movements as it performs tasks like welding or cutting. The robot acts as an extension of the operator's body, responding to their commands and movements. By enabling the human operator to perform tasks with greater precision and accuracy than they could alone, the supervision level of collaboration can boost efficiency and productivity. However, it can also increase the risk of errors or injuries if the human operator lacks adequate training or experience.

- **Peer:** When humans and robots collaborate at the peer level, they have an equal say in decision-making. This type of collaboration is ideal for tasks that require flexibility and adaptability since both parties must work together to maintain the work rate. For instance, in a warehouse, a human operator may work alongside a robot to transfer items to different locations. The robot may detect obstacles or environmental changes, and the human operator may need to cooperate with the robot to adjust their movements or alter their route. This type of collaboration boosts efficiency and productivity by enabling humans and robots to complete tasks more swiftly and effectively than they could alone.
- **Subordinate:** At the subordinate level of collaboration, the interaction between the human operator and the robot is defined as a hierarchical relationship, where the robot acts as the lead. The robot is responsible for guiding and overseeing the actions of the human operator, who acts as the follower. This level of collaboration is appropriate for tasks that require a high level of automation and independence, where the robot has more advanced knowledge or skills than the human operator. For instance, in a medical environment, a robot could be utilized to complete a surgical procedure while a human operator assists with minor duties like adjusting instruments or supplying materials. The robot would be accountable for directing the overall operation and ensuring that it is conducted safely and efficiently. The subordinate level of collaboration can enhance productivity and minimize the risk of human error by allowing the robot to complete tasks

that are challenging or impossible for humans to perform. However, it also raises ethical and safety concerns.

3.3.3 Safety Control Modes

Ensuring the safety of human operators is crucial for the successful implementation of HRC systems. In [47, 48], human errors, environmental conditions, and engineering faults have been identified as potential sources of failure in the human-robot working area. To ensure the safety of human operators and robots during work processes, the International Organization for Standardization (ISO) has established safety standards. ISO 10218-1 and ISO 10218-2 are two of these standards, which provide guidelines for the safe installation and operation of robotic systems. These guidelines aim to prevent injury to human operators[49]. Another standard, ISO 15066, was released in 2016, and it provides enhanced safety control modes for the integration of human-robot collaboration (HRC) systems, focusing on factors such as force and speed [50]. To ensure a safe work environment for both human operators and robots, it is highly recommended to implement mandatory safety modes in the HRC system installation. This involves incorporating safety measures such as emergency stop buttons, protective barriers, and monitoring systems that can instantly detect and respond to any potential hazards. By following these safety standards, the risks associated with HRC systems can be greatly reduced, making it possible for human operators and robots to work collaboratively and safely in industrial settings. The safety tools classification is summarized as follows:

- **Safety-monitored stop:** A safety-monitored stop is an essential safety feature in HRC systems that prioritize the safety of human operators working alongside robots. When activated, the robot will come to a halt immediately

when a human operator enters a defined safety area. This area can be designated by safety sensors or other monitoring devices installed in the work environment. The safety-monitored stop mode is necessary to prevent accidents and injuries that may occur when human operators are near robots during work processes. By stopping the robot's movements when a human operator is detected within the specified safety area, the risk of collision or other forms of contact between the two can be minimized. This safety mode is often used in conjunction with other safety measures such as protective barriers, emergency stop buttons, and safety monitoring systems to ensure the safe and efficient operation of HRC systems, allowing for productive collaboration between human operators and robots.

- **Hand guiding**: In HRC systems, hand guiding is a mode of operation that empowers human operators to manually manoeuvre the robot without external force. This mode is especially beneficial in situations where the robot requires guidance to execute a specific task or operate within limited space with precision. In the hand-guiding mode, the robot's movement is controlled directly by the operator using a joystick or pendant device, enabling the operator to make precise adjustments as necessary. Hand guiding is a versatile mode that enables closer collaboration between humans and robots, making it possible to perform tasks that were previously challenging or impossible to automate using traditional programming methods. By enhancing the flexibility and adaptability of HRC systems, hand-guiding mode makes it possible to use them in an extensive range of industrial applications.

Nonetheless, it is important to exercise caution while using this mode to ensure safety.

- **Speed and separation monitoring:** The safety mode of operation in HRC systems called speed and separation monitoring is crucial in preventing collisions or accidents between robots and human operators. It achieves this by limiting the robot's force and speed within designated safety zones to safe levels. Sensors equipped on the robot monitor the distance between it and the human operator, as well as the speed and force of its movements. If the robot gets too close to the human operator, the sensors trigger a safety stop to prevent a collision. Speed and separation monitoring help to prevent accidents and injuries by limiting the robot's force and speed near the human operator, ensuring a safe working environment for both humans and robots. It is particularly vital in industrial applications, such as assembly lin es or collaborative manufacturing processes, where robots and human operators work closely together. Proper safety measures must be put in place to prevent accidents and ensure a safe operating environment.
- **Power and force limiting**: HRC systems have a safety mode called power and force limiting that restricts the amount of force and torque exerted by the robot. This mode is programmed to keep the robot within a specific range of force and torque to prevent injury to operators. It's particularly handy when the robot must handle delicate materials or meet humans. By limiting force and torque, this safety mode prevents accidents and material damage. The robot's maximum power and force in different directions are limited to avoid exceeding these limits, triggering a safety stop to prevent injury or damage.

Ultimately, power and force limiting is vital safety feature for HRC systems as it ensures the robot can work safely alongside human operators without causing harm or damage.

3.3.4 Communication Interfaces

In the field of human-robot collaboration (HRC), the communication and programming techniques used for controlling and operating robots have evolved to become more intuitive and user-friendly. Unlike traditional programming and interfaces which are based on conventional coding methods, the HRC system leverages more intuitive approaches to facilitate communication between humans and robots [51]. To achieve greater efficiency and flexibility in HRC, it is essential to enhance the level of communication between humans and robots. This allows the robot to adapt to all possible human movements and interactions during work, which is crucial for achieving seamless collaboration between humans and robots.

The latest communication techniques which include body gestures, facial and eye tracking, voice commands, and haptic interfaces [41, 52] aim to enable more natural and intuitive interaction between humans and robots. For example, body gestures, such as pointing or waving can trigger specific actions from the. With facial and eye tracking human facial expressions and eye movements are detected and interpreted, providing the robot with contextual cues for responding appropriately. Voice can issue commands to the robot, while haptic interfaces can be used to provide tactile feedback, such as vibrations or pressure, to the human operator.

Human-robot collaboration (HRC) is an essential area of focus in the smart manufacturing industry. The automotive and food sectors are among the industries with the most significant need for HRC systems. Traditionally, robots have been

utilized in manufacturing to perform repetitive and simple tasks. However, with the advancements in technology, researchers are now exploring ways to integrate human expertise, decision-making, and critical thinking with the strength, repeatability, and accuracy of robots to perform complex tasks [53].

With the increasing adoption of automation technologies in manufacturing, robots are expected to work alongside humans to achieve higher levels of productivity, quality, and flexibility [54]. HRC has emerged as a promising approach to achieving these goals. By working collaboratively, humans and robots can combine their unique strengths and abilities to optimize manufacturing operations. So, the utilization of HRC in manufacturing is changing the traditional approach of utilizing robots, and researchers are increasingly focusing on exploring new ways to exploit human-robot collaboration to enhance manufacturing efficiency and quality [55].

Recent studies have highlighted the benefits of human-robot collaboration in smart manufacturing. One of the key benefits is the improved productivity [56]. By leveraging the strengths of robots, humans and key technologies, manufacturers can achieve higher production rates and faster cycle times. [57]. Recently, the demand for customized products increased and eventually customized manufacturing also increased to meet this demand. Therefore, manufacturers are increasingly transforming their work environments to enhance intelligence, efficiency, and reliability, integrating advanced technologies to optimize operational performance and adaptability. This has resulted in the creation of human-robot collaboration systems in smart manufacturing, where robots and humans operate together harmoniously to achieve better productivity and faster cycle times while preserving

a secure and efficient workplace. By utilizing their respective features, robots can take on tasks that are monotonous or hazardous, while humans can handle more intricate and innovative tasks. These systems' abilities have been further enhanced by machine learning and artificial intelligence, allowing robots to learn from humans and adjust to shifting circumstances. The inclusion of human-robot collaboration systems has revolutionized the industry, giving manufacturers a way to boost competitivity [40].

3.3.5 Summary

This section examined the definition and classification of Human-Robot Collaboration (HRC), emphasizing its role in integrating human cognitive abilities with robotic precision to enhance industrial efficiency. Four levels of collaboration—independent, sequential, simultaneous, and supportive—were analyzed, along with role classifications, including supervision, peer-based, and subordinate interactions.

Key safety control measures, such as safety-monitored stops, hand guiding, speed and separation monitoring, and power and force limiting, were discussed in alignment with international safety standards (ISO 10218-1, ISO 10218-2, ISO 15066). Advances in communication interfaces, including gesture recognition, voice commands, and haptic feedback, were also reviewed as facilitators of intuitive human-robot interaction.

Finally, the section highlighted the impact of HRC in smart manufacturing, particularly in automotive and aerospace industries. The integration of AI, machine vision, and augmented reality has enhanced flexibility and efficiency, positioning HRC as a key driver of innovation within Industry 4.0.

3.4 Smart Manufacturing

During the Third Industrial Revolution, advancements in automation and digital technology redefined manufacturing by significantly increasing production efficiency [58]. The integration of sensors and actuators facilitated real-time process monitoring and control, optimizing production workflows and enhancing operational reliability [59]. These innovations also improved predictive maintenance strategies, minimizing downtime, reducing material waste, and lowering operational expenditures. However, despite these technological strides, Industry 3.0 exhibited inherent limitations, including high implementation costs, rigid production architectures, cybersecurity vulnerabilities, workforce skill gaps, and inefficiencies in real-time data processing [60]. These constraints underscored the necessity for more adaptive, scalable, and interconnected manufacturing paradigms, catalyzing the shift toward Industry 4.0 [61].

With the prevalence of digital transformation, industries are increasingly adopting intelligent, technology-driven frameworks to enhance operational agility. Smart manufacturing exemplifies this evolution, leveraging advanced technologies such as artificial intelligence (AI), machine learning, and robotics to refine precision and accuracy in executing complex manufacturing tasks. This paradigm shift fosters predictive analytics, real-time optimization, and autonomous decision-making, thereby strengthening quality control, reinforcing safety protocols, and augmenting production flexibility. Unlike Industry 3.0, which emphasized mechanized automation with human oversight for process regulation, Industry 4.0 integrates cyber-physical systems (CPS), the Internet of Things (IoT), and AI-driven analytics to enable self-regulating, data-driven manufacturing ecosystems.

By leveraging these advancements, enterprises can achieve measurable improvements such as 10–30% increases in production throughput, 20–40% reductions in defect rates, and 15–25% decreases in material or energy waste, translating into lower operational costs and more efficient resource utilisation. These quantified benefits support the transition toward sustainable and digitally integrated manufacturing practices[62-65].

Furthermore, through advanced data analytics and customer-driven feedback loops, manufacturers can implement mass customization strategies, aligning products and services with dynamic consumer demands to enhance market responsiveness and customer satisfaction [66-68]. Industry 4.0 has also introduced a range of transformative terminologies and concepts, shaping the trajectory of modern industrial innovation outlined in Figure 3.3.

Figure 3.3. Smart manufacturing technological terminologies.

Currently, manufacturers are prioritizing the integration of cyber-physical systems, smart manufacturing, and predictive maintenance to enhance production efficiency and operational resilience. Industry 4.0 applications leverage emerging

technologies such as augmented reality (AR) for real-time assembly guidance and virtual reality (VR) for advanced design and simulation processes. These innovations enable enterprises to gain a competitive advantage and solidify their market position by enhancing precision, reducing errors, and optimizing resource utilization [69]. Smart manufacturing is facilitated through four core technological pillars: the Internet of Things (IoT), cloud computing, big data analytics, and artificial intelligence [70]. These interconnected systems enable real-time monitoring, data-driven decision-making, and seamless automation across production networks. Consequently, the adoption of Industry 4.0 fosters an integrated manufacturing ecosystem, leading to the development of smart factories, autonomous production systems, and customized products and services, ultimately driving industrial transformation and innovation [71].

3.4.1 Smart Manufacturing Technologies

Several key technologies are fundamental to the successful implementation of Human-Robot Collaboration (HRC) in smart manufacturing. These technologies optimize interaction dynamics, enhance adaptability, and enable seamless integration within production environments, ultimately improving efficiency and productivity. The most critical of these technologies are listed below.

3.4.1.1 Artificial intelligence (AI) and Collaborative Robots (Cobot)

Artificial Intelligence (AI) is revolutionizing the manufacturing sector, particularly within Industry 4.0, where Machine Learning (ML) and Deep Learning (DL) optimize production with precision and efficiency [72]. AI-driven smart manufacturing enables advanced automation, optimization, and flexibility by analyzing vast data streams from sensors, machines, and other sources. AI

encompasses a range of theories, methodologies, and technologies designed to augment human intelligence[73]. AI techniques such as ML, DL, and reinforcement learning are enhancing manufacturing by utilizing the gathered data to enhance real-time data quality monitoring interactions, and then processing and analysing data leading to the overall system performance improvements[74-76]

HRC and AI within smart manufacturing facilitate human-like learning, enabling seamless interaction between operators and robots in assembly tasks. Traditional feature-based methods require extensive manual effort for feature design and data labeling, often neglecting task context. To overcome these limitations, automated feature-learning techniques have been introduced, leveraging dual deep-learning inputs and automated labeling [77]. Authors in [78], employed (Cobots) as dynamic resources for assembly line balancing, optimizing task allocation and scheduling across different collaboration modes—sequential, parallel, and joint. Utilizing mathematical modeling approaches, including Mixed-Integer Programming (MIP) and Constraint Programming (CP), alongside metaheuristic algorithms such as Genetic Algorithms (GA) and Particle Swarm Optimization (PSO), they aimed to minimize cycle time, ergonomic risks, and operational costs while enhancing production efficiency and flexibility.

3.4.1.2 Augmented reality (AR)

AR is a distinguished promising technology that can be utilized in smart manufacturing environments. AR is providing support and association information for the human operator which can increase his/her awareness during the work, especially considering assembly tasks and systems design phases [67, 79].

In [80], the authors investigate key aspects of how augmented reality (AR) enhances human-robot collaboration (HRC) systems, particularly in safety, guidance, and quality control. AR improves worker safety by displaying visual warnings, illustrating robot movements, and providing workspace visualization [81]. These visual warnings include alerts for robot startup and shutdown, emergency stops, and general safety notifications. Additionally, AR utilizes two holographic cubical safety volumes—green and red—to indicate safe zones for human operators and robot movement areas. Safety markers are also projected onto the workpiece and the ground to enhance awareness of the robot's actions.

AR technology further assists operators in the assembly process by projecting textual and 3D holographic instructions directly onto the workpiece or a virtual slate. These projections help identify critical areas, indicate correct part placements, and display the necessary tools and components for each task. The system offers real-time updates based on the operator's actions; highlights completed tasks and provides detailed 3D holographic animations.

Moreover, HRC systems incorporating AR technology enhance quality control by detecting defects in handled parts and alerting operators for inspection. A blinking marker is projected onto defective components to prompt human intervention. The system also verifies proper part positioning and screw insertion, notifying the user of any discrepancies. If an error occurs, notifications appear in the same interface used for instructional guidance, further improving quality control.

3.4.1.3 Digital twin (DT)

Digital Twin technology has emerged as a crucial tool in fostering sustainable manufacturing practices within the domain of smart manufacturing. By creating a

digital representation of the physical shop floor, technology facilitates the real-time acquisition of production data [82]. Consequently, it enables manufacturers to identify and implement sustainable enhancements, such as minimizing waste, optimizing energy utilization, and enhancing material efficiency. Digital Twin (DT) technology has demonstrated significant applicability across a range of simulation domains in manufacturing. Mihai et al. in [83] proposed a DT framework for predictive maintenance in CNC machine tools, integrating real-time sensor data with machine learning to predict equipment failures and reduce unplanned downtime. Similarly, Wang et al. in [84] developed a DT-based virtual commissioning approach, enabling the simulation and validation of control systems prior to physical deployment, thereby improving implementation efficiency and reducing commissioning costs. In the context of decision support, a conceptual architecture for digital process twins that facilitates what-if scenario analysis is introduced, allowing organizations to evaluate the impact of process modifications before execution [85]. These studies collectively highlight the versatility of digital twins as a simulation and optimization tool within smart manufacturing environments.

Beyond sustainability, digital twins are extensively utilized for advanced simulation purposes, including what-if scenario analysis, predictive maintenance modeling, and virtual commissioning of manufacturing systems. These simulation capabilities allow manufacturers to evaluate process changes, optimize production strategies, and foresee system failures before they occur, thereby enhancing decision-making and operational robustness.

Digital Twin technology is also compatible with other network-physical integration technologies such as virtual and augmented reality, as well as simulation.

This integration empowers manufacturers to create advanced simulation models of their production processes and test various sustainable initiatives. Virtual and augmented reality technologies provide real-time data and guidance to workers, enabling them to carry out sustainability-related tasks such as identifying and segregating recyclable materials. By providing manufacturers with real-time data, Digital Twin technology has become a vital component of smart manufacturing, and its integration with other technologies can create more sustainable production environments [86, 87].

To create an efficient and cost-effective HRC system for smart manufacturing, it's crucial to carefully design and analyse the system. Digital Twin (DT) technology is essential in improving the interaction between humans and robots, allowing real-time monitoring and dynamic decision-making. However, the challenge lies in creating a DT model that accurately represents the collaborative scenario and relationship between physical components. Additionally, maintaining system consistency can be difficult in sustainable smart manufacturing. In response to these challenges, the authors in [88] propose a four-tuple DT model for HRC systems, which includes a human model, robot model, collaborative environment model, and collaboration relation model. To achieve this goal, the proposed approach concentrates on resolving the challenges associated with optimizing DT, specifically task allocation, path planning, and layout optimization. Additionally, the method considers the consistency of the HRC system while evaluating the model's operational process. Further investigations are necessary to highlight challenges in software capabilities, interoperability, and real-world implementation, calling for

standardized frameworks and AI-driven DT solutions to optimize safety, ergonomics, and efficiency in Industry 4.0.

3.4.1.4 Sensing Technologies

Smart manufacturing environments are characterized by their dynamic work areas, precise production processes, and improved quality control methods geared towards enhancing products[89]. The integration of robotics and sensing systems plays a crucial role in achieving more efficient automation and robust control mechanisms[90]. Notably, ongoing research is concentrated on refining robotic systems for greater flexibility and safety, enabling human operators to collaborate within the work environment. This symbiotic relationship leverages the operator's experience alongside the robot's consistent capabilities, forming what is commonly referred to as a human-robot collaboration (HRC) system [91]. The incorporation of human-robot collaboration systems in smart manufacturing has consistently prioritized the optimization of localization, path planning, and obstacle avoidance challenges.

Villani et al. [13] presented handling, welding, assembly, and automotive as key areas where collaborative robots are utilized noticing the impact on the work efficiency when engaging with human operator in the same work areas. However, key challenge in these environments lies on the intuitive interfaces for broader applications adoption. Ding et al. incorporated Kinect depth sensor-based hand gesture for HRC system in the automotive industry, aiming to enhance ongoing material handling and assembly tasks by harnessing the wealth of information derived from dynamic hand gesture recognition, seamlessly integrated sensing technology and a novel wake-up reminder to enhance timing of gesture

sequences[92]. In contrast, the system's flexibility is limited to the fixed position of the operator as it may perform well with complex gestures. Zhou et al. advanced the use of Inertial Measurement Unit (IMU) devices by integrating them with an attention-based deep learning model to enhance motion recognition and position estimation in human-robot collaboration. Their approach improved the precision of identifying key moments for robotic assistance by merging forward kinematics with deep learning techniques, setting it apart from traditional methods. However, the reliance on controlled experimental conditions raises questions about its effectiveness in more variable real-world environments[93].

The utilized sensing and HRC systems in the manufacturing areas are directed to limited tasks and applications that maintain safe and flexible working environment focusing mainly on the operator's confidence, safety and seamless engagement with the collaborative robot[94]. However, the implementation of sensing systems is essential in industrial applications such as production feedback and control, data exchange, quality assurance, measurement, and machine communication systems. This is particularly critical in environments where collaborative robots operate alongside human workers, as sensing systems significantly influence work efficiency and interaction effectiveness within shared workspaces.

Therefore, the implementation of capacitive sensing technologies has become increasingly widespread in advanced manufacturing systems due to their high sensitivity, low power consumption, and adaptability[95-98]. For example, in additive manufacturing, capacitive sensors are employed for real-time liquid level detection to ensure precise material deposition and process consistency [99]. capacitive sensing plays a critical role in key manufacturing operations, including

pressure measurement, activity recognition, and closed-loop process control, thereby enhancing system monitoring, quality assurance, and overall operational efficiency across industrial applications [100-102].

The utilization of these approaches is attributed to their ability to gather highly sensitive and accurate data, effectively representing the real-time status of ongoing processes and high performance of non-destructive testing [6]. Li et al. in [6] demonstrated a highly sensitive coplanar capacitive sensor that is utilized for liquid film thickness detection to investigate if a liquid film occurs under or above insulation surfaces. The sensor, integrated with AD7745- based system, was tested in a controlled environment using an ultrasonic humidifier. The targeted thickness range is 0 to 1.5 mm and the measuring interval is 0.1 mm[6]. Although the results match the simulation results, the repeatability of this test with the same conditions is challenging. The proposed work in [103], highlighted the application of capacitive sensors, where the deformation of electrodes and dielectric layers under pressure changes their capacitance. This change is key to selecting materials and designing structures, especially for applications needing accurate pressure detection and measurement in flexible and wearable technology. In [104], a developed coplanar capacitive sensing approach is integrated with a printed circuit board (PCB) for non-destructive thickness measurement. Three sensor shapes (spiral, interdigital, round) are designed and optimized for testing and validation with plastic thin film. Results demonstrated a high sensitivity and nearly linear relationship between the voltage and the film thickness up to 90 μm. However, the sensitivity is reduced for thicker films beyond 230 μm. In [105] , authors focused on measuring liquid film thickness in two-phase flow within a square duct. A parallel-plats capacitive sensor and

composite material analysis are involved to predict the capacitance. The approach results stated high accuracy with 0.014 mm and 0.019 mm standard deviations for stratified flow, and 0.17 mm and 0.093 mm for annular up flow and downflow. However, the temperature variations and large fluctuations in film thickness reduce the accuracy in measuring unstable annular flow [105]. On the other hand, the integration between collaborative robots and capacitive sensing technology is mainly focusing on improving and maintaining safety standards specifically in tasks requiring direct physical interactions. However, the temperature variations and large fluctuations in film thickness reduce the accuracy in measuring unstable annular flow [105].

3.4.1.5 Machine Vision

Cobots are known now as a promising technology that is being developed to boost the level of productivity, flexibility, and efficiency in industrial environments specifically smart manufacturing areas [1]. Additionally, classical machine learning and deep learning methods are being deployed to perform image classification task as part of machine vision technology [106]. Both machine vision and robotic technologies are integrated to form novel approaches for monitoring, fault detecting and controlling tasks in industry. T. Brito et al. [107] employed a Cobot to assist human operators in conducting product inspections by manipulating, transporting, or rotating items as needed for thorough examination. The Cobot is equipped with an integrated force-torque sensor and reinforcement learning techniques to enable the cobot to acquire and refine inspection tasks under human guidance. However, this work is currently confined to controlled environments and entails an initial stage in developing the reinforcement learning model, necessitating further refinement and

validation in real-world scenarios. M. Moor et al. [108] introduced a comprehensive system that integrates collaborative robots (Cobots), a vision system, artificial intelligence, and adaptive grippers to perform inspection tasks on IoT modules, specifically focusing on verifying cable placement and functionality. The systems effectiveness was validated through successful tests, demonstrating its capability to automate the inspection process while accommodating various product variations with minimal need for reprogramming. In a controlled laboratory setting, the system achieved a high accuracy in classifying different defect types. However, the scalability and effectiveness of the system in high-volume production environments are constrained by the challenges related to lighting variations and the need for real-world industrial testing. Simultaneously, researchers have advanced quality control inspection techniques for detecting and classifying technical defects in industrial and by leveraging machine vision technology based on classical machine learning and deep learning methods[109, 110]. X. Tao et al. in [111] introduced a machine vision approach aimed at detecting defects in adhesive coatings applied to solid engines. This approach utilized the ResNet101V2 model with transfer learning, achieving a notable validation accuracy of 96.15%. The method is engineered to operate effectively under challenging conditions, including high aspect ratios and varying lighting environments, and has proven its practical viability through real-time deployment. Nonetheless, the approach is limited by its dependence on the specific dataset, the complexity involved in deployment, and its sensitivity to environmental variables, which could impact its generalizability and ease of implementation across different industrial contexts. H. Zhao et al.[112] presented an CNN method for defect detection and classification of coating application based on the deployment of

ResNet50 and DenseNet121 models. The designed ResNet50 model showed the highest detection ability with accuracy of 97.9% and precision of 95.0%. Notable limitations of the system are due to the limited dataset size, variability in detection accuracy and specific conditions for implementation. Also, ResNet-50 VGG-19 have achieved high accuracy rates, with the reported performances in image classification tasks of 93.3% and 94%, respectively[113, 114]. However, these models require considerable computational resources for both training and inference. It is distinguished that the classical machine learning methods such as support vector machine (SVM) are designed to address classification tasks in work processes as stated in [115] [106]. M.Bouamar et.al.[116] proposed a comparative study on Artificial Neural Networks (ANN) and Support Vector Machines (SVM) for water quality classification. Both models achieved similar recognition rates over 86%, highlighting their effectiveness. ANN is faster in training but more susceptible to noise, while SVM, though more noise-resistant, requires significantly more training time. It is important to state that traditional machine learning methods often excel in training but struggle in real-world scenarios due to overfitting, capturing complex and non-linear patterns[117]. In contrast, deep learning models like ResNet-101, though prone to overfitting if not carefully managed, handle intricate feature interactions and generalize better with diverse data.

In the era of advanced manufacturing, quality control inspection is an essential process , as it guarantees that products adhere to specified standards and fulfill customer expectations [118]. Early identification of defects and inconsistencies minimizes waste, reduces production costs, and prevents the distribution of substandard products. In-process inspection is particularly crucial for surface defect

detection in manufacturing. Therefore, machine vision systems, leveraging deep learning, are extensively deployed with robotic systems for real-time monitoring, verification, and fault prediction [119]. This comprehensive approach significantly enhances product reliability, ensures consistent quality, and upholds a company's reputation for excellence in the market [120]. In the automotive industry, coating and painting processes act as protective barriers, offering resistance against corrosion and prolonging the lifespan of materials [121, 122].

However, these procedures encounter notable challenges during production. For instance, they demand substantial energy for heating and air circulation in ovens. Additionally, overspray and paint waste can compromise the overall product quality [123]. In the pharmaceutical sector, uniform coatings safeguard active ingredients, maintaining their stability and efficacy [124]. The development of pharmaceutical coatings involves complexities, operator training, and the need for adequate equipment to ensure even liquid distribution [125]. Consequently, in-process inspection is vital to address production challenges, minimizing quality failures. This scrutiny requires continuous development and technological advancements to effectively address various functional errors and production issues. In industrial applications, coatings are applied to leather, metal, fabric, and composite materials, enhancing their durability and functionality[112]. Liquid spreading over skin mimic substrate is an initiative task that can be conducted to study material specifications and properties before starting production processes to confirm that the liquid can meet the production requirements. For instance, studying the stickiness properties of glue, shampoo or any other liquid that can be used in industrial applications or for production. Spreading the liquid requires precise inspection to confirm the

uniformity of the spreading considering thickness consistency of the spreading and coverage of the spreading area.

3.4.2 Industrial Applications of HRC in Smart Manufacturing

This subsection examines the application of Human–Robot Collaboration (HRC) within two key industries: food and automotive.

In the food industry, robotics and automation are being utilized to improve production processes, enhance food safety, and optimize quality control. Collaborative robots (cobots) assist in repetitive and physically demanding tasks, such as food handling, packaging, and quality inspection, ensuring higher efficiency while maintaining human oversight.

Similarly, in the automotive industry, HRC is revolutionizing assembly lines by allowing robots and human workers to collaborate on complex tasks. Cobots contribute to precision-driven operations such as screwing and component assembly while leveraging vision systems to enhance safety and adaptability. The examination of these industries highlights the practical benefits and challenges associated with implementing HRC in smart manufacturing, emphasizing its role in enhancing productivity and worker well-being while meeting industry-specific demands.

3.4.2.1 Food Industry

The food industry plays a key role in the European economy as some shops produce up to 10,000 meals daily [126]. The manufacturing cycle consists of three major stages: farming, production and finally, ready meals to be sent to the market. Food sector leaders are focusing on transforming the business strategy to be based on demand. This was especially important in the early stages of the COVID-19 pandemic, which negatively impacted supply chain resilience [127]. Therefore, the

emergence of digitalization and Industry 4.0 technological contributions are highly required to lead the transformation of food production to enhance the sustainability of this sector [128].

Robotics in agriculture is enhancing the collection of information about plants, soil and crop growth. The implementation of sensors is increasing the system's reliability through intelligent packaging, as sensors are built to provide real-time data about the expiry date of the products [129]. Fruit harvesting is utilized by employing a robot attached to a gripper camera to perform both picking and inspection processes [130]. By integrating an image processing system with the camera, quality control assurance can be enhanced. In addition, installing a vision system on the cobot will enhance the consumer confidence that this food is safe and clean as the camera will be able to detect foreign bodies like glasses or plastic. According to [126], in catering facilities, there are several processes (e.g., cooking, baking), and the production challenge lies at the end of the line. Food is processed in this area through manual steps, which are light and can be performed by humans, but they require a high level of repetitive ability, which the human worker lacks at this point.

The food industrial sector requires continuous advancements and developments. Challenges may arise due to the adoption of Industry 4.0 technologies and trusting industrial robots to collaborate with human operator to perform tasks. However, a delay in implementing these systems will delay the opportunity to benefit from these technological advances, and therefore no tangible change will occur in the industrial sector. The HRC system adoption will gradually ensure production processes are working ideally considering that some tasks can't be automated and

require human expertise such as feeding machines with components to keep the work continuous.

3.4.2.2 Automotive Industry

Automotive is the largest industrial sector in the world. Considering the UK only, 3.7 million employees are working in the automotive sector and the economic contribution of the UK economy is about $26 billion [127]. In the automotive industry, assembly cells are playing an important role where 83% of production units involve assembly tasks [41]. However, some manual operations are still needing more flexibility and robustness to be performed efficiently; thus, relying on the industrial robot to perform these tasks alone may not be a practical solution as human abilities can't be fully replaced [131]. Therefore, the focus is to combine both abilities of humans and robots to work in collaboration while safety is assured to prevent any accident during the work [50].

In [16], the collaborative robot in the assembly stage is responsible for the screwing task through the sensing integration with a human operator who will be able to share the work area and task. Also, installing the vision system allows the collaborative robot to collect information about the working environment and the human intentions that will be used for further improvements such as path planning and human movement predictions. As a result, the implementation of the HRC system is showing the needed capacity to perform complex tasks.

3.4.2.3 Personal Care Product (PCP) Manufacturing

The personal care product (PCP) industry is characterized by the large-scale manufacturing of high-viscosity formulations, including lotions, creams, and gels,

where stringent quality control is essential to ensure formulation consistency, product safety, and customer satisfaction [132, 133]. Within product validation workflows, particularly during tack testing, the accurate preparation and evaluation of liquid films are critical for obtaining reliable measurements of adhesive strength and spreading behavior [133]. Manual preparation of test specimens is inherently prone to operator-induced variability in both material dispensing and film spreading. Such inconsistencies frequently result in non-uniform film thicknesses, leading to significant deviations in tack force measurements and compromising data reliability [134]. Furthermore, the cleaning of spreading tools, such as precision spreader bars, is often executed manually and lacks standardized verification procedures. This introduces contamination risks and additional measurement uncertainty, ultimately contributing to product rejections, unnecessary material waste, and inefficiencies in quality control. These limitations underscore the pressing need for flexible, automated solutions that integrate advanced sensing, machine vision, and collaborative robotic systems for robust, repeatable test preparation and inspection processes.

Recent advancements in smart manufacturing have accelerated the deployment of collaborative robots (cobots) and machine vision systems in PCP production environments, primarily within downstream operations such as high-speed packaging, filling, labeling, and final inspection [135, 136]. HRC frameworks are increasingly utilized in these settings, operating in sequential, parallel, or responsive modes through sensor-rich controllers that enable task-level autonomy while allowing human operators to retain high-level supervisory and decision-making roles [39]. For example, packaging and decorative sublines in cosmetics manufacturing

often follow principles analogous to those in the food industry, where AI-enabled cobots manage small-batch formats, intricate decorative elements, and frequent product variants, thereby minimizing downtime and improving line flexibility [137]. Similarly, low-payload cobots (≤ 5 kg) equipped with machine vision, force-torque sensing, and gesture-based interaction interfaces have demonstrated capabilities for multi-variant assembly across mixed product lines, directly addressing the PCP sector's demand for high-mix, high-customization manufacturing [138].

Despite these advancements, automation in PCP manufacturing remains predominantly focused on downstream processes, with limited penetration into real-time, in-process quality assurance of viscous film formation during tack testing [139, 140]. Current inspection practices largely rely on manual visual assessments or basic threshold-based image processing techniques that lack the spatial precision, repeatability, and adaptability required for robust quality control. Non-destructive film thickness measurement technologies have not yet been systematically integrated into automated test workflows, leaving critical process variables insufficiently monitored. Likewise, cleaning verification for spreading tools remains a manual, operator-dependent activity, subject to inconsistent execution and error. While collaborative robots have gained traction for material handling and end-of-line operations, their application to AI-driven, sensor-based inspection tasks within PCP manufacturing is still minimal. This gap presents a significant opportunity for research and technological development, specifically in integrating robotic systems with advanced metrology and real-time quality monitoring capabilities to enhance reliability and repeatability in tack testing processes.

3.4.3 Quality Control Inspection in Manufacturing

Accurate in-process Quality Control Inspection (QCI) is essential in liquid-based coating and painting operations, where spreading thickness and uniformity directly affect product reliability and compliance with stringent production standards [9, 141, 142]. Current inspection practices are still dominated by manual visual checks and heuristic assessments, leading to inconsistent quality assurance, operator-dependent variability, and low sensitivity to localized defects, particularly under fluctuating process conditions [143]. These limitations often result in undetected non-uniformities such as thin spreading, centred spreading or empty spreading, causing material waste, costly rework and product assessment failure [144-146].

Therefore, efforts to automate inspection have explored robotic integration, vision based deep learning, and non-contact sensing in related tasks such as level monitoring and surface characterization where defects are detected, classified and localized [147, 148]. However, these implementations provide only global indicators, lacking in real-time monitoring and spatially resolved feedback required during dynamic spreading. Furthermore, viscosity-driven flow behavior and substrate heterogeneity introduce additional uncertainty, making conventional automation strategies inadequate for high precision measurements such as micrometer-scale profiling in production environments. Current inspection methodologies present two fundamental limitations. First, they depend on localized point measurements, such as ultrasonic or eddy-current probes, combined with heuristic visual assessments that are operator-dependent and inherently non-scalable [149, 150]. Second, existing automated systems lack spatial resolution and interpretability achievable with vision-based deep learning frameworks. Current approaches predominantly perform binary

region classification or generate coarse thickness maps without a physically grounded estimation of film uniformity [5, 151, 152]. Addressing this limitation is critical in applications requiring micrometer-scale thickness measurements, as inaccuracies directly influence subsequent manufacturing stages and process decisions. These constraints restrict precise defect localization and impede seamless integration with adaptive process control strategies. In advanced QCI systems for liquid-based surface treatments, including pharmaceutical tablet coating, automotive painting, and consumer product finishing, the inspection process can be formulated as a spatial inference problem. In this context, the uniformity of liquid deposition across the target surface is evaluated by estimating the coating thickness from indirect sensor-derived measurements. [153-157]. Recent progress in robotic-assisted sensing and data-driven modeling provides new opportunities to overcome limitations of current inspection techniques. For instance, capacitive sensing technique is particularly attractive for liquid-film applications due to its high sensitivity to dielectric variations, enabling non-contact estimation of micrometer-scale thickness without disturbing the spreading process [158]-[159]. Capacitive sensing, combined with robot-assisted actuation, enables spatially registered measurements across predefined inspection grids. This configuration facilitates quantification of liquid film thickness with high spatial resolution over the sample surface.

This paper addresses three core challenges in QCI of liquid-based spreading processes. First, existing inspection systems exhibit limited repeatability and inadequate interpretability, primarily due to their dependence on heuristic visual assessments or sparse, contact-based thickness measurements [160]. To address this

limitation, we developed a robot-assisted capacitive sensing platform that estimates micrometre-scale liquid film thickness by mapping analog sensor outputs to calibrated thickness values using a linear regression model derived from empirical calibration data. Unlike rule-based or purely vision-driven approaches, this model is physically grounded and enables consistent estimation across diverse substrates without the need for extensive tuning or domain-specific heuristics.

Second, traditional inspection methods, whether manual or automated, fail to provide sufficient spatial resolution. This limitation results in missed detection of localized non-uniformities such as edge thinning or central pooling [151]. Our method explicitly formulates inspection as a spatial regression task. A UR10e collaborative robot (Cobot) samples nine fixed positions across the spreading area. At each position, the capacitive sensor measures the capacitance and outputs voltage readings based on the capacitive measurement principles. This enables the system to reconstruct the spatial distribution of film thickness in real time.

Third, deep learning solutions in industrial inspection are hindered by data annotation requirements, computational overhead, and limited robustness under variable factory conditions [161]. In contrast, our method does not require large, annotated datasets or high-performance computing infrastructure. In addition, the sensor calibration is achieved using ground-truth thickness measurements. Therefore, the proposed approach is consistent for deployment complex condition environments. Furthermore, the transparency of the regression model supports traceable diagnostics and root-cause analysis, capabilities that are often absent in black-box learning-based pipelines. The system therefore achieves a practical

balance among resolution, interpretability, and industrial deployable ability in quality-critical spreading applications.

3.5 Discussion and Key Research Findings

Industry 4.0 demands AI, robotics, and IoT to enhance manufacturing productivity, efficiency, and cost reduction [162]. Digital transformation requires more than technology adoption; it necessitates leadership, clear vision, and a culture of innovation [163]. Effective leadership communicates technology value, encourages experimentation, and empowers employees. Employee engagement, continuous training, and pilot projects validate transformation benefits before scaling [164] . Collaboration with industry peers enhances knowledge sharing and best practice adoption. Change management strategies emphasize data-driven decisions, analytics investment, and iterative evaluation.

Smart manufacturing integrates AI, Cobots, augmented reality (AR), digital twins (DT), and human-robot collaboration (HRC) to optimize operations, decision-making, and resource use, reducing waste and costs while increasing productivity. Business unit integration improves supply chain management and customer service, ensuring better collaboration, data management, and product traceability [165].

HRC systems enhance flexibility, efficiency, and human-machine collaboration, reducing operational complexity [107]. However, their use is mainly limited to simple production tasks due to technological complexity, affecting operator confidence in critical situations [166]. Defining human-robot roles while maintaining safety is essential.

HRC systems, comprising collaborative robots, human operators, vision/sensing technologies, and machine learning, require expertise in managing complex systems. Skill gaps among operators necessitate significant training investment [164]. High employee turnover further challenges workforce skill retention, requiring ongoing training. AI-driven manufacturing raises ethical and legal concerns, including data privacy, algorithmic bias, and regulatory compliance [167]. Manufacturers must align technology deployment with ethical and legal standards while maximizing HRC benefits in Industry 4.0 [162].

3.5.1 Challenges and Limitations in HRC Systems for In-Process Quality Control Inspection

The integration of Human-Robot Collaboration (HRC) into in-process quality control tasks has emerged as a significant research area, especially in complex and skill-dependent manufacturing processes such as industrial coating and painting processes [168]. Unlike structured manufacturing tasks (e.g., automotive assembly and welding), which rely on well-established QC techniques, liquid-based defect detection presents unique complexities due to its dynamic nature, viscosity variations, and substrate dependencies.

A key challenge lies in the lack of standardized quality inspection methods for liquid spreading applications. Traditional manual inspection methods used in industries are highly subjective and inconsistent, relying heavily on human judgment. Unlike solid-state defects that can be precisely categorized, liquid spreading defects exhibit variable thickness, uniformity, and adhesion, making real-time automated detection significantly more challenging.

To the best of our knowledge, implementing real-time HRC, sensing and vision-based classification of liquid spreading defects application remain underexplored. While machine vision and deep learning have demonstrated success in detecting defects in solid materials, their application in fluid-based processes is still at a nascent stage. The key limitation is the high variability in liquid behavior, which depends on environmental conditions, substrate interactions, material types, and material properties. Moreover, existing capacitive sensing technologies, which have been extensively used in distance and level measurements and industrial safety systems, face significant limitations in liquid-based applications due to environmental interference, material inconsistency, and the dynamic movement of spreading fluids.

From an HRC perspective, most existing sensing systems are optimized for distance and safety measurements at a millimeter or micron level. However, in high precision liquid spreading or coating processes, these systems struggle with real-time adaptability and robustness. Implementing an AI-driven CNN-based defect detection system for liquid spreading, as explored in Chapter 3, requires robust data collection, model optimization, and real-world validation beyond controlled lab environments. Additionally, the development of a regression-based predictive model, detailed in Chapter 4, bridges the gap between sensor data and real-time thickness consistency assessments, advancing HRC-QC systems.

Beyond technical constraints, human involvement in QC decision-making remains an essential yet understudied aspect of HRC systems in quality inspection. While automation can enhance accuracy, efficiency, and repeatability, human operators still play a crucial role in interpreting and validating machine-generated

QC data, particularly in high-stakes production environments where QC failures could result in defective batches, rework costs, or material waste. In Chapter 5, the full system integration including the human operator collaboration is demonstrated and detailed of how the human operator is sharing and collaborating to perform QCI task.

3.5.2 Identified Knowledge Gaps

The challenges outlined above reveal several critical knowledge gaps in the field of HRC-driven quality control for fluidic manufacturing processes:

- Recent deep-learning-based visual inspection research is dominated by surface defect detection on solid materials such as strip steel and metallic products, where CNN and YOLO variants are trained to localize and classify scratches, pits or inclusions on rigid surfaces [169-171]. In contrast, liquid-film and liquid-containing processes are predominantly treated as metrology problems – for example, measuring thin-film thickness or monitoring fluid bags for foreign bodies – rather than as image-based classification of spatial spreading defects on compliant or skin-like substrates [172, 173]. Moreover, the thin-film literature highlights that liquid films are inherently non-uniform and time-varying due to viscosity- and surfactant-driven instabilities, which complicates visual inspection compared with static solid surfaces [174]. To the best of our knowledge, CNN-based QC systems explicitly targeting liquid spreading patterns and classifying them into defect categories (e.g., full, fault, empty) remain largely unexplored, motivating the ResNet-101-based framework proposed in this work. This research addresses this gap by

introducing an AI-based ResNet-101 deep learning model to classify liquid spreading defects, an approach that is extensively detailed in Chapter 4.

- Limited Adoption of Capacitive Sensing for Liquid Thickness Measurement. While capacitive sensors have been widely used for solid-state QC applications, capactive sensing technique is not deployed with HRC-driven quality control systems for real-time liquid thickness evaluation [175] [176]. This study extends capacitive sensing applications by combining them with regression-based predictive models, correlating sensor-based thickness readings with real-time spreading consistency assessments, a novel contribution detailed in Chapter 5.
- Limited Real-World Deployment of HRC-QC Systems. Most HRC-QC research remains confined to laboratory conditions, making it difficult to assess scalability and robustness in industrial settings [177]. The scarcity of real-world industrial deployments of collaborative-robot-based quality control has been repeatedly highlighted in recent systematic reviews, which show that only a small fraction of HRC studies are validated outside controlled experimental setups [137]. This study addresses this limitation by deploying a Proof-of-Concept (PoC) system in a real-world manufacturing case study in collaboration with industrial partner (Unilever) and validating it. Additionally, the sensing-robotic is further validated through another case study focusing on paint coating surface classification.

3.5.3 Proposed Research Approach

To address the above challenges, a novel HRC-based sensing and vision quality control inspection system is proposed, specifically designed for liquid spreading and

coating processes in industrial applications. This system leverages AI-driven defect detection and classification, real-time sensing, and human-in-the-loop decision frameworks to create a scalable, adaptable, and industrially viable QC solution.

- **Key Components of the Proposed System**
  - Machine Vision-Based Defect Classification Using ResNet-101 CNN

The CNN model is trained to classify three primary spreading quality categories:

- Full spreading: a condition where the liquid has been uniformly and completely applied over the target surface area, indicating successful coverage without gaps or inconsistencies.
- Empty spreading: this condition reflects a complete absence of material deposition where spreading is required.
- Faulty spreading: a class capturing partial or irregular spreading patterns, which deviate from the acceptable process specifications.

The ResNet-101 model significantly outperforms traditional machine learning approaches in terms of accuracy, reliability, and processing speed. Deployment in an industrial setting represents a major advancement in AI-powered QC for liquid spreading processes, as discussed in Chapter 3.

- **Capacitive Sensing Integration for Liquid Thickness Measurement**

A regression-based approach is used to predict real-time liquid thickness consistency, correlating sensor readings with spreading behaviour. Real-world

manufacturing data validation ensures robustness and reliability in dynamic QC scenarios as presented and detailed in Chapter 4.

- **Full HRC, Sensing and Vision system for In-Process QC Inspection.**

The system operates in real-time, providing consistent results on spreading quality and thickness consistency. By combining sensing and machine vision insights, this research introduces a comprehensive QC analytics platform that allows human operators to verify and refine defect detection results.

3.6 Summary

This chapter presented a comprehensive review of Human-Robot Collaboration (HRC) in smart manufacturing, covering interaction types, collaboration levels, safety mechanisms, and communication interfaces. The integration of AI, Collaborative Robot (Cobot), Digital Twin (DT), and Augmented Reality (AR) was explored, demonstrating their role in enhancing efficiency, flexibility, and safety in industrial applications, particularly in food and automotive sectors.

Despite the benefits of HRC, challenges remain, particularly in in-process quality control (QC) for dynamic fluid-based processes. To address this, research integrates capacitive sensing, ResNet-101based machine vision subsystem and a UR10e Cobot for liquid spreading inspection on skin-mimic substrates, enhancing consistency, precision and reliability.

Chapter 4. CNN-Based Machine Vision and Robot-Assisted System for Defect Classification

4.1 Introduction

Ensuring uniformity in liquid spreading on skin-mimic substrate materials is a critical aspect of quality control in automated industrial processes. In manufacturing applications such as coating and painting, inconsistencies in liquid spreading can lead to defects that impact product performance and aesthetic quality [3, 110]. As automation continues to advance, the integration of intelligent sensing and vision-based inspection techniques becomes essential for enhancing quality assurance.

This chapter presents a convolutional neural network (CNN)-based approach for visual inspection of liquid spreading on skin-mimic substrate materials. The developed system leverages the ResNet-101 architecture to improve the accuracy and robustness of the quality control process. The proposed system integrates a machine vision subsystem with a UR10e robotic arm, which is responsible for scanning and capturing images under varying lighting conditions. By automating the inspection process, the system ensures consistency and reliability in assessing the quality of liquid spreading.

The spreading process is classified into three distinct categories as presented in Figure 4.1: empty spread, full spread, and fault spread.

(a)

(b)

(c)

Figure 4.1. Liquid spreading status over mimic skin substrate. (a) empty or no spread, (b) fault, and (c) full spreading.

To achieve this, a novel dataset is generated, with images captured and pre-processed for training, validation, and testing purposes. The trained ResNet-101 network effectively categorizes the spreading conditions, demonstrating superior classification performance compared to classical machine learning and alternative deep learning models.

Experimental evaluations highlight the efficacy of the proposed approach, with ResNet-101 achieving a training accuracy of 97.99%. Comparative analysis with traditional models reveals that ResNet-101 not only enhances classification accuracy but also improves the system's robustness in real-world industrial settings. The real-world testing of unseen samples confirms the model's generalization capability and its potential for deployment in automated quality control applications.

The findings presented in this chapter contribute to the advancement of intelligent quality control in automated manufacturing. The proposed CNN-based inspection system provides a promising solution for quality assurance in coating and painting tasks under complex industrial conditions. The following sections will discuss the system architecture, methodology, dataset preparation, experimental results, and the implications of this research in the broader context of industrial automation and human-robot collaboration (HRC) in quality control. The contribution of this research can be outlined as follows:

- A unique dataset specifically is developed for this study by capturing images of liquid spreading under various lighting conditions. This dataset comprises 6900 images classified into: empty, full and fault spreading categories.
- Experimental demonstration of the proposed CNN ResNet-101 -based quality control approach is made on unseen samples of liquid spreading on skin mimic

substrate ensuring its robustness and reliability making the fully developed system well-suited in real-world industrial environments.

4.2 Proposed method

The ResNet (Residual Network), developed by Kaiming He and his team at Microsoft, addresses the degradation problem in deep networks, enhancing feature extraction and classification performance[178, 179]. With a top-5 error rate of approximately 3.57%, ResNet surpasses other architectures in image classification applications [179]. Network selection depends on performance, size, speed, and computational complexity [180], making it crucial to choose an optimal variant for specific tasks., making it crucial to choose an optimal variant for specific tasks.

The proposed method in this chapter leverages ResNet-101, a deep variant well-suited for handling complex feature representations, to classify liquid spreading statuses. Pre-trained on the extensive ImageNet dataset, ResNet-101 is ideal for transfer learning, effectively capturing intricate data patterns. The system integrates this model into a machine vision framework, deployed using a UR10e collaborative robot (Cobot). The Cobot, equipped with a camera on its end effector, provides essential flexibility, precision, and repeatability, significantly improving system performance [2].

As shown in Figure 4.2, the camera is mounted on the Cobot's ende ffector to view the sample area where liquid spreading occurs.

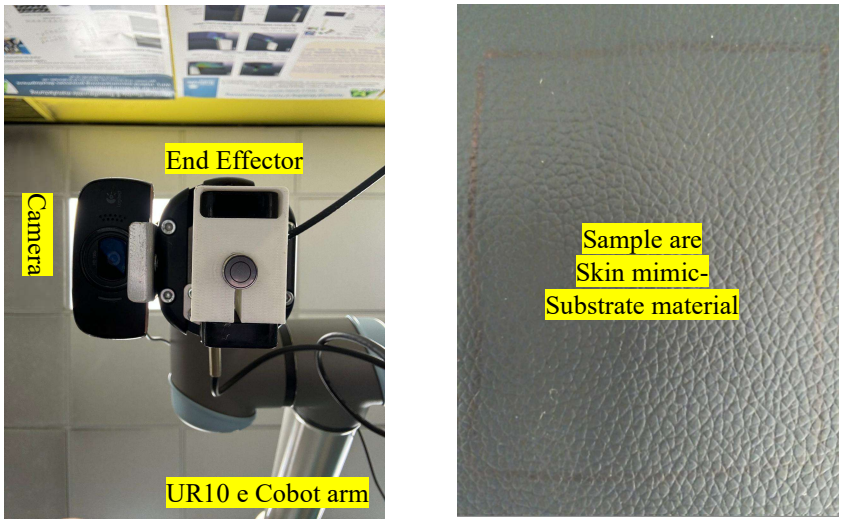

Figure 4.2. Camera setup on UR 10e cobot for liquid spreading defect detection task

4.2.1 Experimental Setup

The proposed setup enables a structured pipeline encompassing data preprocessing, model definition, training, evaluation, and visualization. Each stage is meticulously designed to ensure accurate classification, offering reliable insights into the uniformity of liquid spreading on skin-mimic materials. In the designed system, the collaborative robot (Cobot) plays a critical role in executing precise, controlled movements over the sample area where the liquid is applied. The Cobot's flexibility and accuracy are essential for consistently capturing high-quality images during each inspection cycle. The primary objective of this experimental study is to demonstrate the effectiveness of a CNN-based vision system, supported by a collaborative robot for sensor positioning, in capturing and assessing fault spreading in liquid distribution over skin-mimic surfaces. Figure 4.3 demonstrates non-uniform sample of liquid spreading over the substrate material.

Figure 4.3. Non-uniform liquid spreading sample

This is achieved by capturing detailed images of the skin mimic surface and employing a convolutional neural network (CNN)-based approach for image classification. The tools and materials utilized in this experimental setup are outlined as follows:

- Robotic part: Universal Robot UR10e, configured to move to predefined waypoint through RoboDK. The Cobot is connected to the laptop using an Ethernet cable.
- Vision subsystem: a Logitech 720p HD Webcam is utilized and connected through a USB cable to the laptop. The camera supports 30 frames per second (FPS) at its maximum resolution of 1280 x 720 pixels.

For the camera calibration, a chessboard technique was employed to calibrate the camera for capturing images as presented in figure 4.4.

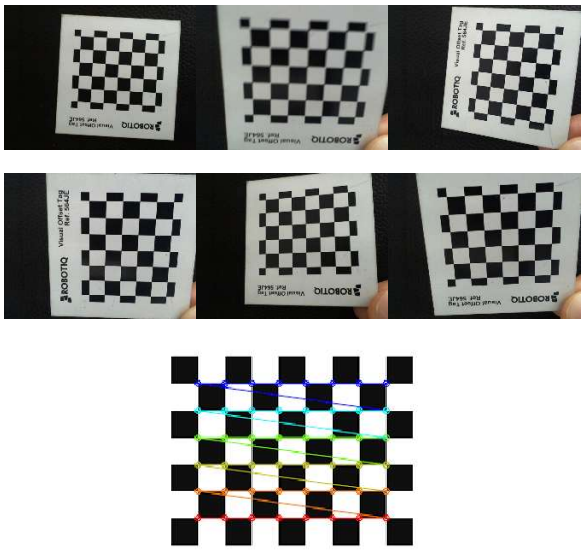

Figure 4.4. Camera calibration using the chessboard technique

The camera calibration matrix and distortion coefficients are as follows:

d_{coeffs}=

$$[0.0416326, 0.03007998, 0.00107624, -0.0068396, -0.51911224] \quad (3.1)$$

$$K = \begin{bmatrix} 699.03176075 & 0 & 324.65701877 \\ 0 & 701.86003627 & 227.7140062 \\ 0 & 0 & 1 \end{bmatrix} \quad (3.2)$$

- Data Acquisition system: Custom Python script for communicating with the Cobot and the camera for capturing, storing and classifying images.

- Materials: skin mimic substrate, magnets, syringe, spreader bar (TQC Sheen VF1500) with four thicknesses, mounting clamp, shampoo, and very flat surface plate used to fix the skin mimic substrate on.
- Power Supply: to provide necessary power for the cobot and the laptop.
- Laptop: Dell Vostro 7510, featuring an Intel Core i7processor, 16GB DDR RAM, and an NVIDIA RTXs studio graphics card. This configuration was utilized to manage both vision and robotic subsystems, as well as to deploy and test the model.
- Software: Python and RoboDK.
- NVIDIA RTX 3090 Graphics Card to train the model, is equipped with 24 GB of GDDR6X Video RAM (VRAM).

In the experimental setup, the skin mimic material is placed on a metal plate to ensure uniform application of the liquid. To maintain a controlled lighting environment, a light diffusion tent is utilized. A flexible light source is then employed to introduce random lighting conditions, facilitating the capture of images for training purposes.

Figure 4.5 illustrates the experimental setup, including the fixed positioning of the tent and the application of random lighting conditions by the designer.

Figure 4.5. Experimental setup with cobot, camera, and lighting conditions

4.2.2 Dataset

A detailed dataset of liquid spreading over a skin-mimic substrate was assembled through controlled laboratory experiments, incorporating varied random lighting conditions to represent a broad range of operational scenarios. The dataset includes 6,900 images, each depicting one of three possible liquid spreading outcomes. These images represent distinct liquid spreading statuses, where "empty" denotes the absence of liquid on the skin mimic, "full" indicates that the spreading process was successfully carried out, and "faulty" highlights issues in the spreading process that may require maintenance or further investigation.

This dataset is intended to support the development of machine learning models for image classification, with a particular emphasis on quality control and inspection of liquid spreading uniformity. The dataset is organized into three main folders: the first folder, labeled "No spread," contains 2,000 images where the spreading area is confirmed to be devoid of liquid; the second folder, "Full spread," holds 3,000 images where the liquid spreading is verified to be flawless; and the third folder, "Fault spreading" comprises 1,900 images that indicate problems with the spreading process, suggesting that the liquid is not spread as intended. Additionally, there is a final folder designated for testing and validation purposes.

The data was split into 70% for training , 20% for validation and 10% for testing on unseen samples, to ensure the robust model evaluation and accurate performance metrics. By providing a varied collection of labelled images, the developed dataset can be served as an asset for developing and enhancing fault inspection of liquid spreading uniformity. Access to high-quality data is essential for the successful creation of machine learning models, and this dataset plays a

significant role in advancing the development of more accurate and reliable tools for evaluating and ensuring the quality of liquid spreading processes.

4.2.3 Pre-processing Stage

In the pre-processing stage, precise image preparation is crucial for optimizing both training and validation. Separate pre-processing pipelines were established for the training and validation datasets to ensure proper formatting for effective model training and evaluation.

For the training dataset, the pre-processing began with data augmentation, including random resized cropping to 224 x 224 pixels, matching the ResNet-101 input dimensions. A random horizontal flip and standardization of brightness, contrast, saturation, and hue were applied to enhance the model's generalization and robustness to varying lighting conditions. Additional augmentations included a random 20-degree rotation and a 10% chance of grayscale conversion, further increasing the model's resilience to diverse visual scenarios. The images were then converted into PyTorch tensors and normalized using the pre-established mean and standard deviation values, aligning with the ResNet-101 pre-trained dataset distribution.

For the validation dataset, images were resized to 256 x 256 pixels and center-cropped to 224 x 224 pixels. The same normalization parameters as the training set were applied to ensure the consistent data scaling, which is critical for reliable model evaluation.

The ResNet-101 architecture, a deep convolutional neural network with 101 layers, was adapted through transfer learning for a three-class classification task. The architecture comprises 33 bottleneck blocks with skip connections to mitigate the

vanishing gradient problem. These blocks, distributed across four stages, capture progressively complex features. An adaptive average pooling layer reduces spatial dimensions to 1x1 before a fully connected layer with a 0.7 dropout rate to prevent overfitting. The model, with 42.5 million trainable parameters and an estimated memory requirement of 8500 MB, demonstrates the significant capacity for high-level feature extraction and classification.

4.2.4 Feature Extraction Stage

The second phase methodology employs a pre-trained ResNet-101 model for feature extraction. Originally trained on the ImageNet dataset, ResNet-101 was adapted via transfer learning by removing its classification layer, transforming it into a feature extractor. The extracted features were subsequently processed through a custom classification layer to evaluate liquid spreading uniformity on skin-mimic substrates. A multi-class classification framework was developed to identify spreading statuses as full, empty, or faulty. The training utilized a batch size of 32, 200 epochs, and an initial learning rate of 1e-6. The network's performance was evaluated on a validation set to ensure accurate classification of spreading conditions. Rather than developing a new model, ResNet-101 was fine-tuned with optimized hyperparameters tailored to the specific dataset. The trained model was subsequently saved for deployment, and its performance was assessed using confusion matrices.

To train the ResNet-101 model deployed in the proposed application, the weights and the learning rate for the architecture are initialized and summarized in Table 4.1.

Table 4.1. Hyperparameter configuration for resnet-101 model training.

Hyperparameters	**Value**
Number of epochs	200
Criterion	CrossEntropyLoss
Optimizer	Adam
Loss-function	Binary_crossentropy
Batch size	32
Initial learning rate	1e-6
Dropout Rate	0.7
Patience for Early Stopping	10

To mitigate overfitting, a multi-faceted strategy was implemented, incorporating data augmentation, dropout regularization, and early stopping. Data augmentation involves random transformations such as resizing, horizontal flipping, color jittering, rotation, and grayscale conversion, which increase the diversity of the training data and reduce the model's tendency to memorize specific features. Dropout regularization is applied in the fully connected layers, with a 70% dropout rate in the final layer, deactivating a subset of neurons during each forward pass to promote better generalization and prevent neuron co-adaptation. Early stopping is used to halt training when no significant improvement in validation accuracy is detected within a predefined patience period, reducing the risk of overfitting by preventing prolonged training. After training, either upon completion of the set number of epochs or triggered by early stopping, final metrics for training and validation are provided, offering a detailed view of the model’s performance. The trained model parameters

are saved for future inference or additional training. Visualizations of training and validation losses, accuracies, and the confusion matrix provide crucial insights into the model's classification performance, helping to detect overfitting and guide decisions on model refinement or deployment.

4.3 Experimental Results

In this section, the proposed method in liquid spreading inspection is evaluated by calculating the four metrics of accuracy, precision, recall and F1-score. For each metric, a defined equation is utilized based on the confusion matrix obtained for validation. The obtained results after the model deployment are presented in terms of confusion matrix, train and validation accuracies and losses graphs.

4.3.1 Evaluation Metrics

- Accuracy is defined as the percentage of correctly classified instances out of the total instances[181]. From the confusion matrix, True Positive (TP), True Negative (TN) , False Positive (TP), and False Negative(FN) values are obtained to aid in the calculation of the system accuracy and other evaluation metrics[182]. Accuracy is measured in (1).

$$Accuracy = \frac{TP+TN}{TP+TN+FN+FP} \quad (1)$$

- Precision measures the accuracy of positive predictions. It is the ratio of correctly predicted positive observations to the total predicted positives [181]. Precision is measured in (2).

$$Precision = \frac{TP}{TP+F} \quad (2)$$

Recall is also known as a sensitivity or true positive rate. It measures the ability of the model to correctly identify all positive instances [181]. It can be measured using (3).

$$Recall = \frac{TP}{TP+F} \quad (3)$$

Finally, F1-Score is the harmonic mean of precision and recall, providing a single metric that balances the two. It is particularly useful when balancing precision and recall is required [181]. It can be measured in (4).

$$F1\ score = 2 \times \frac{Precision \times Recall}{Precision+Reca} \quad (4)$$

4.3.2 Results

In the presented application, the integration of the CNN model for classifying three types of liquid spreading has demonstrated exceptional performance in both training and testing phases. The system was meticulously designed with precise camera calibration and strategically placed waypoints for Cobot movement, ensuring high accuracy in image capture. Among various models evaluated, ResNet-101 consistently outperformed alternatives like DenseNet-121, DenseNet-201, EfficientNet, ResNet-18, ResNet-34, ResNet-50, VGG-16, and VGG-19, as well as traditional machine learning methods such as SVM, KNN, and Bayesian classifiers, especially during deployment.

The models were rigorously trained and validated on a dataset comprising 70% training data (4,830 images) , 20% validation data (1,380 images) and 10% testing data (690 images), enabling a robust comparison. SVM accuracy outperformed KNN and Bayesian methods, as shown in Table 4.2.

Table 4.2 Comparison of classical machine learning methods by cross-validation and validation accuracy.

Classical machine learning methods	Best cross-validation accuracy	Validation accuracy (%)
KNN	0.6091	88%
Bayesian	0.8464	90%
SVM	0.9797	100%

However, ResNet-101 excelled in deep learning models, achieving 100% in validation accuracy, precision, recall, and F1 score, as highlighted in Table 4.3.

Table 4.3. Training and validation accuracy of CNN models

CNN Model	Avg. Training (%)		Avg. Validation (%)		Patience no.
	Loss	Accuracy	Loss	Accuracy	
DenseNet-121	0.1431	95.61%	0.0199	99.71%	46
RenseNet-201	0.1155	96.67%	0.0221	99.76%	36
EfficientNet	0.1413	96.02%	0.0341	99.81%	104
ResNet-18	0.1342	95.30%	0.0130	99.81%	47
ResNet-34	0.1142	95.86%	0.0111	99.66%	37
ResNet-50	0.0777	97.37%	0.0068	99.81%	40
ResNet-101	0.0536	97.99%	0.0009	100.00%	57
VGG-16	0.0606	97.64%	0.0013	100.00%	37
VGG-19	0.0730	97.70%	0.0049	99.86%	27

The distinguishing factor for ResNet-101 was its optimal patience value, a hyperparameter that controls early stopping during training. This exceptional performance is attributed to thorough parameter optimization and effective system integration. With a training accuracy of 97.99%, ResNet-101 proves robust for real-world industrial applications, underscoring its value in quality control for liquid

spreading inspections. The model's classification performance was further validated using a confusion matrix and detailed training and validation loss and accuracy graphs, solidifying the proposed system.

The confusion matrix provides a detailed assessment of the model's predictive accuracy, allowing for precise evaluation of its ability to classify different types of liquid spreading over skin mimic materials specifically fault, empty, and full spreading. Remarkably, the ResNet-101 model achieved flawless classification across all categories, as evidenced by the confusion matrix. Each class was predicted with 100% accuracy, with diagonal values of 900, 600, and 570 for the fault, empty, and full categories, respectively, and no misclassifications present.

However, achieving 100% accuracy in real-world image classification tasks is uncommon and often indicates that the dataset may be highly structured, visually distinct, or limited in variability. In this study, the images were captured under controlled lighting, fixed camera distance, and consistent cobot positioning, which reduced noise and intra-class variation. Additionally, the validation set was relatively small and homogeneous, increasing the likelihood of observing near-perfect performance.

These factors help explain the 100% result, but they also highlight the need for broader testing on more diverse datasets to fully establish the model’s robustness and to rule out any possibility of inadvertent data leakage or overfitting.

The training and validation loss and accuracy curves over 50 epochs showcase the model's efficient learning. Losses rapidly decline and stabilize at low levels, indicating an excellent fit, while consistently low validation loss confirms strong generalization. Accuracy quickly approaches near-perfection, with validation accuracy staying high

(98% to 100%) and stable, highlighting the model's robustness. ResNet-101 was chosen over VGG16 and SVM for its superior performance and reliability, proving its effectiveness in real-world testing. This model is ideal for the rigorous demands of industrial quality control in liquid spreading on skin mimic materials.

The research approach advances current methods, achieving near-perfect validation accuracy, precision, recall, and F1 scores. The novelty lies in creating a new dataset for liquid spreading inspection and enhancing machine vision and robotic systems to improve scanning and inspection. The integration of CNN and machine vision technologies offers the flexibility in complex environments and opens doors for further optimization. The use of a collaborative robot enhances human-machine interaction, supporting safe and intuitive operations. Performance metrics, including the confusion matrix of both validation and testing, training and validation loss, and accuracy graphs, are shown in figures 4.6, 4.7, 4.8,and 4.9 respectively.

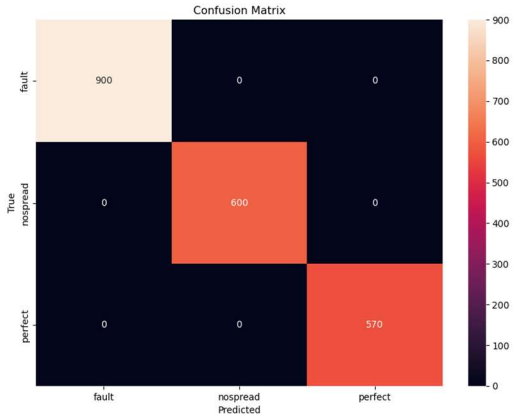

Figure 4.6. Validation confusion matrix of ResNet-101 model

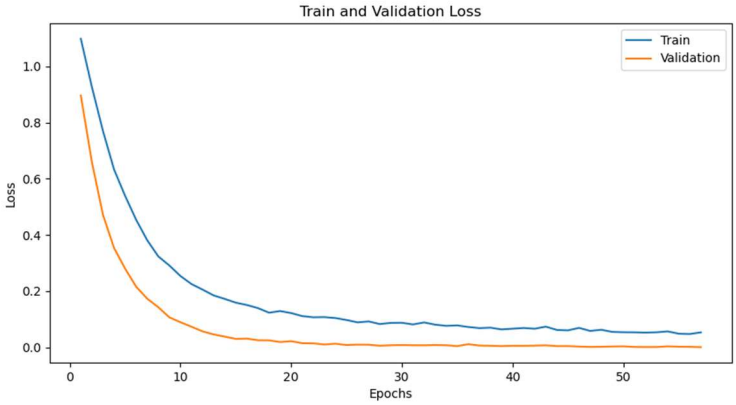

Figure 4.7. Training and validation loss

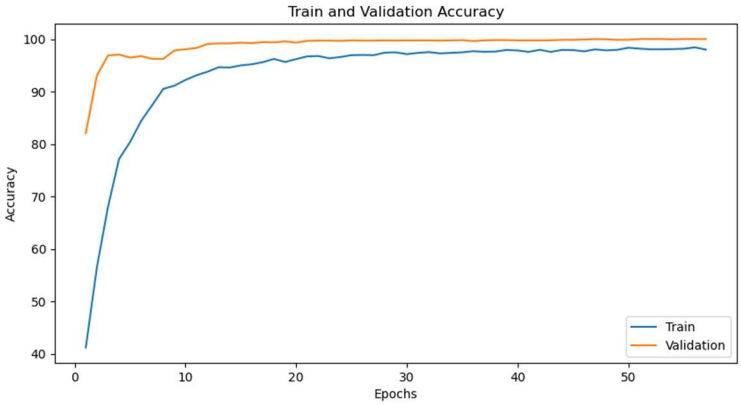

Figure 4.8. Training and validation accuracy

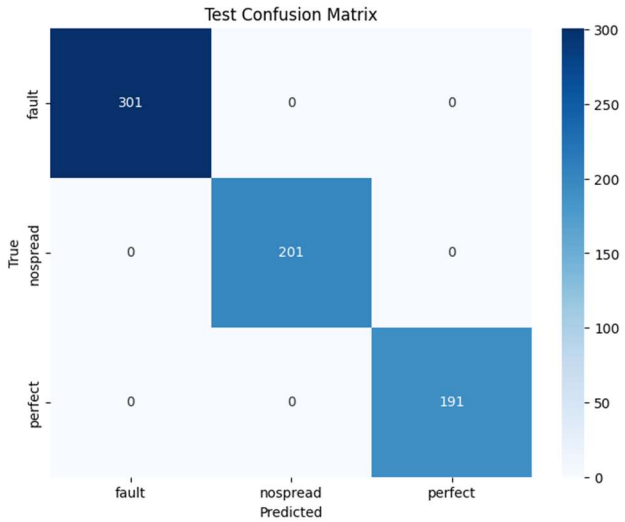

Figure 4.9. Confusion matrix of the test phase showing perfect classification accuracy across the three classes (fault, nospread, perfect) using the trained ResNet-101 model.

The model exhibited highly stable and consistent learning behaviour. Both the training and validation accuracy curves show rapid improvement during the initial epochs, stabilising near 99–100%, which indicates strong convergence and minimal overfitting. The corresponding loss curves decrease sharply and remain near zero, confirming that the model successfully minimised classification errors across both datasets. The validation confusion matrix demonstrates full separation between the three classes (*fault*, *nospread*, *perfect*), confirming that the network learned distinctive visual features for each category. The test confusion matrix further validates this outcome, maintaining perfect prediction consistency on unseen data. Overall, the ResNet-101 model achieved excellent generalisation performance and reliable classification across all phases. Finally, the developed vision-based defect detection system, supported by a collaborative robot for automated sample handling and positioning, was deployed in a real-world setting. Its performance was evaluated using previously unseen and untrained samples to assess generalizability and classification accuracy. The results, as presented in figure 4.9, demonstrate the feasibility of successfully implementing the proposed approach.

(a)

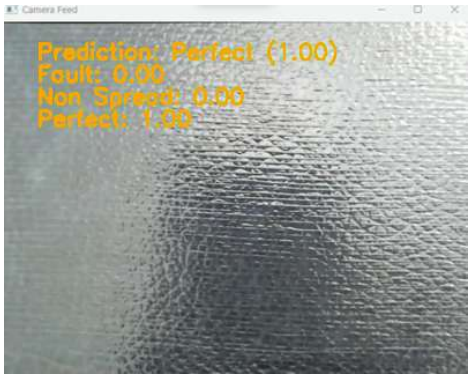

(b)

(c)

Figure 4.10. Three types of liquid spreading on a skin mimic substrate are classified: (a) No spreading or empty; (b) Full spreading and (c). Faulty spreading, indicating an issue with the spreading process.

4.4 Summary

This chapter presented a CNN-based machine vision system for defect classification in liquid spreading over skin-mimic substrates, with robotic assistance used for automated sample positioning and scanning. The proposed approach leverages the ResNet-101 architecture within a machine vision framework, combined with a UR10e robotic system, to ensure precise, automated, and reliable quality control in manufacturing environments. The developed system classifies liquid spreading conditions into three categories: empty, full, and fault spreading, addressing key challenges in industrial coating and painting applications.

To achieve this, a dedicated dataset comprising 6,900 images was generated under various lighting conditions to enhance the robustness of the classification model. The dataset was pre-processed through structured augmentation techniques to improve generalization and performance consistency across diverse conditions. A comparative analysis of classical machine learning models (SVM, KNN, Bayesian classifiers) and deep learning architectures (DenseNet, EfficientNet, ResNet variants, VGG) demonstrated the superiority of ResNet-101, which achieved a validation accuracy of 100%, outperforming alternative models in both classification accuracy and robustness.

Experimental results validated the effectiveness of the proposed approach through structured evaluation metrics, including accuracy, precision, recall, and F1-score, all of which reached 100% for ResNet-101. The confusion matrix confirmed the system's capability to classify all defect types flawlessly, with no misclassifications observed. Additionally, training and validation loss curves

indicated strong generalization and model stability, ensuring reliability in real-world deployment.

The proposed system was deployed in an industrially relevant setting, where unseen test samples were used to validate its robustness and feasibility in automated defect detection. Unlike traditional quality control methods, the CNN-based vision system, supported by a collaborative robot for automated positioning, achieves higher precision and eliminates variability associated with manual inspection. The robot-assisted framework also offers improved adaptability, supporting integration into modern smart manufacturing workflows.

Chapter 5. Robotic and Capacitive Sensing System for Thickness Inspection

5.1 Introduction

Traditional quality inspection methods in liquid spreading processes often involve destructive testing, manual inspections, or fixed vision-based techniques, which may lack the required flexibility, precision, or real-time adaptability [183, 184]. These limitations necessitate the development of an advanced, cost-effective, and non-destructive sensing approach capable of providing high-resolution measurements while maintaining efficiency in production environments.

This chapter presents a capacitive sensing and inspection framework for real-time quality control in liquid spreading applications, supported by a collaborative robot for automated sensor positioning. The proposed system integrates a high-resolution capacitive sensor with a collaborative robot (Cobot), specifically the UR10e, to enable automated and precise quality assessment. The integration of advanced calibration and data acquisition techniques ensures that the system can maintain consistent quality control under variable environmental conditions, capturing detailed voltage readings that correlate with liquid thickness.

A key contribution in this chapter is the application of linear regression analysis to predict liquid thickness, achieving a high R-squared value of 0.915 and a Mean Squared Error (MSE) of 0.00699. These metrics highlight the system's robust predictive capabilities, making it a reliable tool for industrial applications requiring real-time, accurate, and non-destructive inspections. To validate the effectiveness of the proposed approach, an industrial case study in collaboration with Unilever

company conducted. In addition to the first case study which is focused on spearding particular liquids that are produced in the company, another case study was designed to mock the coating on metal material to test the coating consistency and explore the feasibility of utilizing capacitive sensing technology in coating classification tasks.

Focusing on Unilever-sponsored case study, the system is deployed to inspect the uniformity of liquid spread on a skin mimic substrate, which is designed to replicate human skin properties for material testing purposes. Ensuring homogeneity in liquid application is essential in this sector to maintain product consistency and adherence to industry standards.

The second PhD case study will validate the integration of robotic system and capacitive sensing technology for in-process quality inspection in industrial coating applications. The objective is to utilize the sensing technology to distinguish between three types of coating:

- One layer of coating
- Two layers of coating
- Scrap or Scratch (Defect)

The results obtained from the first case study demonstrated the high accuracy and repeatability of the proposed system, underscoring its potential for broader implementation in manufacturing environments. Furthermore, this research contributes to the enhancement of Human-Robot Collaboration in quality control tasks by enabling human operators to participate in inspection processes. By leveraging human expertise in problem-solving and maintenance, the system fosters a more interactive and efficient approach to defect detection and production fault management.

This chapter is structured as follows: Section 2 provides an overview of existing quality control techniques and their limitations. Section 3 discusses the proposed HRC and sensing framework, including sensor selection, system architecture, and calibration techniques. Section 4 presents the experimental setup and methodology, followed by an in-depth analysis of the results in Section 5. Finally, Section 6 discusses key findings, implications for industrial applications, and potential future enhancements.

The primary objective of this study is to develop and validate the novelty of integrating capacitive sensing technology with collaborative robot, part of HRC system, to perform the in-process monitoring and inspection of liquid spreading applications in industrial environments. The following contributions refer specifically to the development and validation of the capacitive sensing subsystem and its robot-assisted implementation, independent of the vision system or the integrated HRC workflow:

- Development of a High-Resolution, Non-Destructive System: the paper presents a system that leverages the high resolution and accuracy of capacitive sensing technology combined with the precision and repeatability of collaborative robots. This system enables non-destructive, real-time monitoring of liquid uniformity, addressing challenges related to maintaining consistent dielectric properties and varying environmental conditions.
- Advanced Calibration and Data Acquisition Techniques: the research details the sophisticated calibration procedures for the CS1 capacitive sensor[185] to ensure accurate baseline measurements. The system

employs custom Python scripts for real-time data acquisition and analysis, capturing 200 readings per point. This enhances the reliability and validity of the collected data for assessing liquid spreading uniformity.

- Mathematical Modeling and Regression Analysis for Predictive Maintenance: the experimental work employs linear regression analysis to develop a mathematical model that describes the relationship between voltage readings and liquid spreading thickness. Validated through Mean Squared Error (MSE) and R-squared metrics, the model provides predictive maintenance capabilities, allowing for the early detection of inconsistencies in the liquid application process.
- Innovative Application of Dual-Dataset Approach for Quality Control Inspection: the research introduces a dual-dataset approach, collecting voltage readings before and after liquid spreading. This method allows for the detailed comparison and analysis of the liquid spreading process, facilitating the identification of pass/fail conditions for quality control.
- Implementation of a Comprehensive Experimental Setup: robust robot-assisted setup involving a Universal Robot UR10e and a capacitive sensing system. The collaborative robot is programmed to traverse predefined waypoints across the sample surface, enabling systematic coverage and spatially resolved thickness measurements. This configuration validates the system's capability to assess liquid spreading consistency over various substrate materials under both controlled and variable conditions.
- The second case study: To generalize the developed approach, a second case study has been initiated to further validate the proposed concept. This

approach is designed for application across various industrial sectors where quality control inspection is critical for improving efficiency, reducing waste, and minimizing the time and costs associated with reproduction processes. In particular, the second case study demonstrates how the integration of robotic and capacitive sensing technologies can be effectively employed for in-process quality inspection during coating applications—a crucial process in both the automotive and aerospace industries.

5.2 Capacitive Sensing Principles and Methodology

This section explains the principles of capacitive sensing for thickness measurement and its implementation in the proposed approach for inspecting non-conductive materials, such as liquid spread over a skin-mimic substrate. The utilization and analysis of sensor readings to determine the status of liquid spreading are discussed, followed by an outline of the design approach for integrating a collaborative robot (cobot) with the sensor. This includes understanding the system and detailing the cobot's movement sequence over the sample, along with sensor readings, to facilitate clear and efficient in-process quality control.

5.2.1 Capacitive Sensor Measurement principles

The underlying reasoning behind the utilization of capacitive sensors in this study diverges from conventional applications where capacitive sensing demonstrated accurate and reliable measurements in challenging working environments. Typically, capacitive sensors operate by measuring changes in capacitance C, defined as the ability of a system to store an electrical charge Q at a

given voltage V [186]. The capacitance C quantifies the effect of the electric field created between the two plates. Its value depends on three factors: the distance d between the plates, the surface area A of the plates, and the dielectric material situated between them. The dielectric material has a specific dielectric constant ε_0, which is crucial for calculating the capacitance of a capacitor given its geometric configuration [12][10][4].

$$C = \varepsilon_r \frac{\varepsilon_0 A}{d}$$

The CS1 capacitive sensor and the metal plate formed a capacitor separated by a dielectric medium. The capacitance of the formed capacitor will be changing based on the dielectric material between the capacitive sensor and the grounded metal plate. The dielectric material could be air, mimic skin material, liquid or a combination of three materials as shown in figure 5.1.

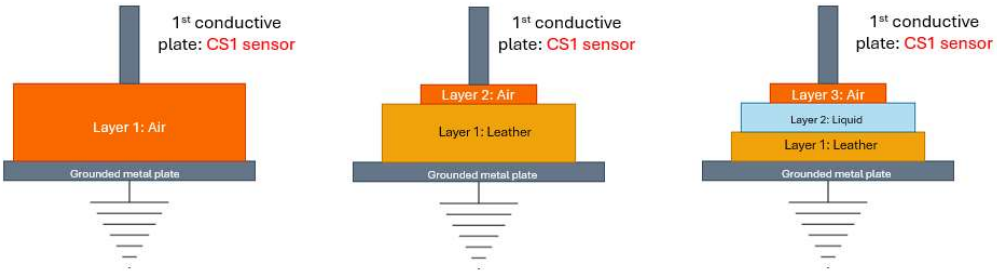

(a) (b) (C)

Figure 5.1. Schematic representation of the CS1 capacitive sensor with different dielectric material configurations. (a) A single-layer dielectric medium consisting of air. (b) A two-layer dielectric medium consisting of a combination of air and leather. (c) A three-layer dielectric medium composed of air, liquid, and leather.

As stated earlier, the capacitance will vary depending on the dielectric constant of the materials and the thickness of each material. So, maintaining a consistent dielectric constant for the examined materials is challenging, as environmental work conditions are not monitored. Additionally, the dielectric constant for a skin mimic substrate will change due to variations in material thickness and roughness from one position to another over the sample area, as the material is not rigid, and the surface is not even. The rigidity of the material surface would ensure a consistent thickness each time the liquid is wiped to repeat the test. Therefore, Therefore, these conditions present significant challenges in applying the ideal capacitance equation principle for accurately estimating the absolute liquid thickness across the sample area.

The objective is to inspect the liquid spreading over a skin-mimic substrate, where the liquid is not applied directly onto the metal sensing plate. Consequently, the uniformity of the spread is evaluated over a non-conductive material. It is therefore necessary to validate that the experimental setup and conditions conform to the principles of capacitive sensing measurement.

As a proof of concept, paper and polypropylene materials, characterized by fixed thicknesses and known dielectric constants, were used to measure the variation in capacitance resulting from incremental increases in the paper layer thickness over the polypropylene substrate. Typically, capacitance affects the voltage output inversely when the current I is constant.

Higher capacitance C results lower reactance X. From Ohm's law, for the given constant current I [12], Higher capacitance C results lower reactance X. From Ohm's law, for the given constant current I [187],

$$V_c = I \times X_c \tag{2}$$

$$X_c = \frac{1}{2\pi f C_{eq}} \tag{3}$$

where X_c is the capacitive reactance, f is the frequency of the AC signal, and C_{eq} is the total capacitance.

The total capacitance C_{eq} of two dielectric materials paper and polypropylene, connected in series, The calculation is as follows:

$$\frac{1}{C_{eq}} = \frac{1}{C_{\text{polypropylene}}} + \frac{1}{C_{paper}} \tag{4}$$

$$C_{\text{polypropylene}} = \varepsilon_{\text{polypropylene}} \times \frac{A}{d_{\text{polypropylene}}}$$

$$C_{paper} = \varepsilon_{paper} \times \frac{A}{d_{paper}}$$

$$C_{eq} = \frac{A \times \varepsilon_{\text{polypropylene}} \times \varepsilon_{paper}}{d_{\text{polypropylene}} \times \varepsilon_{paper} + d_{paper} \times \varepsilon_{\text{polypropylene}}} \tag{5}$$

Ideally, when measuring the change in capacitance between the sensor and the plate with only an air gap between them, the sensor is calibrated to produce a response of 1 volt per 100 microns. Table 5 and Figure 13 below illustrate the capacitance response for a single dielectric material (air) as well as for a combination of two dielectric materials (air and liquid) with varying liquid thicknesses.

This calibration ensures accurate baseline measurements. Different materials are inserted between the sensor and the plate causing the capacitance to increase due

to the varying dielectric properties of these materials. Consequently, the reactance decreases from (3). As a result, the sensor voltage drops when a constant current I is applied. This behavior is crucial for understanding the sensor's response to non-conductive materials. Table 5.1 outlines the specifications of the paper and polypropylene materials used in the simulation as non-conductive materials to test the consistency and reliability of the sensor output when the paper thickness increases over the polypropylene.

Table 5.1. Material specification [187].

Material type	Thickness d (µm)	Dielectric constant ε
Paper	117	2.0 to 3.0
Polypropylene	458	2.2 to 2.3

This proof of concept will justify the liquid spreading consistency check over the skin mimic substrate, which is the primary aim of this novel approach. As the CS1's functional range is up to 1 mm, one layer of polypropylene is fixed, and up to three layers of paper are added on top of the polypropylene. Table 5.2 describes how the capacitance changes against the increase of the paper layers thickness using (5). The measuring area of the sensor is: A = $63.62 \times 10^{-6} m^2$.

Table 5.2. Change in total capacitance against thickness

No. of Polypropylene layers	No. of Paper layers	Total no. of layers	Total Thickness d (µm)	Total Capacitance C_{eq} (F)
1	1	2	575	0.598
1	2	3	692	1.007
1	3	4	809	1.306

The experimental work presented in Table 5.3 validates how the voltage drops against the increase of the paper and polypropylene thicknesses. For instance, when one polypropylene layer is combined with two paper layers, the total thickness is measured at 0.000692 m, resulting in a total capacitance of 1.007 F and a sensor reading of 3.11 V.

Table 5.3. Experimental validation of measuring capacitance against voltage for non-conductive materials

No. of Polypropylene layers	No. of Paper layers	Summing Polypropylene and paper layers	Total Thickness (µm)	Actual thickness total (µm)	Total capacitance (F)	Sensor readings with layers (V)	Sensor readings with air gap (V)
1	1	2	575	578	0.598	2.79	5.76
1	2	3	692	690	1.007	3.11	6.87
1	3	4	809	800	1.306	3.45	8.17

In contrast, with three paper layers, the total thickness increases to 0.000809 m, leading to a higher capacitance of 1.306 F and a sensor reading of 3.45 V. A micrometre was employed to precisely measure the actual thickness of both the paper and the polypropylene layers as shown in figure 5.2.

(a) (b)

Figure 5.2 Measurement of material thickness using a digital micrometer. (a) Measurement of the thickness of a polypropylene layer, displaying a reading of 0.0458 mm. (b) Measurement of the combined thickness paper layer, showing a total thickness of 0.117 mm.

This ensures that the measurements of thickness are accurate and reliable, contributing to the validity of the experimental simulation results. The data collected from these experiments not only confirm the theoretical assumptions but also provide practical insights into the behavior of the sensor under varying conditions, especially measuring the liquid spreading consistency over the skin mimic substrate. Nonetheless, the scenario posited in this study presents some challenges to implementing standard measurement principles due to uncontrolled environmental conditions such as humidity, temperature and variations in the thickness and roughness of the skin mimic substrate. These factors lead to loss in the consistency of permittivity calculations, subsequently affecting capacitance readings. As an alternative, this research leverages the voltage readings derived from the sensor to glean insights into the test status. Novelty is to harness the high resolution, accuracy, and non-destructive measurement capabilities of capacitive sensing, alongside the Cobot's repeatability, precision, and flexibility, to monitor the uniformity of liquid spreading. This is achieved without direct reliance on material permittivity. Voltage readings are collected and catalogued into two datasets: one representing the pre-spreading and the other post-spreading conditions. These datasets will assess the uniformity of the liquid spread, enabling the operator to evaluate the spreading status as either pass or fail digitally.

5.2.2 Experiment Setup

The primary aim of the experimental work is to demonstrate the capability of the robot-assisted sensing system to assess the consistency of liquid spreading over a skin-mimic substrate. This is achieved by capturing voltage readings before and after spreading, targeting four predefined thickness levels: 15, 30, 60, and 90

microns. The tools and materials utilized in the experimental procedures are detailed as follows:

- Robotic part: Universal Robot UR10e, configured to move to the predefined waypoints through RoboDK as shown in figure 5.3.

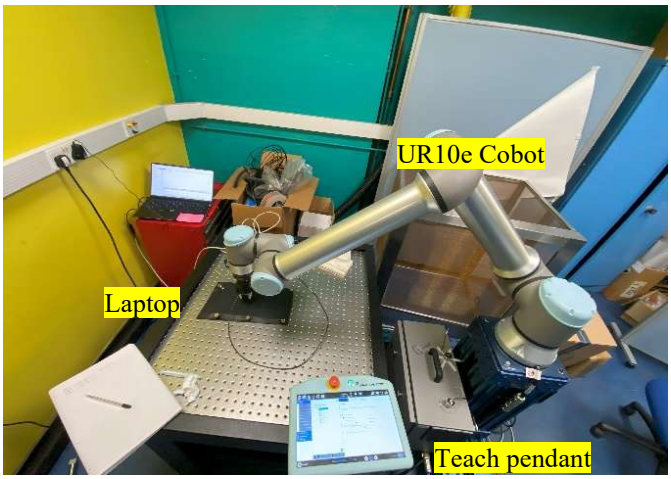

Figure 5.3. Robotic system utilized in the system

- Sensing part: IF1032 interface module, DT6110 controller[188] to produce an amplified voltage internally, Ethernet cable to connect the system to the laptop, and CS1 capacitive sensor, calibrated to 1 volt per 100 microns, in ideal conditions as shown in figure 5.4.

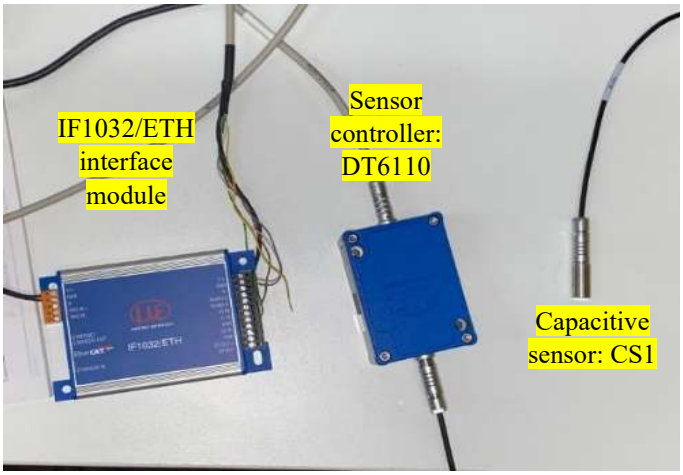

Figure 5.4. Sensing system utilized in the designed system

- Data Acquisition system: Custom Python script for data collection and analysis.
- Materials: skin mimic, magnets, syringe, spreading bar (TQC Sheen VF1500)[186] with four thicknesses, mounting clamp, testing liquid, and very flat surface plate used to fix the skin mimic substrate on and to act as a second conductive plate with the sensor.
- Power Supply: to provide necessary power for the Cobot and the sensor.
- Laptop: to control both the sensing and the robotic systems and process the collected data.
- Software: Python, RoboDK, Sensor Tool and Excel.

Figure 5.5 illustrates the method by which the skin mimic substrate is affixed to the metal plate, demonstrating the precise attachment mechanism. Additionally, it shows the configuration of the CS1 sensor, detailing how it is securely mounted to the Cobot's end effector via the custom-designed sensor holder.

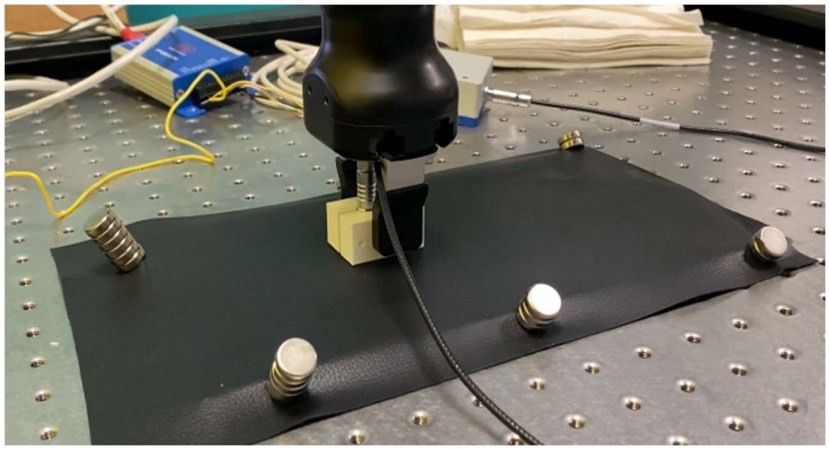

Figure 5.5. Experimental setup showing mimic skin material attachment and sensor integration

Figure 5.6 illustrates the full robot-assisted capacitive sensing system used for the inspection process. The Cobot and sensing system are connected to the laptop via Ethernet cables using a switch for proper IP communication.

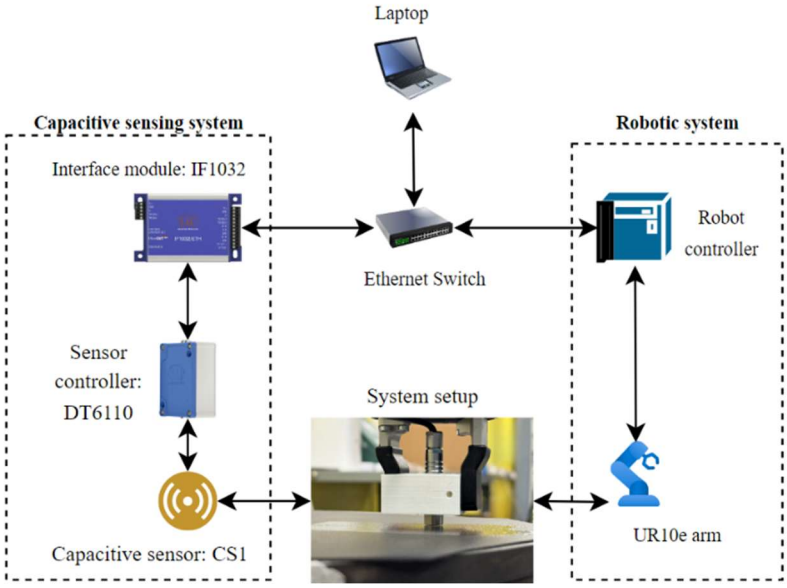

Figure 5.6. Robotic and sensing system structure

5.2.3 Experimental Protocol and Conditions

In this study, the UR10e cobot's repeatability specification of ±0.05 mm has direct implications for the experimental protocol, particularly when working with a capacitive sensor that operates within a 0–1 mm measurement range and exhibits a sensitivity of 1 V per 100 µm. At this level of precision, even small positional deviations can introduce measurable voltage variation.

Given that a ±0.05 mm positional shift corresponds to approximately ±50 µm, this translates to an expected fluctuation of ±0.5 V in the sensor output solely due to cobot positioning tolerances. Consequently, the repeatability of the UR10e forms a non-negligible source of measurement variability. However, because all scanning trajectories and approach paths were executed consistently using pre-defined waypoints, this positional uncertainty remained systematic rather than random. As a

result, its effect on the measurements is stable and predictable, allowing the regression model to absorb such deviations without compromising the comparative assessment of liquid spreading uniformity.

To ensure protocol robustness, all data acquisition sequences were repeated under identical motion commands, and the cobot's full-speed Cartesian approach was kept constant to minimise dynamic deviations. Thus, while UR10e's repeatability introduces a measurable baseline offset, it does not obstruct pattern detection, thickness differentiation, or the overall reliability of the capacitive sensing pipeline. Table 5.4 and figure 5.7 presents the collected data from the capacitive sensing system when an air gap between the sensor and the plate against when liquid is spread on the metal plate with four thicknesses.

Table 5.4.Output V readings of air and liquid as dielectric materials between the sensor and the metal plate

Distance d_t (mm)	**Voltage air V**	**Voltage liquid and air V**			
		15 μm	**30 μm**	**60 μm**	**90 μm**
0.5	5.03	4.71	4.65	4.52	4.26
0.6	6.03	5.71	5.63	5.52	5.26
0.7	7.06	6.71	6.66	6.52	6.25
0.8	8.06	7.71	7.66	7.52	7.23
0.9	9.06	8.74	8.66	8.52	8.23

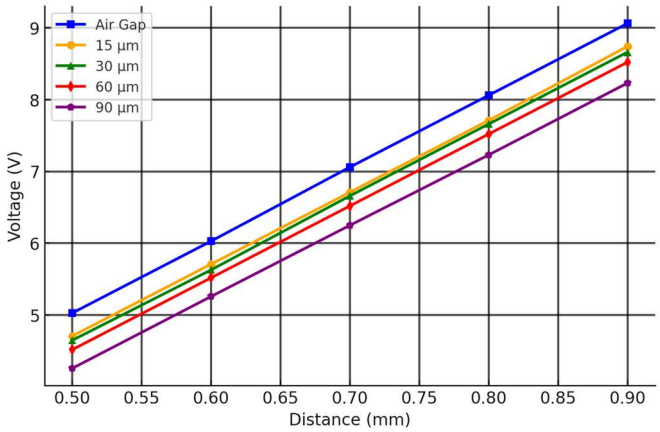

Figure 5.7. Voltage readings change when two layers of dielectric materials are positioned within the capacitor range

From Table 4.4, the collected readings indicated that having two dielectric materials between the sensor and the plate resulted in a voltage drop as a response to the increased capacitance. Additionally, at the same height of 0.5 mm, when the liquid thickness increased from 15 to 90 microns, the voltage dropped accordingly.

The voltage drop is not uniform due to material properties and environmental factors like temperature and humidity, which affect the dielectric constant. For example, at 30 µm thickness, voltage readings ranged from 5.3958 V (Position 1) to 5.4625 V (Position 5). Despite these variations, the aim is to differentiate between the four thicknesses and accurately identify the targeted liquid thickness. As shown in Table 8, the sensor provided consistent and repeatable readings, such as 5.6108 V at 60 µm (Position 1) and 5.6612 V at the same thickness (Position 5).

Spreading the liquid over the skin mimic is the main part of this conducted research. The experiment is conducted in an area of 70 mm by 70 mm square, over which the Cobot is meticulously programmed to traverse 9 waypoints for data acquisition, as shown in figure 5.8.

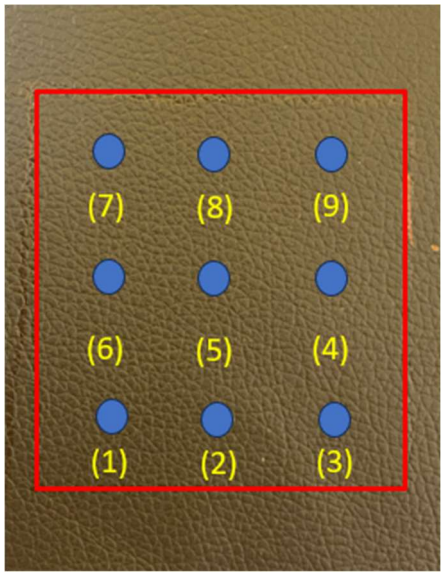

Figure 5.8. A set of waypoints where the Cobot is assigned to move over

The waypoints are strategically placed as 35 mm between each adjacent point on X and Y axes to ensure the comprehensive coverage of the sample area, enabling a detailed analysis of the surface treatment's consistency. Table 5.5. demonstrates the waypoints coordinates that are being assigned to the Cobot to move over the sample.

Table 5.5. Waypoint coordinates assigned to the cobot to move on using RoboDK.

Way point	X (mm)	Y(mm)	Z(mm)
1	-460	-105	24.7
2	-460	-140	24.62
3	-460	-175	24.72
4	-425	-105	24.76
5	-425	-140	24.76
6	-425	-175	24.76
7	-390	-105	25.07
8	-390	-140	24.97
9	-390	-175	24.88

It is important to note that the Z values are assigned based on the sensor being calibrated to 10 V above each waypoint, which means that before spreading, the sensor readings are at 10 V. The standard deviation between the Z values indicates that the skin mimic surface is not uniformly flat across all points, with a standard deviation of 0.142 among the 9 waypoints. The experimental waypoints are configured to enable the CS1 sensor to conduct voltage measurements across the sample area in two separate instances. The sensor is allocated 3.5 seconds at each waypoint, divided into a 0.5-second stabilization period to ensure the cobot's positional stability, followed by a 3-second data acquisition period, during which data is transferred in real-time to a CSV file for subsequent analysis in Excel. During this period, 200 readings are collected per point. This dual-measurement approach, capturing both pre-spreading and post-spreading data sets, facilitates the evaluation of the liquid's spreading uniformity. Variations in voltage readings are expected to

correlate with the applied liquid thicknesses. These variations can be analyzed to derive a differential voltage data set across waypoints. To ensure robustness, the experiment will be replicated three times for each thickness level, providing a substantial data set for developing a quality control methodology.

5.2.4 Mathematical Model Development

Linear regression analysis is implemented in this unique experimental work to mathematically describe the relation between the voltage (dependent variable) and liquid spreading thickness (independent variable) over the skin mimic [189].

$$Y = b_0 + b_1 \cdot X, \tag{6}$$

Where,

Y is the voltage readings (dependent variable),

X is the liquid thickness (independent variable),

b_0 is the intercept term (voltage when the thickness is zero),

b_1 is the slope coefficient (change in Y for a one-unit change in X).

Both intercept and slope coefficients are derived as follows

$$b_1 = \frac{\sum(X - \bar{X})(Y - \bar{Y})}{\sum(X - \bar{X})^2} \tag{7}$$

and

$$b_0 = \bar{Y} - b_1\bar{X} \tag{8}$$

where $\bar{Y}$ is the mean of Y values (voltage readings), and $\bar{X}$ is the mean of X values (thickness); The development of a mathematical model for the conducted work enables the prediction of material thickness based on the collected voltage readings. The mathematical model efficiency is evaluated by calculating R-squared.

An ideal regression behavior is indicated when the value of R-squared is close to one. R-squared measures the proportion of the variance in the dependent variable that is predictable from the independent variable(s). It is calculated as:

$$R^2 = 1 - \frac{\sum(Y_i - \hat{Y})^2}{\sum(Y_i - \bar{Y})^2} \quad (9)$$

Where $\hat{Y}$ is the predicted value of Y.

5.3 Experimental Finding and Results

5.3.1 Liquid Spreading Statistical Findings

Experimental findings for the liquid spreading over the skin mimic substrate outline the voltage difference per thickness. As mentioned earlier, the sensor is programmed to capture 200 readings per point, pre spreading and after spreading. In total, A total of 3600 readings is obtained for one cycle, with the test repeated three times for each thickness to ensure consistency and repeatability. The average readings of 9 waypoints are calculated per point. Table 5.6 provides the summary of the voltage readings for the thickness range of testing liquid spread over the skin mimic substrate.

Table 5.6. Voltage Readings Summary of Testing Liquid Spreading Over Mimic Skin Material

Position	Voltage Readings -15 μm	Voltage Readings -30 μm	Voltage Readings -60 μm	Voltage Readings -90 μm
1	5.0276	5.3958	5.6108	5.8198
2	5.2210	5.4271	5.6208	5.8828
3	4.9739	5.3174	5.6367	5.8330
4	5.2061	5.3706	5.7472	5.9690
5	5.2627	5.4625	5.6612	5.9212
6	5.1917	5.4300	5.6596	5.8864
7	5.0061	5.4316	5.6061	5.7979
8	5.1153	5.3539	5.6578	5.8761
9	5.1850	5.4339	5.7377	5.9367

These results are unique for a specific type of testing liquid. This experimental concept can be adopted for further liquid types and identify new custom criteria that can be used for testing. Figure 5.9 presents the main experimental work result in inspecting the liquid spreading consistency and identifying the targeted thickness.

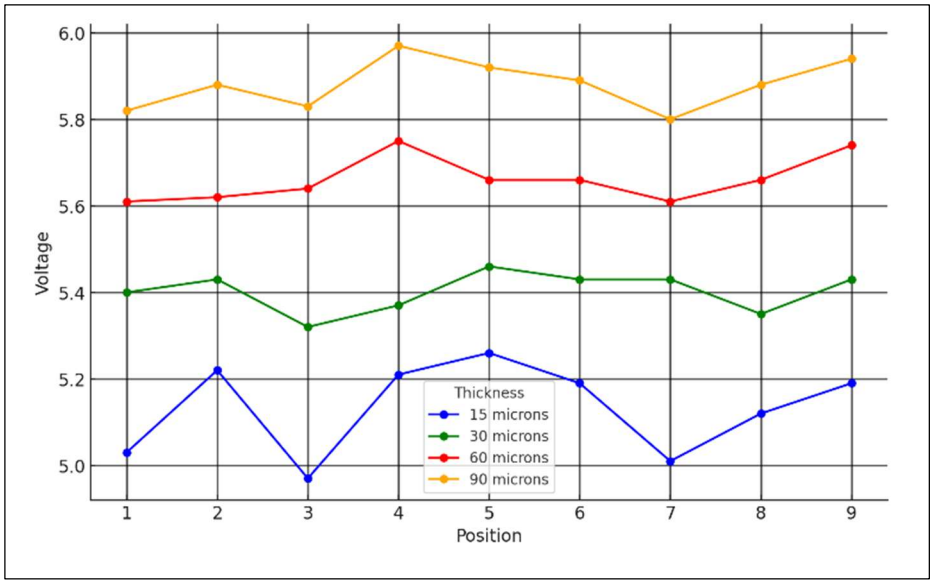

Figure 5.9. Experimental work results. voltage readings against way points.

Every targeted thickness has a unique voltage range and voltage average. These two key factors are considered as identifiers that can be utilized to measure the testing liquid spreading consistency. Table 5.7 outlines the results for the key factors per thickness.

Table 5.7. Key features for liquid spreading consistency identification

Variable	15 μm	30 μm	60 μm	90 μm
Voltage Readings Range	Min: 4.97 Max: 5.26	Min: 5.32 Max: 5.46	Min: 5.61 Max: 5.75	Min: 5.80 Max: 5.97
Voltage Difference Average	5.13	5.40	5.66	5.88

5.3.2 Regression Analysis and Validation Results

To derive the mathematical model describing the relationship between the voltage readings and the liquid spreading thickness, the coefficients b_1 and b_0 from (7) and (8) must be determined. The first step involves calculating the mean values of the voltage and thickness, as expressed in the following equations:

$$\bar{X} = \frac{\sum x_i}{N} = \frac{195}{4} = 48.75$$

N denotes the number of target thickness levels considered in the analysis,

$$\bar{Y} = \frac{\sum y_i}{N} = \frac{198.96}{36} = 5.5267$$

N denotes the number of waypoints defined for each thickness level (N = 9 x 4 = 36).

The required summations are then calculated as follows:

$$\sum (X - \bar{X})(Y - \bar{Y}) =$$

$$\sum (X - 48.75)(Y - 5.5267) = 160.2375$$

$$\sum (X - \bar{X})^2 = \sum (X - 48.75)^2 = 16903.125$$

Substituting in (7) and (8)

$$\frac{\sum (X - \bar{X})(Y - \bar{Y})}{\sum (X - \bar{X})^2} = \frac{160.2375}{16903.125} = 0.0095$$

$$b_0 = \bar{Y} - b_1 \bar{X} =$$

$$5.5267 - (0.0095 \times 48.75) =$$

$5.5267 - 0.463125 = 5.063575$

Thus, from (6) the regression equation is:

$$Y = 0.0095 \cdot X + 5.063575 \qquad (10)$$

Using the regression equation, the predicted voltage values $\hat{Y}$ for given thicknesses are calculated by substituting in (10) as shown in Table 5.8.

Table 5.8. Predicted Voltage Values (Y^) For Different Material Thicknesses Using the Linear Regression Equation.

Thickness (microns)	**Predicted voltage ($\widehat{Y}$)**
15	5.206325
30	5.351075
60	5.640
90	5.930075

To measure the efficiency of the derived model from (10) for the conducted experimental work, the Mean Squared Error (MSE) and R-squared are calculated using actual voltage readings Y, predicted voltage readings $\hat{Y}$ and mean voltage readings $\bar{Y} = 5.5267$. Conducted calculations are outlined in Table 5.9.

Table 5.9. Actual and predicted voltage readings calculations to determine the efficiency of the regression mathematical model used to describe the system behavior of liquid spreading inspection

Thickness	**15 microns**			**30 microns**			**60 microns**			**90 microns**		
Position	Y	$Y-\widehat{Y}$	$(Y-\widehat{Y})^2$	Y	$Y-\widehat{Y}$	$(Y-\widehat{Y})^2$	Y	$Y-\widehat{Y}$	$(Y-\widehat{Y})^2$	Y	$Y-\widehat{Y}$	$(Y-\widehat{Y})^2$
1	5.0276	-0.1787	0.03194	5.3958	0.0447	0.00200	5.6108	-0.0298	0.00089	5.8198	-0.1103	0.01216
2	5.2210	0.0147	0.00022	5.4271	0.0760	0.00578	5.6208	-0.0197	0.00039	5.8828	-0.0473	0.00223
3	4.9739	-0.2325	0.05404	5.3174	-0.0337	0.00113	5.6367	-0.0039	0.00002	5.8330	-0.0971	0.00942
4	5.2061	-0.0002	0.00000	5.3706	0.0196	0.00038	5.7472	0.1067	0.01138	5.9690	0.0389	0.00152
5	5.2627	0.0564	0.00318	5.4625	0.1114	0.01240	5.6612	0.0206	0.00043	5.9212	-0.0088	0.00008
6	5.1917	-0.0146	0.00021	5.4300	0.0789	0.00623	5.6596	0.0191	0.00036	5.8864	-0.0437	0.00191
7	5.0061	-0.2002	0.04009	5.4316	0.0805	0.00648	5.6061	-0.0345	0.00119	5.7979	-0.1321	0.01746
8	5.1153	-0.0910	0.00828	5.3539	0.0028	0.00001	5.6578	0.0172	0.00030	5.8761	-0.0540	0.00292
9	5.1850	-0.0213	0.00045	5.4339	0.0828	0.00686	5.7377	0.0972	0.00944	5.9367	0.0066	0.00004

From Table 4.9, MSE and R-squared of the regression analysis are computed after calculating the summation of $(\boldsymbol{Y} - \widehat{\boldsymbol{Y}})^{\boldsymbol{2}}$ for the four targeted thicknesses as presented in Table 5.10.

Table 5.10. The squared summations of the difference between actual and predicted voltage values for the four thicknesses

Thickness (microns)	$\sum(\boldsymbol{Y} - \widehat{\boldsymbol{Y}})^{\boldsymbol{2}}$
15	0.13841
30	0.04128
60	0.02432
90	0.04774

Substituting the squared summations of the difference between actual and predicted voltage values for the four thicknesses set in (11),

$$\text{MSE} = \frac{1}{N}\sum(Y - \hat{Y})^2 \tag{11}$$

$$\text{MSE} = \frac{0.25182}{36} = 0.00699$$

Also, the summation of the squared difference between the actual voltage readings and the mean voltage is calculated as follows:

$$\sum(Y - \bar{Y})^2 = 2.977$$

So,

$$R^2 = 1 - \frac{\sum\left(Y_i - \hat{Y}\right)^2}{\sum(Y_i - \bar{Y})^2} = 1 - \frac{0.25182}{2.977} = 0.915$$

Both the MSE and R-squared metrics demonstrate the model's robustness and predictive capability.

In figure 5.10, the result of the regression analysis is presented using a scatterplot of the voltage against the thickness.

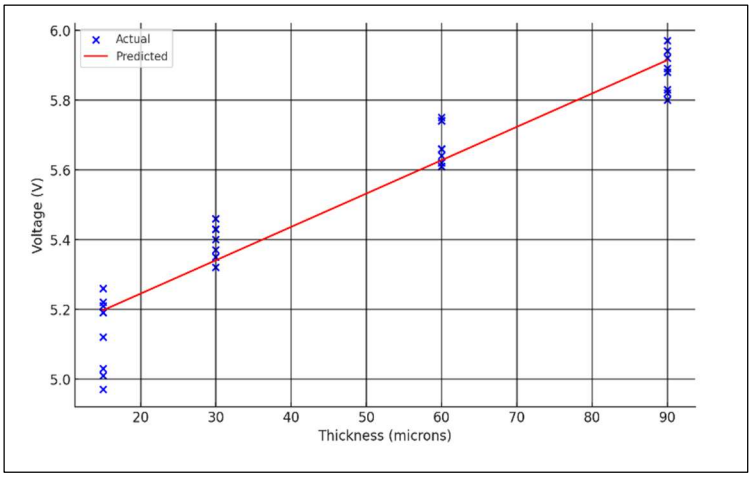

Figure 5.10. Regression fit showing the relationship between thickness and voltage.

5.3.3 Coating Inspection case Study

To generalize the developed approach, which integrates robotic and capacitive sensing technologies in collaboration with a human operator, a second case study has been initiated to further validate the proposed concept. This approach is designed for application across various industrial sectors where quality control inspection is critical for improving efficiency, reducing waste, and minimizing the time and costs associated with reproduction processes. In particular, the second case study demonstrates how the integration of robotic and capacitive sensing technologies can be effectively employed for in-process quality inspection during coating applications—a crucial process in both the automotive and aerospace industries.

5.3.4 Proposed Methodology

Given that the coating process is applied to car bodies, the proposed approach is validated by measuring coating consistency both prior to and following the application of the coating.

- The metal plate was segmented into evenly distributed areas to define 12 waypoints for the cobot. Four inspection classes were established for evaluation using the proposed approach. As illustrated infigure 5.11, the the metal plate was partitioned into equal-sized squares.

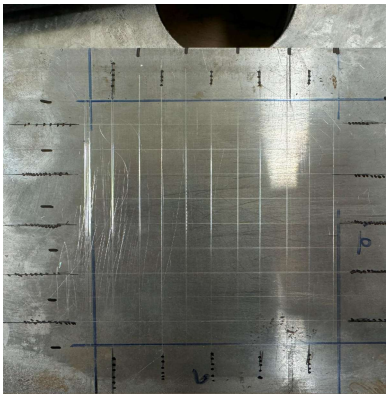

Figure 5.11. Grid Division of the Metal Plate.

- Now, the sensor is calibrated before coating at 10V over the 12 waypoints as shown in figure 5.12.

Figure 5.12. Sensor calibration over the sample area before coating.

- After the sensor calibration is successfully performed, the metal plate is coated. Four classes over the metal plate were identified to be inspected as shown in figure 5.13.

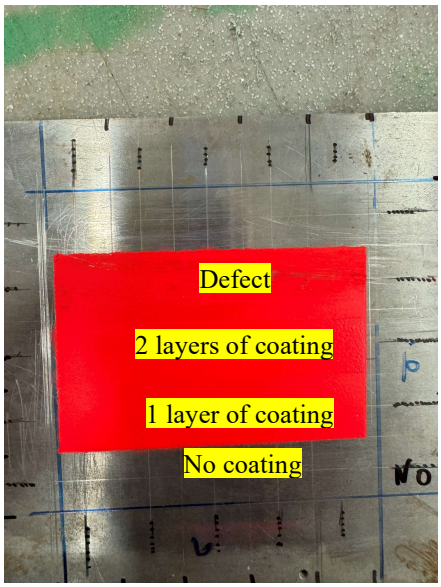

Figure 5.13. Coating Area on a Metal Plate

- For each class, three waypoints were designated for inspection using the sensor, as illustrated in figure 5.14.

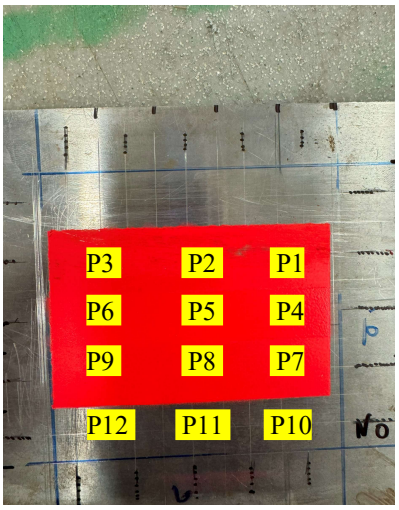

Figure 5.14. Measurement Points on the Coated Plate. The figure shows designated sensor points (P1–P12) for coating evaluation

- The Cobot is programmed to move over each point. The duration as discussed in the first case study is decided to be 3.5 second. So, the cobot will take 0.5 second to settle, and then 3 seconds to measure the thickness.

5.3.5 Results

The experimental evaluation was conducted without predefined coating standards or reference measurements. This case study investigates the feasibility of a robot-assisted capacitive sensing system for real-time, in-process coating inspection, targeting operational applicability within complex manufacturing environments. The acquired voltage data, demonstrate a direct correlation between coating thickness and voltage reading across four distinct coating classifications: scrab (defective coating), over-coating (two layers), good coating (one layer), and no coating presented in Table 5.11 and figure 5.15.

Table 5.11. Voltage measurements at different positions, comparing coating types based on the recorded differences before and after coating

Coating Type	Position	Voltage before Coating	Voltage after Coating	Difference
Scrab (Defect)	P1	10	9.85	0.15
	P2	10	9.93	0.07
	P3	10	9.83	0.17
2 Layers (Over Coating)	P4	10	9.56	0.44
	P5	10	9.56	0.44
	P6	10	9.58	0.42
1 Layer (Good)	P7	10	9.78	0.22
	P8	10	9.77	0.23
	P9	10	9.75	0.25
No Coating	P10	10	9.9	0.1
	P11	10	9.9	0.1
	P12	10	9.9	0.1

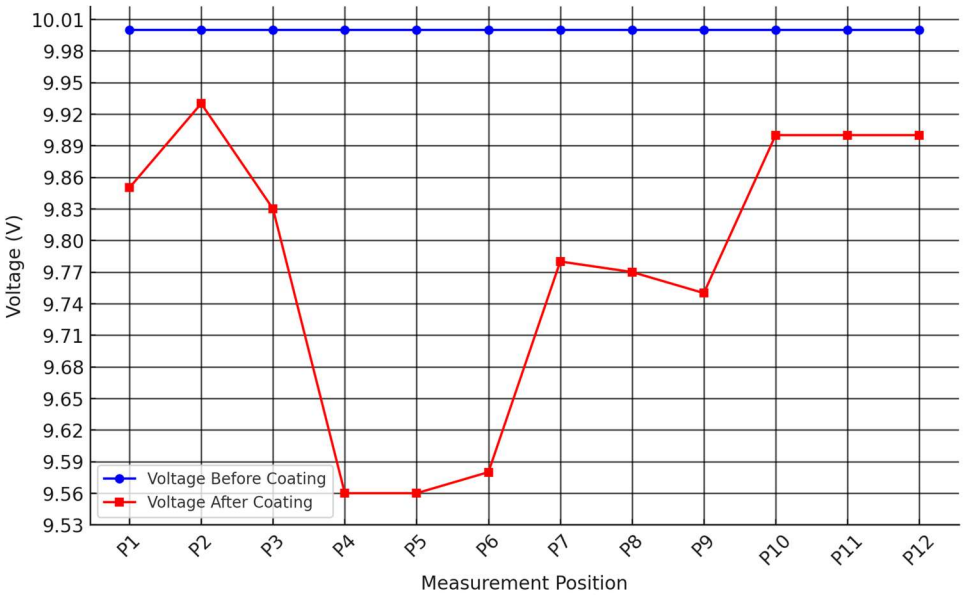

Figure 5.15. Voltage before and after coating, highlighting the correlation between coating thickness and voltage drop, with over-coated areas showing the highest reduction and uncoated regions the least

Uncoated regions exhibited minimal voltage deviations of 0.1V, indicating negligible surface modification. In contrast, defective coatings displayed slight variations, with voltage differences ranging from 0.07V to 0.17V, while good coatings (one layer) resulted in moderate deviations between 0.22V and 0.25V. Over-coated areas (two layers) exhibited the most significant variations, with differences reaching up to 0.44V, indicating excessive material deposition. The consistency of voltage measurements within each coating classification confirms the repeatability and reliability of the sensing system in distinguishing different coating conditions. These findings highlight the potential of the proposed approach for automated and non-destructive coating assessment in industrial applications.

5.4 Summary

In this chapter, a capacitive sensing system supported by a collaborative robot for automated sensor positioning has been developed and evaluated for in-process quality inspection of liquid spreading and coating applications. The primary objective was to design a non-destructive, real-time, and high-resolution inspection framework that leverages capacitive sensing technology in combination with a collaborative robotic system (UR10e) to enhance quality control in industrial environments.

Initially, existing quality inspection techniques and their limitations were reviewed, highlighting challenges related to environmental dependencies, manual inspections, and the need for high-precision, real-time assessment methodologies. To address these challenges, the proposed system was designed to integrate advanced calibration techniques, data acquisition frameworks, and regression-based predictive modeling for accurate thickness measurement and defect detection.

The capacitive sensing mechanism was rigorously analyzed, focusing on its ability to measure dielectric variations corresponding to liquid thickness. A proof-of-concept study demonstrated that the capacitive sensor exhibited consistent and repeatable voltage responses, correlating capacitance changes to variations in liquid thickness. The experimental setup validated the sensor's capability to distinguish between different material configurations and provided key insights into the challenges posed by environmental factors such as humidity, temperature fluctuations, and substrate surface irregularities.

To quantify the system's performance, a linear regression model was employed to predict liquid thickness based on voltage readings, yielding an R-squared value of

0.915 and a Mean Squared Error (MSE) of 0.00699, signifying high predictive accuracy. Furthermore, the dual-dataset approach implemented in this research enabled effective differentiation between pre-spreading and post-spreading conditions, establishing a robust methodology for pass/fail classification in industrial inspection processes.

Experimental validation was conducted in collaboration with Unilever, wherein the system was deployed for real-time inspection of liquid spreading on a skin-mimic substrate, simulating industrial product application processes. The obtained results confirmed the repeatability and robustness of the proposed sensing system, reinforcing its potential for large-scale manufacturing environments. The integration of robotic automation with capacitive sensing demonstrated significant advancements in Human-Robot Collaboration (HRC), enabling operators to engage in inspection supervision, defect analysis, and decision-making.

A secondary industrial case study was introduced to evaluate the feasibility of the developed system in coating quality assessment applications, particularly for defect detection and classification of coating layers. Experimental results showed that the capacitive sensing system was able to differentiate between defective coatings, single-layer coatings, and over-coated surfaces, based on characteristic voltage variations. This confirms the system's suitability for automated in-process inspection in high-precision applications such as automotive and aerospace industries.

In summary, the proposed robotic and capacitive sensing framework has demonstrated a high degree of accuracy, reliability, and adaptability in liquid spreading and coating quality control applications. Future enhancements may include

the integration of machine learning techniques for real-time defect classification, expansion of the sensing framework to accommodate multi-layered material structures, and further refinement of environmental compensation models to enhance robustness under diverse industrial conditions. The contributions of this research pave the way for next-generation, AI-driven, real-time quality inspection systems, promoting efficiency, reducing waste, and enhancing production consistency in automated manufacturing environments.

Chapter 6. Human-Robot Collaborative, Vision and Capacitive Sensing System

6.1 Introduction

This chapter presents an innovative approach to in-process quality control inspection in manufacturing, leveraging the integration of Human-Robot Collaboration (HRC), vision systems, and capacitive sensing technologies. These advanced technologies collectively enhance production processes by enabling consistent, efficient, and real-time quality control during manufacturing. Addressing critical challenges such as liquid spreading uniformity and coating quality, this approach has the potential to transform industrial practices, particularly in high-precision sectors like automotive and aerospace.

Effective quality control is essential in industries where coating and painting processes not only serve aesthetic purposes but also ensure the durability and functionality of products. Uniform application of coatings is vital to protect the external surfaces of vehicles and machinery [190-192]. However, conventional methods face challenges in ensuring even application, as issues such as liquid spreading irregularities or coating non-uniformity can significantly degrade product quality. Furthermore, traditional inspection methods often rely on post-production testing, which is time-consuming and reactive, leading to production delays and increased costs. These challenges highlight the need for innovative solutions capable of real-time, in-process quality control.

The integration of cutting-edge technologies—HRC, capacitive sensing, and CNN-based vision systems—offers a promising solution. The flexibility, accuracy,

and repeatability of collaborative robots (cobots) facilitate seamless automation of repetitive tasks. At the same time, capacitive sensing and vision systems provide complementary inspection capabilities: the former for precise thickness measurements and the latter for surface classification. This synergistic integration ensures timely detection and resolution of defects, minimizing downtime and enhancing process efficiency.

6.1.1 Novelty and Key Contributions

This section outlines the novelty and key contributions of the proposed human-robot collaborative quality control framework. The system combines collaborative robotics, capacitive sensing, and convolutional neural network (CNN)-based machine vision to address long-standing challenges in in-process quality inspection—particularly in coating and liquid spreading operations.

Unlike conventional methods that depend solely on manual inspection or fully automated systems, the proposed solution integrates real-time sensing, classification, and robotic execution within a closed-loop inspection environment. Collaborative robots (Cobots) offer the precision and repeatability needed for consistent motion handling, while capacitive sensing—traditionally used in fluid-level monitoring—is repurposed here for non-contact, micron-scale thickness measurement. At the same time, a tailored implementation of ResNet101 enables robust surface state classification. This approach ensures high inspection accuracy and real-time responsiveness, even in variable production environments.

The following contributions refer to the fully integrated HRC-QC system, where the sensing subsystem, the vision subsystem, and the collaborative workflow are combined into a unified multimodal inspection framework:

- **Robot-Assisted Real-Time Inspection Framework:** Developed and validated a system that combines collaborative robotics (UR10e for automated sensor and camera positioning), CNN-based vision (ResNet-101), and capacitive sensing to enable real-time, in-process inspection of liquid spreading quality.
- **Capacitive sensing for micron-scale thickness assessment:** Proposed a novel use of capacitive sensors to non-destructively measure liquid film thickness during spreading, achieving sensitivity suitable for detecting micro-level coating inconsistencies.
- **Human-in-the-loop data labeling strategy:** Designed a labeling approach where human operators utilize both sensor readings and visual inspection to generate high-accuracy ground truth datasets for training the CNN model.
- **Sensor–vision fusion for enhanced defect detection:** Demonstrated a multi-modal inspection pipeline in which capacitive sensor data is used to cross-validate vision-based classification, reducing classification ambiguity and increasing robustness under varied lighting and surface conditions.
- **Customized ResNet101 classification model:** Adapted and trained the ResNet101 architecture to classify spreading states

("Full," "Fault," "Empty") with high accuracy, achieving robust performance despite visual noise and variation.

- **Human-Robot Collaboration in quality control implementation**: Implemented a collaborative setup where cobots execute repeatable inspection motions, while human operators intervene only for system supervision, maintenance, and error handling — enhancing inspection consistency and human-machine synergy.

Collectively, these contributions offer a scalable and adaptable solution to the limitations of conventional inspection techniques. The system was validated through a two-year industrial case study in collaboration with Unilever, demonstrating its effectiveness in detecting coating defects, maintaining process uniformity, and reducing downtime. This validation highlights the potential of the proposed approach to advance quality assurance practices in smart manufacturing environments.

6.2 Approach

6.2.1 Problem Identification

The primary challenge addressed by this research is the need for in-process quality control inspections in manufacturing environments, particularly within the automotive and aerospace sectors, where coating and liquid spreading processes play a crucial role. Ensuring uniformity and precision in these processes is essential to maintain production standards and avoid defects [193, 194]. Traditional post-production inspection methods are insufficient to meet the real-time quality demands of modern manufacturing industries. In-process inspection, enabled through Human-Robot Collaboration (HRC), computer vision, and sensing technologies, provides a more responsive and adaptive solution [195].

One of the key challenges in these sectors is achieving uniformity in coating and liquid spreading. Variations in film thickness and surface coverage can introduce defects that compromise both the aesthetic and functional quality of the final product. The proposed robot-assisted approach addresses this challenge by performing inspection during production, allowing for immediate detection and correction of faults. This minimizes delays, reduces rework, and enhances overall process efficiency.

Key areas targeted for inspection include the uniformity of the coating as an application of applying protective or functional film on substrate, and the consistency of liquid spreading which can be part of the coating process where liquid is initially covering areas across surfaces. Two main parameters are critical for inspecting the quality of the coating or liquid spreading processes: the thickness of the coating and the surface quality after application. The case study with Unilever, discussed later in this chapter, outlines specific measurements that are used to assess the liquid spreading uniformity. The voltage readings before and after spreading the liquid are utilized mainly to measure the quality of the liquid spreading over the substrate. This is further detailed in Chapter 4, where the subsystem integrating capacitive sensing and robotic technologies is described.

Additionally, surface uniformity is evaluated using a vision system combined with Convolutional Neural Networks (CNN). The system classifies captured images into three categories: *Full*, *Fault*, and *Empty*, enabling the real-time assessment of the coating's quality. Voltage readings obtained while measuring the thickness of the liquid are utilized to identify the spreading status. Simultaneously, utilizing a trained ResNet-101 model will visually assess the spreading status and provide information

to indicate the spreading class.This classification process is vital in determining whether the application meets the required standards and addressing any defects during production. Through this methodology, the research addresses a critical gap in real-time quality control for coating and liquid spreading, which current autonomous systems rarely tackle. By integrating robotics, advanced sensing, and vision systems with human expertise, this study develops a flexible solution to ensure uniform coatings while reducing time, waste, and human effort. This approach bridges the gap between advanced technology and its application in complex industrial QC tasks, contributing to both scientific progress and industrial efficiency.

6.2.2 Task Selection and Allocation

The inspection process in this research involves various interconnected operations performed collaboratively by the human operator, the collaborative robot (cobot), the capacitive sensing system, and the vision system. The design of the task allocation is critical to ensure that each resource contributes effectively to the overall process.

To achieve this, tasks were carefully distributed based on the unique capabilities of each resource:

- Cobot: Handles repetitive and precise tasks such as moving to defined waypoints and stabilizing for accurate measurements.
- Vision System: Captures images at specific waypoint for surface assessment and classifies the status of liquid spreading (full, fault, or empty).

- Capacitive Sensing System: Measures the liquid thickness at nine predefined waypoints, ensuring uniformity and compliance with production standards.
- Human Operator: Oversees the process, calibrates the setup, evaluates results from the sensing and vision systems, and performs necessary maintenance tasks and addressing equipment issues.

The breakdown of the tasks and their allocation to each resource is summarized in Table 6.1. This table details the specific jobs, tasks, operations, and corresponding resources involved in the inspection process. The allocation is designed to maximize efficiency and accuracy while ensuring smooth collaboration between humans and machines.

Table 6.1. This table outlines the distribution of jobs, tasks, and specific operations among various resources, including the collaborative robot, vision system, sensing system, and human operator. Each resource's role is optimized to ensure accurate and efficient inspection of liquid spreading and coating uniformity.

Job	Task	Operation	Resource
In-process Quality Control	Prepare Inspection Cell	Move inspection cell into position	Human Operator
		Perform initial calibration based on production needs	Human Operator
		Set cobot to home position	Cobot (UR10e)
Pre-Coating Inspection	Vision System Setup	Move cobot to waypoint 1	Cobot (UR10e)
Pre-Coating Inspection	Vision System Setup	Capture pre-coating image	Vision System (Webcam 920/720 HD)
Pre-Coating Inspection	Scanning	Move cobot to 9 waypoints	Cobot (UR10e)
Pre-Coating Inspection	Scanning	Stabilize cobot for 0.5 seconds	Cobot (UR10e)
Pre-Coating Inspection	Scanning	Measure surface data for 3 seconds at each waypoint	Capacitive Sensor (CS1, DT6110, IF1032)

Pre-Coating Inspection	Scanning	Move cobot to home position after each waypoint	Cobot (UR10e)
Spreading/Coating	Perform Liquid Spreading	Activate liquid spreader (manual or automated)	Liquid Spreader
Post-Coating Inspection	Scanning and Data Collection	Repeat cobot motion to 9 waypoints	Cobot (UR10e)
Post-Coating Inspection	Scanning and Data Collection	Stabilize cobot for 0.5 seconds	Cobot (UR10e)
Post-Coating Inspection	Scanning and Data Collection	Measure surface data for 3 seconds at each waypoint	Capacitive Sensor (CS1, DT6110, IF1032)
Post-Coating Inspection	Scanning and Data Collection	Move cobot to home position after each waypoint	Cobot (UR10e)
Post-Coating Inspection	Image Classification	Capture post-coating images	Vision System (Webcam 920/720 HD)
Result Analysis	Visualize and Assess Results	Display sensor voltage readings (9-waypoints)	Laptop
Result Analysis	Visualize and Assess Results	Display classification outputs (full/fault/empty)	Laptop
Result Analysis	Evaluate results and decide next actions		Human Operator
Maintenance	Ensure Setup Functionality	Refill liquid if empty	Human Operator
Maintenance	Ensure Setup Functionality	Inspect for damage to substrate or system	Human Operator
Maintenance	Ensure Setup Functionality	Clean surface using paper tissue	Human Operator
Safety Measures	Ensure Safe Operation	Monitor cobot movement in safe zone	Human Operator & Emergency Stop Button
Safety Measures	Ensure Safe Operation	Wear protective eyewear	Human Operator

6.2.3 Work Environment Design

The design of the inspection cell is central to the successful integration of human-robot collaboration (HRC), vision, and sensing technologies for in-process

quality control. This section outlines the physical layout, accessibility features, safety measures, ergonomic considerations, and environmental factors of the inspection cell, highlighting how these elements contribute to its functionality and adaptability.

The inspection cell is configured in a university laboratory environment to simulate real-world manufacturing conditions. The core components include a collaborative robot (cobot), a capacitive sensing system, a vision system, and a fixed inspection plate. The cobot is positioned adjacent to the inspection plate, where the mimic substrate is affixed for testing purposes. Both the capacitive sensor and the vision system are mounted on the cobot's end effector, enabling seamless integration for surface scanning and image capture tasks. This compact design ensures precise synchronization between the sensing and vision functionalities while minimizing the footprint of the cell.

The Cobot itself is mounted on a mobile base equipped with wheels, making the system modular and flexible. This mobility allows the inspection cell to be repositioned easily, accommodating diverse workspace layouts or evolving operational requirements. Such flexibility ensures the setup can be adapted to different industrial environments without significant reconfiguration. Figure 6.1 presents how the Cobot is directed to the inspection area where the mimic material is positioned on a metal plate.

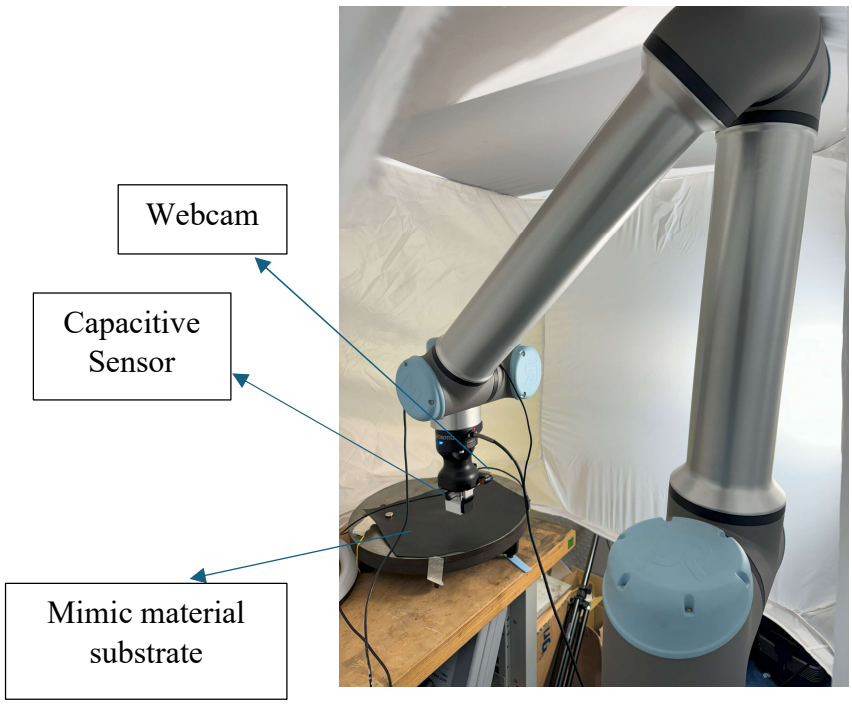

Figure 6.1. representation of the inspection cell layout, showing the positions of the cobot, vision system, sensing system, and inspection plate.

Accessibility has been prioritized to ensure ease of operation and maintenance. The Cobot's mobility allows it to be positioned optimally within the workspace, and its components are mounted at waist height to facilitate ergonomic interaction. This design simplifies key tasks, such as system calibration and hardware maintenance, reducing the physical strain on the operator. For example, the operator can adjust the capacitive sensing system and the vision system on the cobot's end effector without the need for additional tools or equipment. The inspection plate is also positioned to ensure seamless interaction between the cobot and the substrate, further streamlining the process.

To ensure a safe working environment, several safety measures were integrated into the inspection cell. For instance, during Cobot operation, the operator must maintain a safe distance and monitor the inspection results remotely via a laptop screen. This minimizes any potential physical interaction between the operator and

the moving Cobot. The cobot is equipped with an emergency stop button on its teach pendant, enabling the operator to halt its movements immediately if necessary as shown in Figure 6.2. Additionally, the operator is required to wear protective eyewear throughout the operation to guard against unforeseen risks.

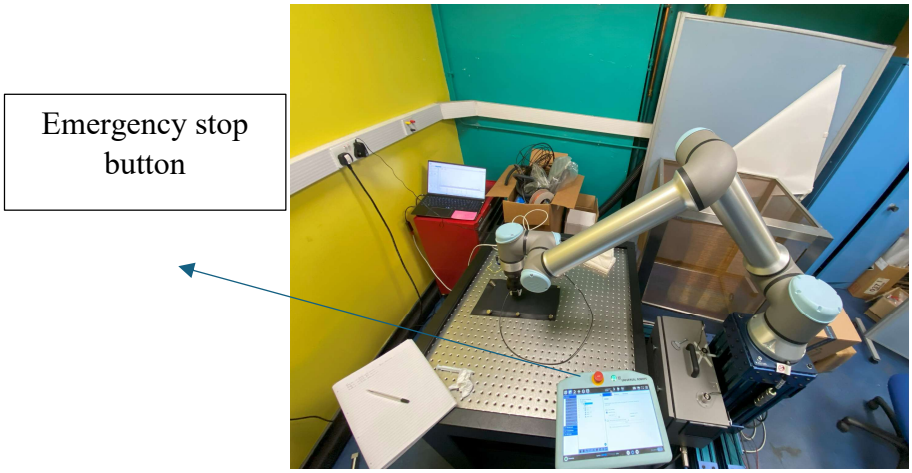

Figure 6.2. Inspection cell including how the emergency button is always available for emergency cases.

The ergonomic design of the workspace further enhances operator comfort and efficiency. The Cobot and its components are positioned at a height that allows the operator to perform setup and maintenance tasks while standing upright, eliminating the need for bending or awkward postures. The laptop displaying inspection results is strategically placed at eye level, ensuring the operator can monitor sensor readings and vision system classifications without straining their neck. Anti-fatigue mats have been added to the floor to reduce physical discomfort during extended periods of operation. Additionally, a task chair is available, enabling the operator to alternate between sitting and standing while reviewing results, thereby minimizing fatigue.

Beyond physical interaction, the human operator plays a central role in the operation and supervision of the inspection cell. During the training phase, the

operator is responsible for labeling image data by reviewing both visual input and capacitive sensing measurements to generate accurate annotations for the CNN model. During live operation, the operator monitors the output of the vision and sensing systems, interprets alerts or classification flags, and decides on corrective actions such as rework, system adjustment, or escalation. The operator also performs periodic system calibration, error recovery, and safety checks, ensuring reliable and safe execution of collaborative tasks. This human-in-the-loop framework ensures that the system remains adaptive, responsive to anomalies, and aligned with quality control standards.

The inspection cell has also been designed to handle certain environmental challenges. Although the workspace operates under general laboratory conditions with no controlled environment, measures have been taken to mitigate potential issues. For example, random lighting conditions were accounted for during the training phase of the vision system's CNN model, ensuring robust image classification under varying light intensities as detailed in Chapter 4.

In summary, the inspection cell has been designed with careful attention to physical layout, accessibility, safety, and ergonomics, creating a flexible and operator-friendly system. These design considerations—along with the clearly defined role of the human operator—support seamless human-robot collaboration and enhance the efficiency, adaptability, and accuracy of the quality control inspection process.

6.3 Technology Implementation

This section outlines the hardware and software components of the developed system, focusing on the roles of the Cobot, vision system, and capacitive sensing technologies. These three key aspects form the foundation of the inspection process, as detailed in Chapters 3 and 4. A brief overview of their implementation and functionality is provided below, with results discussed in detail in Section 6 of this chapter.

- Cobot: The collaborative robot (UR10e) is programmed to perform precise, repetitive movements along predefined waypoints. With a pose repeatability of ±0.05 mm, its primary role is to enable systematic scanning of the target area, ensuring consistent data acquisition for the vision and sensing systems. The cobot's flexibility and accuracy make it integral to the inspection process, allowing seamless integration with complex tasks in wider manufacturing range and applications.
- Vision System: The vision system consists of a webcam setup paired with a Convolutional Neural Network (CNN) for image classification, specifically using the ResNet101 architecture. This system captures and processes images of the surface, identifying and categorizing areas into three classes: Full, Fault, or Empty. This classification provides critical information on coating or liquid spreading uniformity and is essential for quality assessment.
- Sensing System: The capacitive sensing system is employed for both pre coating and post coating measurements. In the pre coating stage, the sensor is calibrated at a predefined voltage to establish a stable baseline for

subsequent comparisons. Post coating, the same sensor is used to gather measurements that assess the uniformity and thickness of the applied coating or liquid spread. Using a single calibrated sensor for both stages is essential because it ensures consistent sensitivity, calibration stability, and noise characteristics, allowing any change in voltage output to be attributed directly to the applied coating rather than differences between sensing devices. This practice is consistent with established capacitive metrology literature, where maintaining the same sensor across sequential measurements improves repeatability and increases accuracy when detecting micrometre scale variations in dielectric layers. Studies on thin film and coating thickness evaluation have demonstrated that capacitive sensors achieve higher reliability when the pre measurement and post measurement readings are taken with the same probe, as shown in [4], by film thickness measurement systems using capacitive methods [196], and by coating evaluation work using capacitive and hybrid electromagnetic sensors [196]. This dual stage application therefore strengthens the inspection methodology and improves confidence in detecting coating uniformity.

6.3.1 Integration Architecture

The proposed system shown in Figure 6.3 integrates a vision system, capacitive sensing system, and robotic system (Cobot) through a centralized laptop running Python and RoboDK, interconnected via USB and Ethernet. The vision system connects to the laptop via USB for image capturing, processing and classification, while the capacitive sensing system and robotic controller communicate through an

Ethernet switch, enabling real-time data exchange. The laptop, acting as the control hub, processes visual and sensor data in Python and uses RoboDK to simulate and send precise motion commands to the cobot. The physical integration of the camera, sensor, and cobot ensures synchronized operations for advanced automation tasks.

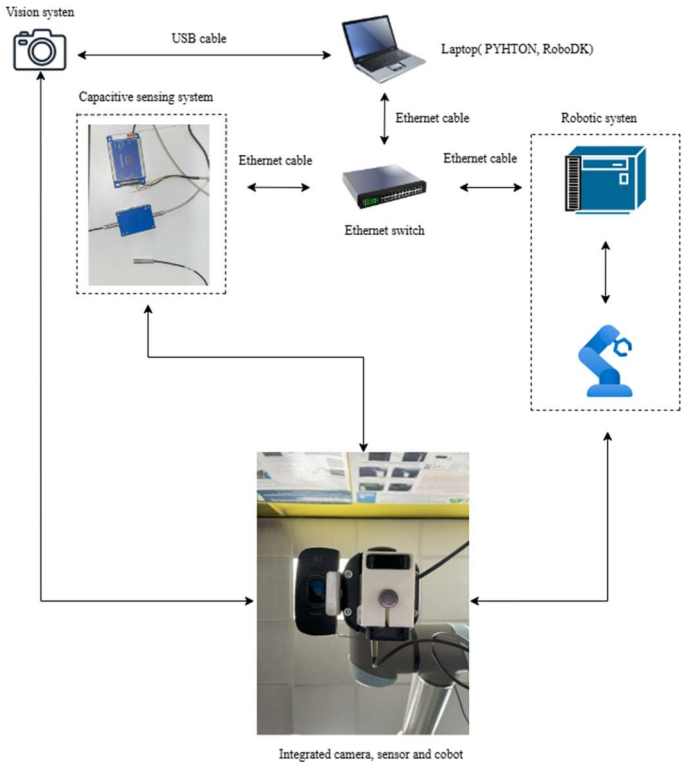

Figure 6.3. System architecture showing the integration of a vision system, capacitive sensor, and cobot, connected via USB and Ethernet to a laptop running Python and RoboDK for synchronized control and automation

6.4 System Workflow

In the pre-coating assessment, the capacitive sensor is calibrated at a predefined voltage, and initial measurements are recorded to establish a baseline reference for subsequent comparisons of thickness uniformity. Simultaneously, the camera is assigned to capture pre-coating images at scheduled inspection intervals. This ensures both sensor and visual data are logged prior to material application, providing a full pre-coating dataset for operator reference. For reference, baseline sensor

readings typically yield an estimated value of 10 V, while the vision system classifies these images as “Empty.”

In the post-coating assessment, the collaborative robot (Cobot) executes precise, preprogrammed movements along designated waypoints to collect synchronized post-coating data from both the capacitive sensor and the vision system. This stage includes the initial automated analysis, where the system applies trained CNN models and threshold-based sensing logic to classify the surface condition (e.g., “Full,” “Fault,” or “Empty”). These results form the preliminary pass/fail assessment, which is then presented for further evaluation.

Finally, in the Human Operator Intervention stage, a human operator reviews the classified results from both systems. The operator may confirm the system’s decisions, override incorrect classifications, or initiate corrective actions such as system calibration, rework, or equipment maintenance. Although this research does not specify all operator responsibilities in detail, the system is designed to support human-in-the-loop collaboration for decision-making, error resolution, and system supervision during in-process quality control. Below, a set of figures that are presenting the three stages of the inspection process.

6.4.1 Pre-liquid spreading

When the mimic substrate material is clean and empty as shown in Figure 6.4

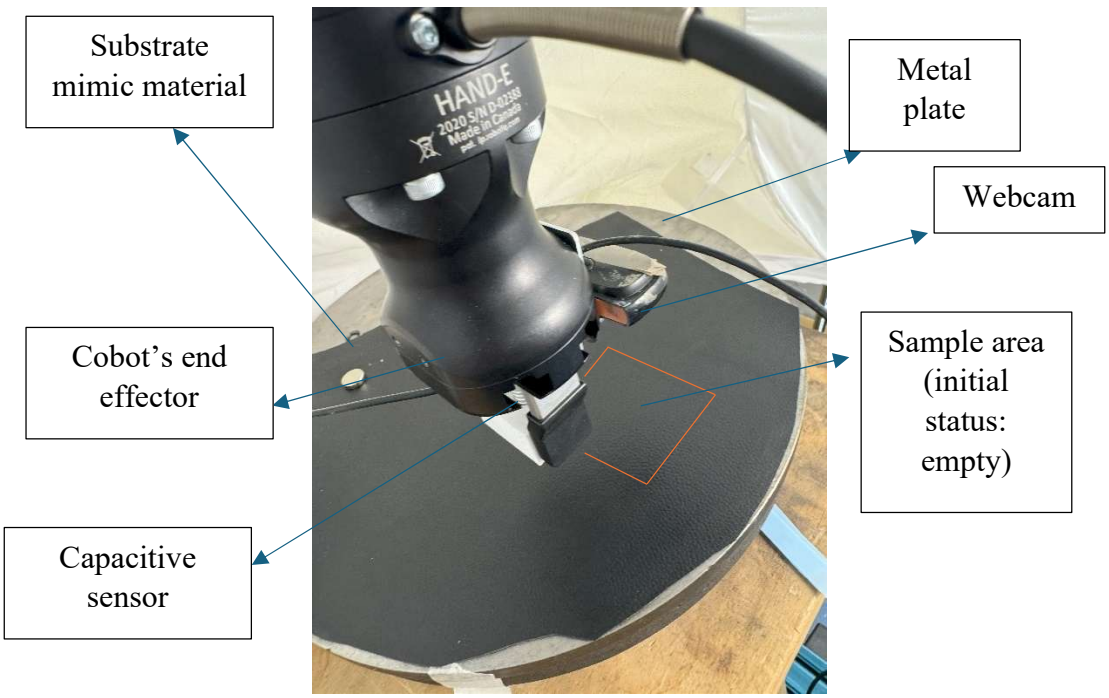

Figure 6.4. Pre-liquid spreading scanning

6.4.2 Post- Liquid Spreading

When the liquid is being spread on the mimic substrate material, the cobot will then carry out the scanning process again as shown in Figure 6.5.

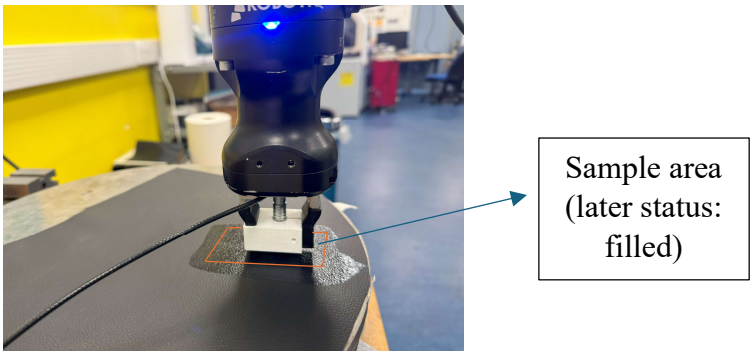

Figure 6.5. Post- liquid spreading scanning

6.5 Post-Data Collection

The operator reviews the results generated by the capacitive sensor and vision system for further assessment, as illustrated in Figure 6.6. A key aspect of this process is the simultaneous implementation of collaboration between the human operator and the Cobot. While the Cobot performs automated tasks such as precise scanning and data acquisition, the human operator focuses on the critical evaluation of the collected data to identify potential defects or irregularities. Notably, the collaboration in this approach does not involve direct physical interaction between the human and the Cobot. Instead, both operate within the same work environment, each focusing on distinct yet complementary tasks that align with the overarching objective of achieving robust and reliable in-process quality control inspection. This parallel interaction ensures efficiency, minimizes interference, and leverages the strengths of both automated precision and human decision-making.

(a) (b)

Figure 6.6. (a) Operator is monitoring the scanning stage and data collection, (b) Operator is acting by checking the setup

6.5.1 Feedback Assessment

The inspection assessment form presented in Table 6.2, provides a systematic framework for operators to evaluate production quality during scheduled inspections,

ensuring consistency and traceability throughout the process. By recording key parameters such as the date, time, operator name, and liquid type, the form ensures that each inspection is contextually aligned with production requirements.

It integrates automated outputs from the vision and capacitive sensing systems, enabling the operator to document surface classification results as Full, Fault, or Empty, based on predefined criteria such as surface uniformity, defects, or the absence of coating, and verify whether voltage readings align with the specified coating thickness range. In cases where discrepancies are detected, the form facilitates pinpointing issues to specific waypoints within the inspection grid, enhancing the precision of fault identification. Additionally, the form incorporates a section for qualitative feedback, allowing the operator to document observations, note anomalies, and recommend corrective actions. This structured approach not only fosters collaboration between human oversight and automated technologies but also ensures that inspection results are systematically recorded, facilitating real-time quality control and informed decision-making in dynamic production environments.

Table 6.2. Inspection Assessment Form for Recording Quality Control Data During Scheduled In-Process Inspections.

Inspection Item	**Details**	**Operator Input**
Date	**Enter the date of the inspection.**	
Time	**Enter the time the inspection is performed.**	
Operator Name	**Name of the operator performing the inspection.**	
Liquid Type	**Specify the type of liquid being used in the coating/spreading process.**	
Camera Inspection Results	**Indicate the surface quality based on camera assessment:** **☐ Full: Uniform coating** **☐ Fault: Defective area(s)** **☐ Empty: No coating applied**	☐ Full ☐ Fault ☐ Empty
Sensing Results	**Indicate whether the voltage readings are within the acceptable range for the required thickness. If 'No', specify waypoints with issues below.**	☐ Yes ☐ No
Waypoints with Issues	**Select the specific waypoints (as shown in Figure 6) where sensing results indicate issues.**	☐ (1) ☐ (2) ☐ (3) ☐ (4) ☐ (5) ☐ (6) ☐ (7) ☐ (8) ☐ (9)
Additional Notes	**Provide comments on issues or observations during the inspection.**	

6.5.2 System's Workflow Chart

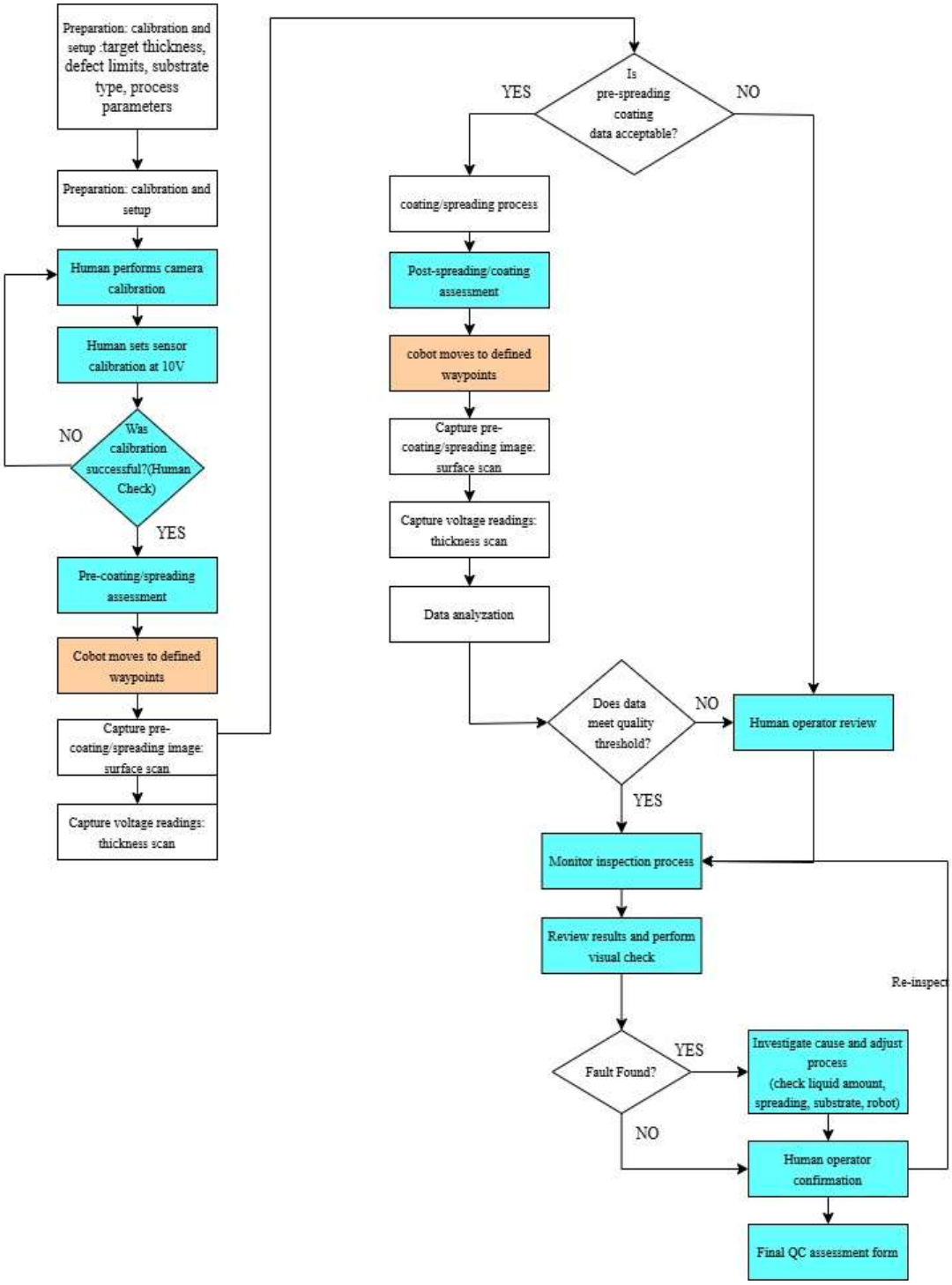

Figure 6.7. Full HRC, vision and sensing system's workflow chart

6.6 Results

This section presents the results of the case study supported by Unilever, which serves as a proof of concept for inspecting a testing liquid spread over a mimic substrate material. As established in Chapters 4 and 5, the integration of vision and sensing technologies with a robotic system has proven to be highly beneficial for manufacturing processes. The operation of the complete system is demonstrated to illustrate its capability for delivering seamless and efficient quality control inspections. The proposed quality control approach relies on the collection, analysis, and classification of data from both the capacitive sensor and the vision system. The operator successfully identified and analyzed three distinct scenarios:

- The substrate was empty, with no testing liquid applied.
- The liquid was spread fully, achieving one of the four targeted thickness levels: 15, 30, 60, or 90 microns.
- A fault occurred during the spreading process, specifically while applying the 30-micron thickness, which was identified and documented by the operator as a technical issue.

6.6.1 Empty spreading

Typically, when the spreading area is empty, both pre-spreading and post spreading stages will result same voltage values of 10 V, which indicate that the liquid is not being applied. As shown in Table 6.3, voltage values remained constant before and after spreading.

Table 6.3. Voltage Readings Before and After Spreading with corresponding differences across inspection positions for Empty spreading status.

Position	Voltage readings before spreading	Voltage readings after spreading	Voltage difference
1	9.99	9.97	0.02
2	9.98	9.95	0.03
3	9.96	9.96	0.00
4	9.96	9.97	-0.01
5	9.97	10.01	-0.04
6	9.98	10.03	-0.05
7	9.99	10.03	-0.04
8	9.99	9.99	0.00
9	9.99	9.99	0.00

The vision and sensing output as should be presented to the operator are presented in Figure 6.8 below.

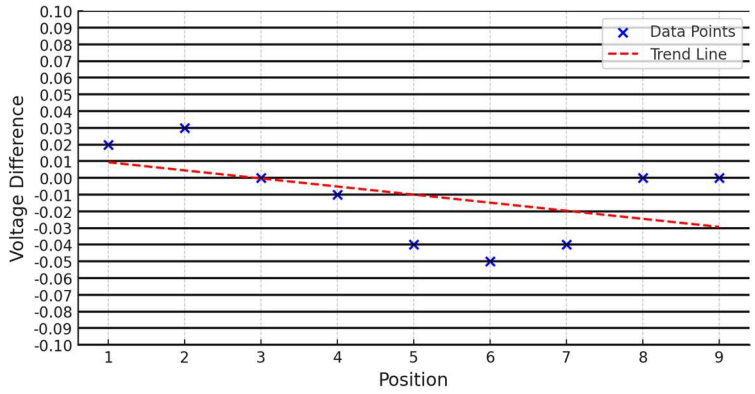

(a)

Figure 6.8.(a) Voltage differences across nine positions during the inspection process, (b) Visual prediction output from the vision system indicating a "Non-Spread/Empty" result.

(b)

Once the results are ready for the operator, the form assessment is completed accordingly as stated in Appendix C, Table C-1.

6.6.2 Full Spreading

Full spreading means that the testing liquid spreading is uniform, and the spreading area is covered evenly with testing liquid. According to Unilever, the targeted thicknesses are 15, 30, 60 and 90 microns. In this part of the results, the measurements of the four thickness levels and the corresponding assessment forms for each are presented.

6.6.2.1 Thickness 15 microns

Thickness 15 microns is when the spreader bar is set at 15 microns and being assigned for spreading. Table 6.4 presents the collected values of testing liquid spreading at 15 microns.

Table 6.4 Voltage readings before and after spreading with corresponding differences across inspection positions of 15 microns thickness

Position	Voltage readings before spreading	Voltage readings after spreading	Voltage difference
1	10.05	4.89	5.16
2	10.03	4.81	5.22
3	10.00	4.83	5.17
4	10.02	4.81	5.21
5	10.03	4.77	5.26
6	10.06	4.87	5.19
7	10.00	4.79	5.21
8	10.03	4.79	5.24
9	10.03	4.84	5.19

In Figure 6.9, the output results from the sensing and vision systems are presented to the operator.

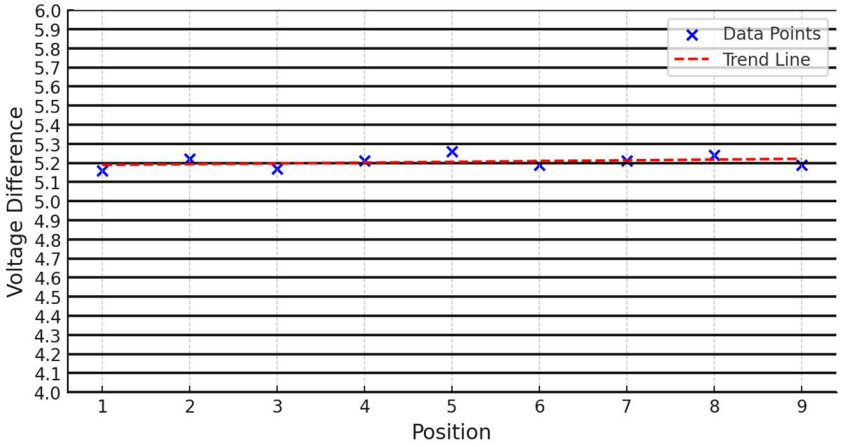

(a)

(b)

Figure 6.9. (a) Voltage differences across nine positions during the inspection process of 15 microns, (b) Visual prediction output from the vision system indicating a "Full" result.

The operator then established the assessment form of the obtained results outlined in Appendix C, Table C-2.

6.6.2.2 Thickness 30 microns

Now, considering thickness 30 microns, in Table 6.5, the results obtained from the sensing system are outlined as follows:

Table 6.5 Voltage readings before and after spreading with corresponding differences across inspection positions of 30 microns thickness

Position	Voltage readings before spreading	Voltage readings after spreading	Voltage difference
1	10.08	4.68	5.4
2	10.01	4.59	5.43
3	10.05	4.73	5.32
4	10.02	4.65	5.37
5	10.02	4.56	5.46
6	10.09	4.66	5.43
7	10.03	4.6	5.43
8	10.0	4.65	5.35
9	10.04	4.6	5.43

In Figure 6.10, the output results from the sensing and vision systems are presented to the operator.

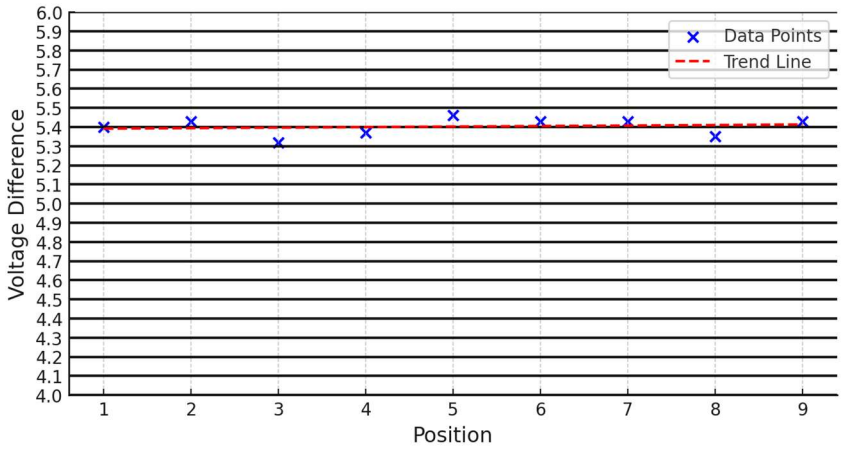

(a)

(b)

Figure 6.10. (a) Voltage differences across nine positions during the inspection process of 30 microns, (b) Visual prediction output from the vision system indicating a "Full" result.

The operator then established the following assessment form of the obtained results outlined in Appendix C, Table C-3.

6.6.2.3 Thickness 60 microns

Now, considering thickness 60 microns, in Table 6.6, the results obtained from the sensing system are outlined as follows:

Table 6.6. Voltage readings before and after spreading with corresponding differences across inspection positions of 60 microns thickness

Position	Voltage readings before spreading	Voltage readings after spreading	Voltage difference
1	10.06	4.45	5.61
2	10.02	4.4	5.62
3	10.01	4.37	5.64
4	10.03	4.38	5.65
5	9.99	4.33	5.66
6	10.06	4.4	5.66
7	10.03	4.42	5.61
8	10.01	4.35	5.66
9	10.06	4.32	5.74

In Figure 6.11, the output results from the sensing and vision systems are presented to the operator.

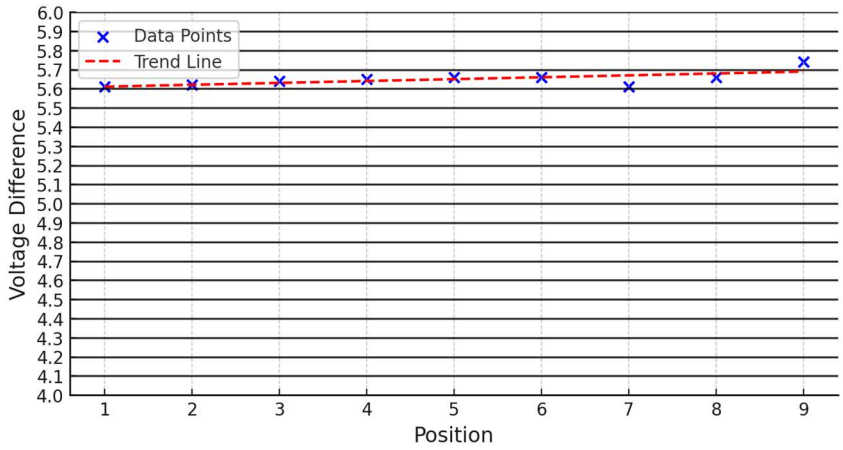

(a)

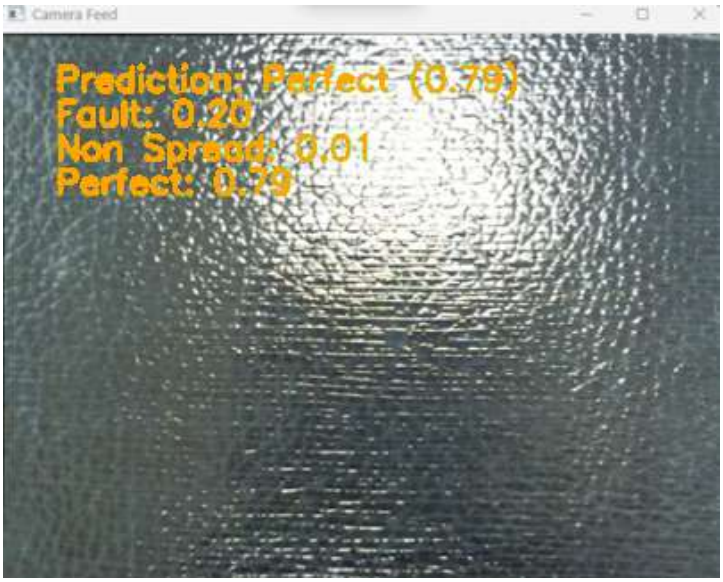

(b)

Figure 6.11 (a) Voltage differences across nine positions during the inspection process of 60 microns, (b) Visual prediction output from the vision system indicating a "Full" result.

The operator then established the assessment form of the obtained results outlined in Appendix C, Table C-4.

6.6.2.4 Thickness 90 microns

Finally, Table 6.7 below outlines the voltage output of the fourth targeted thickness 90 microns.

Table 6.7. Voltage readings before and after spreading with corresponding differences across inspection positions of 90 microns thickness

Position	Voltage readings before spreading	Voltage readings after spreading	Voltage difference
1	10.05	4.23	5.82
2	10.04	4.16	5.88
3	9.98	4.14	5.83
4	10.03	4.06	5.97
5	10.02	4.1	5.92
6	10.06	4.17	5.89
7	10.04	4.24	5.8
8	10.01	4.13	5.88
9	10.0	4.06	5.94

Figure 6.12 summarizes the output results from the sensing and vision systems are presented to the operator.

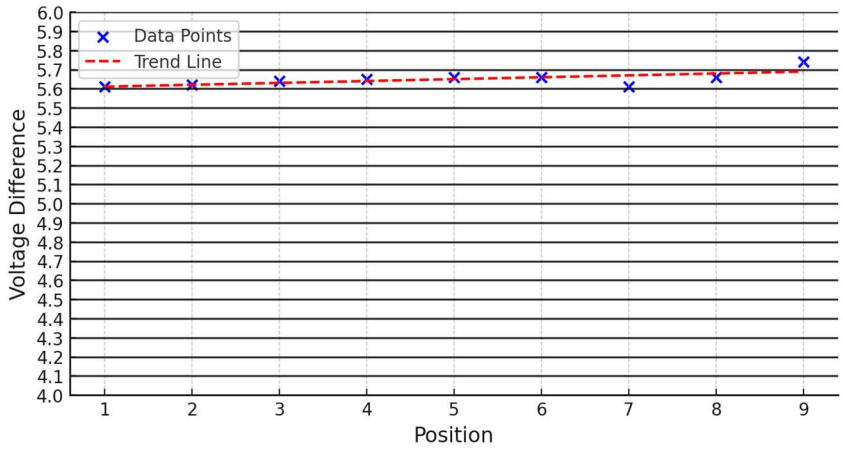

(a)

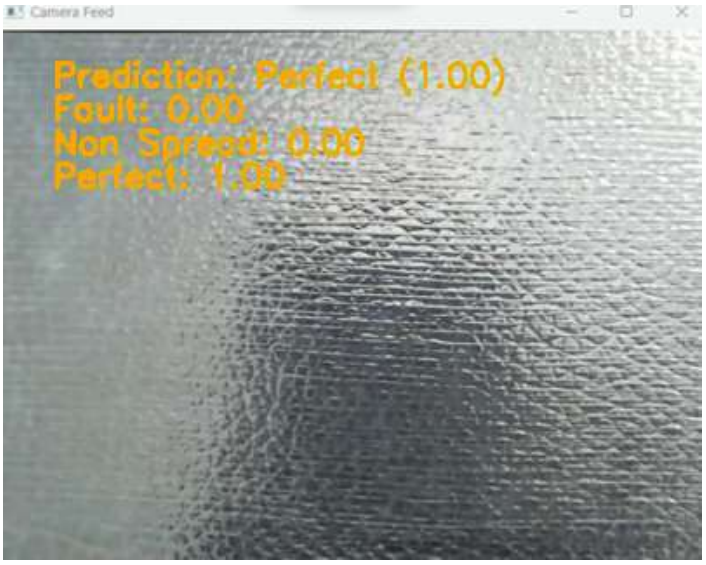

(b)

Figure 6.12.(a) Voltage differences across nine positions during the inspection process of 90 microns, (b) Visual prediction output from the vision system indicating a "Full" result.

The operator then established the assessment form of the obtained results outlined in Appendix C, Table C-5.

6.6.3 Fault Spreading

While testing the approach, the operator intended to examine the approach by inspecting fault spreading that form one form of the estimated technical problems that may occur in production. Both results of sensing and vision systems indicate that a technical problem is valid and require further assessment and action to be taken and sort the issue. The operator has recorded the case using the assessment form and the results are presented.

Table 6.8 represents the voltage data collected before and after scanning as seen below.

Table 6.8. Voltage readings before and after spreading with corresponding differences across inspection positions where defect was noticed in different positions.

Position	Voltage readings before spreading	Voltage readings after spreading	Voltage difference
1	10.00	4.68	5.32
2	10.00	9.95	0.05
3	10.01	9.97	0.04
4	10.00	9.99	0.01
5	10.00	9.85	0.15
6	10.01	4.66	5.35
7	10.01	4.6	5.41
8	10.01	9.94	0.07
9	10.00	9.94	0.06

Simultaneously, the operator has viewed the output from the vision system and the corresponding voltage chart that assist in assigning the exact positions where technical issue occurs. Figure 6.13 outlines the visual results.

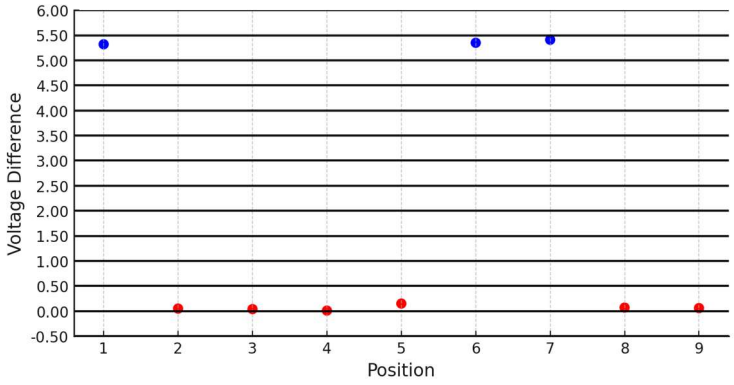

(a)

(b)

Figure 6.13. (a) Voltage differences across nine positions during the inspection process of fault spreading, (b) Visual prediction output from the vision system indicating a "Fault" result.

To evaluate fault propagation, no predefined target thickness was assigned, allowing the operator to utilize the thickness prediction equation developed in Chapter 5. By applying this equation, the operator conducted a comprehensive assessment of fault propagation by accurately identifying the locations of the anomalies and correlating them with the predicted target thickness values. This approach ensures that the identified issues are directly associated with the

corresponding production records. In Appendix C, Table C-6 the assessment framework employed in this case is presented.

6.7 Summary

The integration of HRC, vision systems, and capacitive sensing technologies represents a significant advancement in quality control methodologies for manufacturing. By combining real-time precision, human expertise, and advanced automation, the proposed system addresses the limitations of manual and fully automated workflows. The case study with Unilever demonstrated the practical benefits of the designed approach, including reduced downtime, enhanced adaptability, and superior defect detection capabilities. These findings establish a strong foundation for future industrial applications, paving the way for improved quality control practices that meet the evolving demands of modern manufacturing environments.

Chapter 7. Discussion

7.1 Introduction and Overview

This thesis addressed the need for a robust in process quality control framework for liquid spreading and coating operations where both surface condition and micron scale thickness uniformity must be assessed within the production window. The research aimed to develop and validate an integrated system that combines collaborative robotics, CNN based machine vision, and capacitive sensing within a human robot collaborative inspection workflow. The objective was not to replace the operator, but to structure inspection tasks so that the robot executes repeatable scanning and data acquisition, the AI modules provide rapid classification and quantitative estimation, and the human operator supervises calibration and resolves exceptions.

This discussion chapter is structured around the major findings of the vision system, the robotic capacitive sensing model, and the full integrated HRC inspection cell. The chapter first interprets the key experimental outcomes. It then positions these outcomes within the literature base reviewed in the thesis, focusing on the knowledge gaps that motivated the multimodal approach. A system level comparison of manual, fully automated, and HRC enabled inspection paradigms is then presented using the content originally developed in Section 6.7. The chapter concludes with the practical implications, contributions to knowledge and limitations

7.2 Interpretation of Key Findings

7.2.1 Vision based classification of spreading states

The vision subsystem was designed to classify the surface state of liquid spreading into Full, Fault, and Empty categories. The adopted model was ResNet 101 pretrained on ImageNet and fine-tuned on the developed dataset. The dataset was structured across three main classes with 2,000 images for No spread, 3,000 images for Full spread, and 1,900 images for Fault spreading, then split into 70% training, 20% validation, and 10% testing to evaluate generalisation on unseen samples. This design decision provides a clear and defensible separation between model development and model evaluation within the scope of the thesis.

The reported performance of the ResNet 101 model indicates a strong capability to extract high level discriminative features from spreading textures and boundary characteristics. The model achieved a training accuracy of 97.99% and a validation accuracy of 100.00%. This outcome suggests that, under the controlled acquisition conditions of the inspection cell and the structured dataset, the three classes present separable visual signatures that can be learned effectively by deep residual architectures. The reliability of the classification is further supported by the comparative evaluation against alternative models and classical baselines in the vision chapter.

The critical interpretation is not that perfect performance will necessarily hold across all industrial deployment contexts. Rather, the most defensible meaning of the result is that robot assisted and repeatable image capture, combined with a carefully curated dataset, can produce a stable classification pipeline for quality control tasks where the visual variability is bounded by cell design and acquisition protocol. This

provides a robust foundation for scaling the vision subsystem to broader production variability in future work.

This outcome aligns with the broader deep learning inspection direction reported in the literature that I reviewed, where residual networks are widely justified for industrial texture and defect discrimination because of their stable gradient flow and high-level feature abstraction. The ResNet family originally proposed by He et al. provides the theoretical and architectural basis for this selection, and my results confirm that ResNet 101 remains an effective choice when the acquisition protocol and class definitions are tightly controlled by the inspection cell design. In this thesis, I extend this baseline by demonstrating a robot assisted data capture protocol that reduces viewpoint and lighting variability at the point of inspection, which is a practical improvement over purely vision only pipelines that do not explicitly control spatial repeatability as part of the model performance assumptions.

7.2.2 Capacitive sensing for micron scale thickness estimation

The capacitive sensing subsystem was developed to quantify liquid thickness and to provide spatial uniformity assessment across nine predefined waypoints. The CS1 sensor was calibrated to operate over a defined measurement window, with a stated sensitivity of approximately 1 V per 100 μm within the relevant experimental protocol. The thickness targets for industrial validation were 15, 30, 60, and 90 microns. These levels were selected to reflect realistic industrial deposition conditions while remaining within a narrow operational range where the voltage thickness relationship is stable for regression-based modelling.

The linear regression model achieved an R squared value of 0.915 and a mean squared error of 0.00699. Within the experimental scope, this indicates that a linear

mapping is a suitable engineering approximation of the sensor behaviour for the tested thickness conditions. The key meaning is not that capacitive sensing is universally linear across all coating ranges, but that the effective experimental window used in this thesis supports a reliable linear calibration model for industrial pass-fail discrimination and thickness category separation.

The dual stage sensing logic of pre spreading baseline establishment followed by post spreading measurement provides a practical method to reduce ambiguity introduced by substrate variability. This framework strengthens the interpretability of thickness deviation during real time inspection and is consistent with the system level requirement to detect insufficient coverage even when surface appearance alone may be misleading.

The second case study on coating inspection extends the relevance of the sensing approach beyond the primary liquid spreading context. The results indicate that the robotic capacitive sensing concept can be transferred to coating uniformity assessment where the discrimination between different layer conditions and defective regions is necessary for high value manufacturing environments.

Prior work in capacitive sensing for thin films and dielectric variation confirms that high sensitivity thickness inference is feasible when the measurement window is narrow and the dielectric system is well characterised. The state of the art reviews and application studies that I cited, including the coplanar capacitive sensing review and the water film thickness study, support the rationale for using capacitive sensing as a non-destructive alternative to optical only inspection for thin liquid layers. My results extend this literature by demonstrating a cobot assisted calibration and spatial scanning strategy that enables repeatable point wise thickness categorisation across

nine locations, and by validating this approach through both liquid spreading and a second coating oriented case study designed to generalise the sensing concept beyond a single industrial scenario.

7.2.3 Robot assisted spatial scanning and synchronised acquisition

The UR10e collaborative robot provides controlled and repeatable sensor and camera positioning for consistent spatial sampling. The nine-waypoint strategy establishes a structured inspection grid for both voltage acquisition and image capture. In the integrated workflow, the robot executes deterministic movement and stabilisation, while the sensing and vision systems acquire synchronised measurements aligned to each waypoint. This architecture reduces the variability that would otherwise be introduced by manual repositioning and enables valid pre and post comparison at a point wise level.

The technical significance of robotic assistance is not limited to automation. It establishes controlled conditions for multimodal data correlation. This improves the reliability of sensor vision cross validation and supports a coherent inspection logic suitable for supervised autonomy.

The HRC literature reviewed emphasises that effective collaboration in manufacturing depends on exploiting complementary strengths, where robots provide repeatability and humans provide contextual decision making. Surveys and industrial frameworks in this area highlight safety, role allocation, and interface design as central pillars of successful deployment. In this thesis, I extend these principles into a quality control specific workflow for liquid spreading and coating by showing that UR10e guided waypoint execution is not only a logistics enabler but a methodological requirement for reliable cross modality correlation between image

and voltage data. This strengthens the argument that robot repeatability should be treated as part of the measurement integrity of multimodal inspection systems, not merely as an automation convenience.

7.3 Contextualization within Existing Literature

The literature review in this thesis established that quality control inspection for liquid spreading and coating remains constrained by two persistent limitations. The first is the reliance on manual inspection or visually dominant approaches that struggle to provide reliable micron scale thickness verification during production. The second is the limited availability of HRC frameworks that integrate surface classification, thickness sensing, and operator supervision within a single structured workflow. These gaps were identified through the HRC and smart manufacturing studies reviewed earlier, including foundational surveys that define collaboration levels, safety modes, and role assignment, and which implicitly highlight that most industrial HRC demonstrations still focus on assembly, handling, or polishing motifs rather than liquid film quality control.

From an HRC standpoint, the system architecture developed in this thesis is consistent with the direction described by Villani et al. and Hentout et al., where safe and intuitive collaboration is achieved through clear task partitioning and the use of cobots for repetitive precision tasks. My work extends this base by situating HRC directly inside an in-process inspection loop for liquid spreading, where the robot is not only a safe co-worker but a repeatable metrology carrier for both vision and sensing. In this context, the nine-waypoint strategy and the calibration inspection decision sequence operationalise a supervised autonomy model that is more specific than the general HRC paradigms reported in these surveys.

In relation to vision based inspection, the literature I cited supports the adoption of CNN architectures as the dominant approach for industrial surface state recognition under complex texture variability. The ResNet family introduced by He et al. provides the technical rationale for deep residual learning in this domain, and my selection of ResNet 101 follows the thesis criteria of performance, robustness, and transfer learning suitability. I extend this vision literature by presenting a dataset and a robot assisted acquisition protocol tailored to liquid spreading on a skin mimic substrate, where class definitions are linked to the production logic of Full, Fault, and Empty states. The high validation performance should therefore be interpreted as evidence that a controlled HRC inspection cell can bound visual variability enough to enable stable deep classification, rather than as a claim of universal generalisation to all unconstrained factory environments.

For thickness inspection, my capacitive sensing results are positioned against studies and reviews that investigate non-destructive dielectric-based measurement for thin films. The coplanar capacitive sensing review by Abdollahi Mamoudan et al. and the water film thickness study by Li et al. show that capacitive approaches can achieve high sensitivity for thin liquid layers when calibration and material assumptions are clearly defined. My work builds on this foundation by integrating a commercial CS1 sensor with cobot guided spatial sampling and by demonstrating that a linear regression model provides a valid engineering approximation within the narrow 15 to 90 microns operating window used in the Unilever spreading case study. This is further supported by the second coating-oriented case study, which broadens the relevance of the proposed sensing logic into coating uniformity contexts aligned with high value sectors.

The key advancement beyond the reviewed literature is therefore not a single algorithmic improvement in vision or a standalone calibration improvement in sensing. It is the demonstrated closed loop coupling of three elements that are rarely validated together in the cited body of work. These elements are ResNet 101 surface state classification, cobot assisted capacitive thickness inference, and cross modality validation mediated by human oversight. This integration addresses the known limitation that automated systems often detect surface defects without reliable in process thickness quantification, and it provides an HRC grounded pathway for deploying multimodal inspection without removing the operator from final interpretive control.

7.4 System level comparison of inspection paradigms and HRC impact

This section synthesises the subsystem level findings into a system level interpretation of inspection effectiveness. The comparison of manual, fully automated, and HRC enabled workflows is used to evaluate how the proposed multimodal architecture addresses the limitations identified in the literature review and to clarify the practical significance of integrating UR10e guided scanning, ResNet101 classification, and CS1 based thickness estimation within a supervised autonomy model.

7.4.1 Discussion of integrated framework

The presented novel system framework integrates Human-Robot Collaboration (HRC), vision systems, and capacitive sensing technologies to address critical challenges in in-process quality control within manufacturing. By enabling real-time assessment of liquid spreading uniformity, the proposed system offers a robust

solution for achieving precision during production. Supported by a case study conducted with Unilever, the methodology demonstrated the effectiveness of combining Convolutional Neural Networks (CNN) for image classification and capacitive sensing for quantitative thickness evaluation. This integration ensures accurate detection of anomalies and consistency in achieving target thickness levels (15, 30, 60, and 90 microns).

The findings validated the effectiveness of the proposed system in addressing common limitations of existing quality control methods. The contributions of this research represent significant advancements in industrial quality control practices, including:

1. **Real-time inspection:** Immediate detection and correction of defects, resulting in reduced downtime and lower rework costs.
2. **Human-robot synergy:** Leveraging collaborative robots (cobots) for repetitive, precise tasks, allowing human operators to focus on critical decision-making and maintenance.
3. **Flexible system design:** A modular, ergonomic system that adapts to diverse manufacturing environments, enhancing scalability and usability.
4. **System workflow:** A structured inspection process supported by assessment forms that ensure consistency, traceability, and operational efficiency.

7.4.1.1 Manual workflow without HRC

In a manual workflow, quality control relies on human operators using visual inspections and basic measurement tools. While widely employed, this method suffers from several limitations:

- **Human error:** Fatigue, judgment variability, and operator inconsistencies can result in missed defects and reduced accuracy.
- **Precision challenges**: Traditional tools lack the capability to detect micron-level variations when it comes to complex industrial applications, a critical requirement in high-precision manufacturing.
- **Scalability limitations:** Manual processes are labor-intensive, inefficient for high-volume production, and prone to delays and increased operational costs.

7.4.1.2 Automated Workflow Without HRC

Fully automated systems address some limitations of manual methods but have their own drawbacks:

- **Incomplete capabilities:** While effective in detecting surface defects, current systems struggle to measure liquid film thickness with the level of accuracy required for micrometre scale applications. In contrast, the capacitive sensing model developed in this work achieved an R squared value of 0.915 and a mean squared error of 0.00699, allowing reliable discrimination between the tested thickness levels.
- **Inflexibility:** Automated systems are limited in adapting to unexpected anomalies or dynamic production changes, often requiring reprogramming or human intervention, leading to costly inefficiencies.
- **Maintenance challenges:** Automated systems require specialized expertise for maintenance, which can disrupt production schedules and increase operational downtime.

7.4.1.3 HRC- System Workflow

The system has been engineered to reflect a structured, task-divided collaboration between human operators and robotic automation. This collaboration is embedded across three main phases: calibration, inspection execution, and decision-making, and is directly represented in the color-coded workflow diagram.

- **Precision and consistency:** repetitive physical tasks such as sensor alignment, image capture, and positional scanning are executed by the collaborative robot. Once the human operator sets the initial calibration values (10V reference for the capacitive sensor and image calibration), the robot moves to pre-defined waypoints with millimeter-level repeatability to perform surface scanning. Each movement is embedded in the robot control script and executed via Python-based command sequences to ensure spatial and temporal alignment between image frames and voltage measurements. This repeatability allows valid before/after comparisons of each inspection point and prevents data inconsistency due to human handling.
- **Enhanced decision-making**: decision making is concentrated around human interpretation of flagged cases and supervision of ambiguous or borderline outcomes. In real world operation, human intervention is not continuous; it typically occurs at three stages. First, at the beginning of each inspection cycle to verify that sensor and camera calibration have been completed successfully. Second, on demand when the system detects cases outside the acceptable threshold range, such as a voltage deviation that indicates insufficient coating or when the CNN model flags a low quality spreading pattern. Third, at the end of the cycle for final QC validation. During stable production, such interventions are infrequent because most samples fall within expected limits. Real world observations from liquid spreading lines show that flagged

cases typically account for a small fraction of total samples, often less than ten percent, meaning the human operator's workload remains manageable. The operator cross validates the visual and sensor outputs, compares them against expected spreading behaviour, and determines whether the anomaly is a true coating fault, a process drift that requires adjustment, or a sensor related issue that requires recalibration. The system's automation handles the high frequency scanning and data capture, allowing the operator to focus on exception handling rather than continuous monitoring. This supervised autonomy approach enables the human to keep pace with the inspection rate because the robot executes all repetitive scanning at high speed, and the operator is only prompted when the system encounters a case that requires human judgment. As a result, the operator's involvement scales with the number of exceptions rather than the total inspection volume, ensuring that the human remains able to keep up with the process even when the robot operates at faster cycle times..

- **Comprehensive quality control:** the developed quality control approach for inspection is not dependent on a single modality. Capacitive sensing is used to quantify the actual thickness of the applied liquid at each scanning point. Deviation from the reference indicates insufficient coverage, even when the image may appear visually correct. Meanwhile, the ResNet101 model classifies surface images into three categories: "Full," "Fault," or "Empty." These classifications are made per scan point and are cross validated against the sensor readings. If there is a mismatch—such as a visually "Full" classification with low voltage—the sample is automatically flagged for

manual review. This dual-modality architecture improves detection sensitivity and reduces false positives or undetected faults.

- **Improved efficiency:** the overall inspection workflow is structured to automate all repetitive and deterministic tasks (robot movement, image capture, voltage reading, and data logging), while delegating judgment and anomaly handling to the human operator. This division reduces operator fatigue, improves focus, and speeds up inspection throughput. Moreover, the system resilience increases by enabling dynamic human re-engagement only when necessary (e.g., outliers, failed calibration, or post-inspection confirmation).

7.5 Practical Implications and System Significance

The integrated results indicate that a multimodal inspection cell combining CNN based surface classification and capacitive thickness estimation can provide a more complete representation of liquid spreading quality than single modality inspection. The Unilever case study shows that the structured pre and post spreading logic, supported by robot assisted waypoint scanning, enables consistent evaluation of target thickness conditions alongside surface state assessment. The capacitive sensing outcomes demonstrate that the proposed calibration and regression strategy is suitable for discriminating the tested micron scale thickness levels, while the vision system provides rapid categorisation of spreading state under the acquisition conditions defined in the inspection cell. The secondary coating case study further suggests that the sensing and robotic concept can be adapted to coating uniformity contexts where thickness variation and defect separation are critical quality variables. Together, these findings support the industrial relevance of a supervised autonomy

inspection model in which high frequency scanning and data capture are automated, and the operator is engaged primarily for calibration confirmation and exception handling.

7.6 Limitations and Weaknesses

The scope of this research is bounded by the experimental conditions and industrial contexts investigated. The vision model performance was validated within the dataset and acquisition protocol defined in the thesis. The 100.00% validation accuracy should therefore be interpreted as reflecting strong class separability under the current data characteristics and controlled capture conditions, rather than as evidence of universal generalisation across all production variability. For capacitive sensing, the regression model is justified within the tested thickness window and calibration strategy. The linear mapping should not be assumed to hold outside the experimentally validated range or under significantly different dielectric conditions. The sensing chapter also acknowledges potential sensitivity to environmental factors such as humidity and temperature, which defines the present operational envelope. At the system level, the nine-waypoint strategy provides structured spatial assessment but limits resolution to the selected sampling grid, while the workflow design retains human supervision for calibration verification and anomaly resolution.

Chapter 8. Conclusion and Future Research

8.1 Conclusions

In this thesis, Human-Robot Collaboration (HRC), capacitive sensing, and vision system has been developed to enhance in-process quality control (QC) inspection in complex manufacturing environments. The proposed system helps addresses critical challenges associated with defect detection, liquid spreading uniformity, and thickness consistency, utilizing a combination of machine vision, capacitive sensing, and robotic automation. By leveraging advanced CNN-based defect detection, real-time capacitive sensing, and collaborative robotic workflows, this research significantly improves QC inspection accuracy and reliability in industrial applications.

A comprehensive review of existing quality control methods identified the limitations of traditional inspection techniques, particularly in liquid-based applications such as coating, spreading, and painting processes. Conventional manual inspections are subjective, error-prone, and inefficient, while existing automated approaches often lack adaptability, real-time feedback, and multi-modal sensing capabilities. To overcome these limitations, a hybrid QC system was designed, integrating collaborative robots, a CNN-powered vision system, and capacitive sensing technology.

The defect detection component of this system was developed using a CNN-based vision model trained on a high-resolution dataset of liquid spreading defects. Experimental results demonstrated that this model outperforms traditional feature-based image classification techniques, achieving high accuracy in defect classification across various lighting conditions and surface textures. Furthermore,

capacitive sensing was utilized to provide real-time, non-destructive thickness measurements, addressing a critical gap in conventional vision-based inspections. The capacitive sensing system was rigorously validated through regression analysis, confirming its ability to provide micron-level precision in thickness estimation.

The integration of these technologies into a single HRC-QC framework resulted in a real-time inspection system capable of detecting and quantifying defects. Experimental validation demonstrated that the proposed system significantly enhances QC inspection efficiency, improves defect classification accuracy, and reduces material waste in manufacturing processes.

8.2 Contributions to Knowledge

This thesis makes several key contributions to the field of smart manufacturing and industrial quality control:

- **Comprehensive review of HRC and key technologies implementation in industry.** A detailed review of existing technologies, QC inspection methodologies highlighted the limitations of manual and automated approaches in liquid-based defect detection. An in-depth evaluation framework was developed to benchmark the proposed system against conventional inspection techniques.
- **Novel CNN-Based defect detection system:** A deep learning-based vision model was designed and trained to detect and classify defects in liquid spreading application on skin mimic substrate. The model demonstrated high accuracy, robustness to lighting variations, and superior performance compared to traditional machine learning approaches.

- **Capacitive sensing for thickness measurement:** The implementation of a capacitive sensing system provided real-time, non-destructive measurements of liquid thickness during the spreading process. The developed regression model accurately predicted thickness variations, ensuring enhanced quality control.
- **HRC- system inspection framework:** A human operator was assigned with robotic, vision and sensing technologies to create a fully automated QC workflow. The system achieved adaptive decision-making, based on human intervention for validating the obtained results, applying any maintenance action needed while maintaining high precision and reliability.
- **Experimental validation and industrial case studies:** The proposed system was tested in real-world manufacturing conditions, demonstrating significant improvements in defect detection accuracy, QC process efficiency, and material waste reduction. A case study conducted in collaboration with Unilever validated the system's effectiveness in addressing liquid spreading inconsistencies in production. Unilever case study was utilized in developing both vision and sensing system. and for the generalization purpose, another case study was conducted for the sensing- robotic system.

8.3 Recommendations for Future Work

Despite the high accuracy and reliability achieved in liquid spreading defect detection, certain limitations still persist, potentially restricting broader industrial applications. The proposed system demonstrated strong performance in detecting defects, but further improvements are necessary to enhance adaptability, scalability, and real-time processing capabilities.

Firstly, computational complexity remains a key factor influencing the system's real-time performance and capacity. The current processing speed, while sufficient for many applications, can be further optimized to meet the stringent requirements of high-speed manufacturing lines. To address this, research will be directed towards optimizing the defect detection pipeline by incorporating adaptive thresholding mechanisms and machine learning-based calibration techniques. These enhancements will enable more precise defect detection while reducing the system's computational load, thereby improving real-time performance.

Secondly automation and robotics integration present additional opportunities for advancing quality control capabilities. While the system currently requires manual sensor calibration, future work will focus on developing automated calibration techniques to reduce human intervention and improve operational efficiency.

Another critical aspect of future research is how to improve the system's scalability and deployment across various industrial settings. While initial trials have demonstrated promising results, further industrial testing will be conducted to assess adaptability and robustness across different manufacturing environments, including multi-layered applications such as composite materials and biomedical coatings. Ensuring the system's seamless integration into existing production lines will be a key focus, with an emphasis on optimizing its compatibility with diverse manufacturing processes.

Finally, the advancement of condition monitoring systems (CMS) will be a vital area of investigation. Enhancing data capture and processing efficiency will be crucial in addressing latency and storage constraints, particularly in large-scale

production environments. Future research will also explore adaptive learning techniques to refine real-time performance in defect assessment, ensuring more accurate and efficient quality control.

References

[1] U. Othman and E. Yang, “Human–robot collaborations in smart manufacturing environments: Review and outlook,” *Sensors*, vol. 23, no. 12, p. 5663, 2023, doi: 10.3390/s23125663.

[2] U. Othman and E. Yang, “An overview of human-robot collaboration in smart manufacturing,” in *Proc. 27th Int. Conf. Automation and Computing (ICAC)*, Birmingham, U.K., Sept. 1–3, 2022, pp. 1–6, doi: 10.1109/ICAC55051.2022.9911168

[3] U. Othman, M. A. Ait Ameur, E. Yang., & O. Torres.." CNN-based ResNet-101: a high-accuracy quality control inspection approach for industrial applications in liquid spreading on skin-mimic substrates". In K. Dahal, Z. Pervez, & M. Gilardi (Eds.), 2025 International Conference on Software, Knowledge, Information Management & Applications (SKIMA) IEEE. https://doi.org/10.1109/SKIMA66621.2025.11155456.

[4] N. Kozamernik, J. Zaletelj, A. Košir, *et al.*, “Visual quality and safety monitoring system for human–robot cooperation,” *Int. J. Adv. Manuf. Technol.*, vol. 128, pp. 685–701, 2023, doi: 10.1007/s00170-023-11698-2.

[5] F. Abdollahi-Mamoudan, C. Ibarra-Castanedo, and X. P. V. Maldague, “Advancements in and research on coplanar capacitive sensing techniques for non-destructive testing and evaluation: A state-of-the-art review,” *Sensors*, vol. 24, no. 15, p. 4984, Aug. 2024, doi: 10.3390/s24154984.

[6] N. Li, M. Cao, X. Yu, J. Jia, and Y. Yang, “High sensitive capacitive sensing method for thickness detection of the water film on an insulation surface,”

IEEE Access, vol. 7, pp. 96384–96391, 2019, doi: 10.1109/ACCESS.2019.2929585.

[7] K. Maize, Y. Mi, M. Cakmak, and A. Shakouri, "Real-time metrology for roll-to-roll and advanced inline manufacturing: A review," *Adv. Mater. Technol.*, vol. 8, no. 2, p. 2200173, 2023, doi: 10.1002/admt.202200173.

[8] G. Zhao, Y. Huang, W. Zhang, C. Wang, and J. Chen, "Advances in high-precision displacement and thickness measurement based on eddy current sensors: A review," *Measurement*, vol. 243, p. 116410, Feb. 2025, doi: 10.1016/j.measurement.2024.116410.

[9] N. E. Sánchez-Arriaga, E. Canzini, N. J. Espley-Plumb, M. Farnsworth, S. Pope, A. Leyland, and A. Tiwari, "Enhancing thin-film wafer inspection with a multi-sensor array and robot constraint maintenance," *arXiv preprint arXiv:2503.05853*, 2025. [Online]. Available: https://arxiv.org/abs/2503.05853.

[10] R. Mohandas, P. Mongan, and M. Hayes, "Ultrasonic weld quality inspection involving strength prediction and defect detection in data-constrained training environments," *Sensors*, vol. 24, no. 20, p. 6553, 2024, doi: 10.3390/s24206553.

[11] S. Grahn, V. Gopinath, X. V. Wang, and K. Johansen, "Exploring a model for production system design to utilize large robots in human–robot collaborative assembly cells," *Procedia Manuf.*, vol. 25, pp. 612–619, 2018, doi: 10.1016/j.promfg.2018.06.094.

[12] "Executive Summart World Robotics 2020 Industrial Robots," https://ifr.org/img/worldrobotics/Executive_Summary_WR_2020_Industrial_Robots_1.pdf, 2020].

[13] V. Villani, F. Pini, F. Leali, and C. Secchi, “Survey on human–robot collaboration in industrial settings: Safety, intuitive interfaces and applications,” *Mechatronics*, vol. 55, pp. 248–266, 2018, doi: 10.1016/j.mechatronics.2018.02.009.

[14] M. A. Goodrich and A. C. Schultz, “Human–robot interaction: A survey,” *Found. Trends Hum.-Comput. Interact.*, vol. 1, no. 3, pp. 203–275, 2007, doi: 10.1561/1100000005.

[15] A. Hentout, M. Aouache, A. Maoudj, and I. Akli, “Human–robot interaction in industrial collaborative robotics: A literature review of the decade 2008–2017,” *Adv. Robot.*, vol. 33, no. 15–16, pp. 764–799, 2019, doi: 10.1080/01691864.2019.1636714.

[16] L. Wang, R. Gao, J. Váncza, J. Krüger, X. V. Wang, S. Makris, and G. Chryssolouris, “Symbiotic human–robot collaborative assembly,” *CIRP Ann.—Manuf. Technol.*, vol. 68, no. 2, pp. 701–726, 2019, doi: 10.1016/j.cirp.2019.05.002.

[17] C. Gaz, E. Magrini, and A. De Luca, “A model-based residual approach for human–robot collaboration during manual polishing operations,” *Mechatronics*, vol. 55, pp. 234–247, Nov. 2018, doi: 10.1016/j.mechatronics.2018.02.014

[18] S. Mikhel, D. Popov, S. Mamedov, and A. Klimchik, “Development of typical collision reactions in combination with algorithms for external impacts

identification," *IFAC-PapersOnLine*, vol. 52, no. 13, pp. 253–258, 2019, doi: 10.1016/j.ifacol.2019.11.177.

[19] E. Magrini, F. Ferraguti, A. J. Rongo, F. Pini, A. De Luca, and F. Leali, "Human–robot coexistence and interaction in open industrial cells," *Robot. Comput.-Integr. Manuf.*, vol. 61, p. 101846, Feb. 2020, doi: 10.1016/j.rcim.2019.101846.

[20] Z. Huang, Y.-J. Mun, X. Li, Y. Xie, N. Zhong, W. Liang, J. Geng, T. Chen, and K. Driggs-Campbell, "Seamless interaction design with coexistence and cooperation modes for robust human–robot collaboration," *arXiv preprint arXiv:2206.01775*, 2022. [Online]. Available: https://arxiv.org/abs/2206.01775.

[21] T. Mina, S. S. Kannan, W. Jo, and B.-C. Min, "Adaptive workload allocation for multi-human multi-robot teams for independent and homogeneous tasks," *IEEE Access*, vol. 8, pp. 152697–152712, 2020, doi: 10.1109/ACCESS.2020.3017659.

[22] A.-B. Karami, L. Jeanpierre, and A. Mouaddib, "Human–robot collaboration for a shared mission," in *Proc. 5th ACM/IEEE Int. Conf. Human–Robot Interaction (HRI)*, 2010, pp. 155–156, doi: 10.1109/HRI.2010.5453219.

[23] F. Flacco, T. Kröger, A. De Luca, *et al.*, "A depth space approach for evaluating distance to objects," *J. Intell. Robot. Syst.*, vol. 80, suppl. 1, pp. 7–22, 2015, doi: 10.1007/s10846-014-0146-2

[24] Fujii, M., Murakami, H., & Sonehara, M., "Study on application of a human-robot collaborative system using hand-guiding in a production line," *IHI Engineering Review*, vol. 49, no. 1, pp. 24–29, 2016..

[25] F. Semeraro, A. Griffiths, and A. Cangelosi, “Human–robot collaboration and machine learning: A systematic review of recent research,” *Robot. Comput.-Integr. Manuf.*, vol. 79, p. 102432, 2023, doi: 10.1016/j.rcim.2022.102432

[26] A. Mörtl, M. Lawitzky, A. Kucukyilmaz, M. Sezgin, C. Basdogan, and S. Hirche, “The role of roles: Physical cooperation between humans and robots,” *Int. J. Robot. Res.*, vol. 31, no. 13, pp. 1656–1674, 2012, doi: 10.1177/0278364912455366.

[27] X. V. Wang, A. Seira, and L. Wang, “Classification, personalised safety framework and strategy for human–robot collaboration,” in *Proc. 48th Int. Conf. Computers and Industrial Engineering (CIE)*, Dec. 2–5, 2018, Curran Associates, Inc., pp. 2302–2311.

[28] Y. Liu, G. Caldwell, M. Rittenbruch, M. B. F. Teixeira, A. Burden, and M. Guertler, “What affects human decision making in human–robot collaboration?: A scoping review,” *Robotics*, vol. 13, no. 2, p. 30, 2024, doi: 10.3390/robotics13020030.

[29] A. Baratta, A. Cimino, M. G. Gnoni, and F. Longo, “Human robot collaboration in Industry 4.0: A literature review,” *Procedia Comput. Sci.*, vol. 217, pp. 1887–1895, 2023, doi: 10.1016/j.procs.2022.12.389.

[30] S. G. Ponnambalam, Q. Chang, R. Y. Zhong, *et al.*, “Human–robot collaboration in the next generation manufacturing and logistics system,” *Flex. Serv. Manuf. J.*, vol. 35, pp. 975–978, 2023, doi: 10.1007/s10696-023-09506-w.

[31] W. Li, Y. Hu, Y. Zhou, and D. Pham, “Safe human–robot collaboration for industrial settings: A survey,” *J. Intell. Manuf.*, vol. 35, 2023, doi: 10.1007/s10845-023-02159-4.

[32] L. Pérez, E. Diez, R. Usamentiaga, and D. F. García, “Industrial robot control and operator training using virtual reality interfaces,” *Comput. Ind.*, vol. 109, pp. 114–120, Aug. 2019, doi: 10.1016/j.compind.2019.05.001.

[33] F. Saffre, H. Hildmann, E. Heikkilä, T. Malm, and D. Pakkala, “Dynamic and probabilistic safety zones for autonomous mobile robots operating near humans,” *Results Eng.*, vol. 23, p. 102731, Sept. 2024, doi: 10.1016/j.rineng.2024.102731.

[34] R. Gervasi, L. Mastrogiacomo, and F. Franceschini, “Towards the definition of a human–robot collaboration scale,” in *Proc. IES 2019 – Statistical Evaluation Systems at 360°: Techniques, Technologies and New Frontiers*, Rome, Italy, Jul. 4–5, 2019, pp. 75–80.

[35] M. Ronzoni, R. Accorsi, L. Botti, and R. Manzini, “A support-design framework for cooperative robots systems in labor-intensive manufacturing processes,” *J. Manuf. Syst.*, vol. 61, pp. 646–657, Oct. 2021, doi: 10.1016/j.jmsy.2021.10.008.

[36] J. de Gea Fernández, D. Mronga, M. Günther, T. Knobloch, M. Wikus, M. Schröer, M. Tramper, S. Stiene, E. Kirchner, V. Bargsten, T. Bänziger, J. Teiwes, T. Krüger, and F. Kirchner, “Multimodal sensor-based whole-body control for human–robot collaboration in industrial settings,” *Robot. Auton. Syst.*, vol. 94, pp. 102–119, Aug. 2017, doi: 10.1016/j.robot.2017.04.007.

[37] E. Matheson, R. Minto, E. G. G. Zampieri, M. Faccio, and G. Rosati, “Human–robot collaboration in manufacturing applications: A review,” *Robotics*, vol. 8, no. 4, p. 100, 2019, doi: 10.3390/robotics8040100.

[38] P. S. Parra, O. L. Calleros, and A. Ramirez-Serrano, “Human–robot collaboration systems: Components and applications,” in *Proc. 7th Int. Conf. Control Systems and Robotics (CDSR)*, Niagara Falls, ON, Canada, Nov. 9–11, 2020, Paper no. 150, pp. 1–9, doi: 10.11159/cdsr20.150

[39] M. Dhanda, B. A. Rogers, S. Hall, E. Dekoninck, and V. Dhokia, “Reviewing human–robot collaboration in manufacturing: Opportunities and challenges in the context of Industry 5.0,” *Robot. Comput.-Integr. Manuf.*, vol. 93, p. 102937, June 2025, doi: 10.1016/j.rcim.2024.102937.

[40] M. Lavit Nicora, R. Ambrosetti, G. Wiens, and I. Fassi, “Human–robot collaboration in smart manufacturing: Robot reactive behavior intelligence,” *J. Manuf. Sci. Eng.*, vol. 143, 2020, doi: 10.1115/1.4048950.

[41] P. Segura, O. Lobato, A. Ramirez-Serrano, and I. Soria, “Human–robot collaborative systems: Structural components for current manufacturing applications,” *Adv. Ind. Manuf. Eng.*, vol. 3, p. 100060, Sept. 2021, doi: 10.1016/j.aime.2021.100060.

[42] S. El Zaatari, M. Marei, W. Li, and Z. Usman, “Cobot programming for collaborative industrial tasks: An overview,” *Robot. Auton. Syst.*, vol. 116, pp. 162–180, June 2019, doi: 10.1016/j.robot.2019.03.003.

[43] P. K. Murali, K. Darvish, and F. Mastrogiovanni, “Deployment and evaluation of a flexible human–robot collaboration model based on AND/OR graphs in a

manufacturing environment," *Intell. Serv. Robot.*, vol. 13, pp. 439–457, 2020, doi: 10.1007/s11370-020-00332-9

[44] A. Castro, F. Silva, and V. Santos, "Trends of human–robot collaboration in industry contexts: Handover, learning, and metrics," *Sensors*, vol. 21, no. 12, p. 4113, 2021, doi: 10.3390/s21124113.

[45] X. V. Wang, Z. Kemény, J. Váncza, and L. Wang, "Human–robot collaborative assembly in cyber-physical production: Classification framework and implementation," *CIRP Ann.—Manuf. Technol.*, vol. 66, no. 1, pp. 5–8, 2017, doi: 10.1016/j.cirp.2017.04.101.

[46] C. E. Harriott, G. L. Buford, J. A. Adams, and T. Zhang, "Mental workload and task performance in peer-based human–robot teams," *J. Human-Robot Interact.*, vol. 4, no. 2, pp. 16–96, 2015, doi: 10.5898/JHRI.4.2.Harriott.

[47] J. Carlson and R. R. Murphy, "How UGVs physically fail in the field," *IEEE Trans. Robot.*, vol. 21, no. 3, pp. 423–437, June 2005, doi: 10.1109/TRO.2004.838027.

[48] M. Vasic and A. Billard, "Safety issues in human–robot interactions," in *Proc. IEEE Int. Conf. Robot. Autom. (ICRA)*, 2013, pp. 197–204, doi: 10.1109/ICRA.2013.6630576.

[49] J. V. S. Teixeira, A. M. Reis, F. B. Mendes, and L. G. L. Vergara, "Collaborative robots," in *Occupational and Environmental Safety and Health*, Cham, Switzerland: Springer Int. Publ., 2019, pp. 791–796.

[50] S. Hjorth and D. Chrysostomou, "Human–robot collaboration in industrial environments: A literature review on non-destructive disassembly," *Robot. Comput.-Integr. Manuf.*, vol. 73, p. 102208, Feb. 2022, doi: 10.1016/j.rcim.2021.102208.

[51] V. Villani, F. Pini, F. Leali, C. Secchi, and C. Fantuzzi, “Survey on human–robot interaction for robot programming in industrial applications,” *IFAC-PapersOnLine*, vol. 51, no. 11, pp. 66–71, 2018, doi: 10.1016/j.ifacol.2018.08.236.

[52] D. Andronas, G. Apostolopoulos, N. Fourtakas, and S. Makris, “Multi-modal interfaces for natural human–robot interaction,” *Procedia Manuf.*, vol. 54, pp. 197–202, 2021, doi: 10.1016/j.promfg.2021.07.030.

[53] R. R. Raffik, R. R. Sathya, V. Vaishali, S. Balavedhaa, and N. J. Lakshmi, “Industry 5.0: Enhancing human–robot collaboration through collaborative robots – A review,” in *Proc. 2nd Int. Conf. Advancements in Electrical, Electronics, Communication, Computing and Automation (ICAECA)*, Coimbatore, India, 2023, pp. 1–6, doi: 10.1109/ICAECA56562.2023.10201120.

[54] A. Rodić, I. Stevanović, and M. Jovanović, "Smart Cyber-Physical System to Enhance Flexibility of Production and Improve Collaborative Robot Capabilities – Mechanical Design and Control Concept," *Advances in Service and Industrial Robotics.* pp. 627-639.

[55] H. Liu and L. Wang, “Gesture recognition for human–robot collaboration: A review,” *Int. J. Ind. Ergon.*, vol. 68, pp. 355–367, Nov. 2018, doi: 10.1016/j.ergon.2017.02.004..

[56] T. Yu, J. Huang, and Q. Chang, “Optimizing task scheduling in human–robot collaboration with deep multi-agent reinforcement learning,” *J. Manuf. Syst.*, vol. 60, pp. 487–499, July 2021, doi: 10.1016/j.jmsy.2021.07.015.

[57] J. Arents, V. Abolins, J. Judvaitis, O. Vismanis, A. Oraby, and K. Ozols, “Human–robot collaboration trends and safety aspects: A systematic review,” *J. Sens. Actuator Netw.*, vol. 10, no. 3, p. 48, 2021, doi: 10.3390/jsan10030048.

[58] Z. Jiang, S. Yuan, J. Ma, and Q. Wang, “The evolution of production scheduling from Industry 3.0 through Industry 4.0,” *Int. J. Prod. Res.*, vol. 60, no. 11, pp. 3534–3554, June 2022, doi: 10.1080/00207543.2021.1925772.

[59] R. E. Haber Guerra, J. Jiménez, C. R. Peres, and J. Alique, “An investigation of tool-wear monitoring in a high-speed machining process,” *Sens. Actuators A Phys.*, vol. 116, pp. 539–545, Oct. 2004, doi: 10.1016/j.sna.2004.05.017..

[60] B. M. Hamad and M. K. Jawad, “The fourth industrial revolution: A historical and conceptual review,” *J. Econ. Admin. Sci.*, vol. 30, no. 141, pp. 154–172, 2024, doi: 10.33095/gh3a7g38.

[61] K. Vinitha, R. Ambrose Prabhu, R. Bhaskar, and R. Hariharan, “Review on industrial mathematics and materials at Industry 1.0 to Industry 4.0,” *Mater. Today Proc.*, vol. 33, pt. 7, pp. 3956–3960, 2020, doi: 10.1016/j.matpr.2020.06.331.

[62] K. R. Nayan, “Strategic roadmaps for digital transformation in manufacturing enterprises,” *Eur. J. Comput. Sci. Inf. Technol.*, vol. 13, no. 4, pp. 95–111, Apr. 2025, doi: 10.37745/ejcsit.2013/vol13n495111.

[63] V. Tripathi, S. Chattopadhyaya, A. Bhadauria, S. Sharma, C. Li, D. Y. Pimenov, K. Giasin, S. Singh, and G. D. Gautam, “An agile system to enhance productivity through a modified value stream mapping approach in Industry 4.0: A novel approach,” *Sustainability*, vol. 13, no. 21, Art. no. 11997, 2021, doi: 10.3390/su132111997.

[64] J. Lario, J. Mateos, F. Psarommatis, and Á. Ortiz, “Towards zero defect and zero waste manufacturing by implementing non-destructive inspection

technologies," *J. Manuf. Mater. Process.*, vol. 9, no. 2, Art. no. 29, 2025, doi: 10.3390/jmmp9020029.

[65] A. Billey and T. Wuest, "Energy digital twins in smart manufacturing systems: A case study," *Robot. Comput.-Integr. Manuf.*, vol. 88, Art. no. 102729, Aug. 2024, doi: 10.1016/j.rcim.2024.102729.

[66] O. Givehchi, K. Landsdorf, P. Simoens, and A. Colombo, "Interoperability for industrial cyber-physical systems: An approach for legacy systems," *IEEE Trans. Ind. Informat.*, early access, Aug. 2017, doi: 10.1109/TII.2017.2740434.

[67] J. Zenisek, N. Wild, and J. Wolfartsberger, "Investigating the potential of smart manufacturing technologies," *Procedia Comput. Sci.*, vol. 180, pp. 507–516, 2021, doi: 10.1016/j.procs.2021.01.269.

[68] D. Jaspert, M. Ebel, A. Eckhardt, and J. Poeppelbuss, "Smart retrofitting in manufacturing: A systematic review," *J. Clean. Prod.*, vol. 312, Art. no. 127555, Aug. 2021, doi: 10.1016/j.jclepro.2021.127555.

[69] J. Posada, C. Toro, I. Barandiaran, D. Oyarzun, D. Stricker, R. de Amicis, E. B. Pinto, P. Eisert, J. Döllner, and I. Vallarino Jr., "Visual computing as a key enabling technology for Industrie 4.0 and Industrial Internet," *IEEE Comput. Graph. Appl.*, vol. 35, no. 2, pp. 26–40, Mar.–Apr. 2015, doi: 10.1109/MCG.2015.45.

[70] A. G. Frank, L. S. Dalenogare, and N. F. Ayala, "Industry 4.0 technologies: Implementation patterns in manufacturing companies," *Int. J. Prod. Econ.*, vol. 210, pp. 15–26, 2019, doi: 10.1016/j.ijpe.2019.01.004

[71] B. Meindl, N. F. Ayala, J. Mendonça, and A. G. Frank, “The four smarts of Industry 4.0: Evolution of ten years of research and future perspectives,” *Technol. Forecast. Soc. Change*, vol. 168, Art. no. 120784, 2021, doi: 10.1016/j.techfore.2021.120784.

[72] T. Kotsiopoulos, P. Sarigiannidis, D. Ioannidis, and D. Tzovaras, “Machine learning and deep learning in smart manufacturing: The smart grid paradigm,” *Comput. Sci. Rev.*, vol. 40, Art. no. 100341, May 2021, doi: 10.1016/j.cosrev.2020.100341.

[73] H. Wang, Z. Liu, D. Peng, and Y. Qin, “Understanding and learning discriminant features based on multiattention 1DCNN for wheelset bearing fault diagnosis,” *IEEE Trans. Ind. Informat.*, vol. 16, no. 9, pp. 5735–5745, Sep. 2020, doi: 10.1109/TII.2019.2955540.

[74] C. Scholl, A. Tobola, K. Ludwig, D. Zanca, and B. M. Eskofier, “A smart capacitive sensor skin with embedded data quality indication for enhanced safety in human–robot interaction,” *Sensors*, vol. 21, no. 21, Art. no. 7210, 2021, doi: 10.3390/s21217210.

[75] F. Liu, K. Puthuveetil, A. Padmanabha, K. Khokar, Z. Temel, and Z. Erickson, “SkinGrip: An adaptive soft robotic manipulator with capacitive sensing for whole-limb bed bathing assistance,” arXiv:2405.02772, 2025.

[76] C. Taesi, F. Aggogeri, and N. Pellegrini, “COBOT applications—Recent advances and challenges,” *Robotics*, vol. 12, no. 3, Art. no. 79, 2023, doi: 10.3390/robotics12030079.

[77] Y. Sun, W. Wang, Y. Chen, and Y. Jia, “Learn how to assist humans through human teaching and robot learning in human–robot collaborative assembly,”

IEEE Trans. Syst., Man, Cybern., Syst., vol. 52, no. 2, pp. 728–738, Feb. 2022, doi: 10.1109/TSMC.2020.3005340.

[78] P. Chutima, "Assembly line balancing with cobots: An extensive review and critiques," *Int. J. Ind. Eng. Comput.*, vol. 14, pp. 785–804, 2023, doi: 10.5267/j.ijiec.2023.7.001.

[79] J. de Assis, N. F. Ayala, and A. G. Frank, "Smart working in Industry 4.0: How digital technologies enhance manufacturing workers' activities," *Comput. Ind. Eng.*, vol. 163, Art. no. 107804, Jan. 2022, doi: 10.1016/j.cie.2021.107804.

[80] G. M. Costa, M. R. Petry, and A. P. Moreira, "Augmented reality for human–robot collaboration and cooperation in industrial applications: A systematic literature review," *Sensors*, vol. 22, no. 7, Art. no. 2725, Apr. 2022, doi: 10.3390/s22072725.

[81] R. Lunding, S. Hubenschmid, T. Feuchtner, *et al.*, "ARTHUR: Authoring human–robot collaboration processes with augmented reality using hybrid user interfaces," *Virtual Real.*, vol. 29, Art. no. 73, 2025, doi: 10.1007/s10055-025-01149-6.

[82] W. Kritzinger, M. Karner, G. Traar, J. Henjes, and W. Sihn, "Digital twin in manufacturing: A categorical literature review and classification," *IFAC-PapersOnLine*, vol. 51, no. 11, pp. 1016–1022, 2018, doi: 10.1016/j.ifacol.2018.08.474.

[83] S. Mihai, W. Davis, D. Hung, R. Trestian, M. Karamanoglu, B. Barn, R. Prasad, H. Venkataraman, and H. Nguyen, *A digital twin framework for predictive maintenance in Industry 4.0*, 2021.

[84] J. Wang, X. Niu, R. X. Gao, Z. Huang, and R. Xue, “Digital twin-driven virtual commissioning of machine tool,” *Robot. Comput.-Integr. Manuf.*, vol. 81, Art. no. 102499, Jun. 2023, doi: 10.1016/j.rcim.2022.102499.

[85] I. Compagnucci, B. Re, E. Serral Asensio, and M. Snoeck, “A digital process twin conceptual architecture for what-if process analysis,” in *Enterprise Design, Operations, and Computing. EDOC 2024 Workshops*, Springer, 2025.. pp. 373-388.

[86] A. A. Malik and A. Brem, “Digital twins for collaborative robots: A case study in human–robot interaction,” *Robot. Comput.-Integr. Manuf.*, vol. 68, Art. no. 102092, Apr. 2021, doi: 10.1016/j.rcim.2020.102092.

[87] S. Ma, W. Ding, Y. Liu, S. Ren, and H. Yang, “Digital twin and big data-driven sustainable smart manufacturing based on information management systems for energy-intensive industries,” *Appl. Energy*, vol. 326, Art. no. 119986, Nov. 2022, doi: 10.1016/j.apenergy.2022.119986.

[88] X. Ma, Q. Qi, J. Cheng, and F. Tao, “A consistency method for digital twin model of human–robot collaboration,” *J. Manuf. Syst.*, vol. 65, pp. 550–563, Oct. 2022, doi: 10.1016/j.jmsy.2022.10.012.

[89] S. Grabowska, “Smart factories in the age of Industry 4.0,” *Manag. Syst. Prod. Eng.*, vol. 28, no. 2, pp. 90–96, 2020, doi: 10.2478/mspe-2020-0014.

[90] J. Singh, C. Banerjee, and S. K. Pandey, “Smart automation in manufacturing process using industrial internet of things (IIoT) architecture,” *Innov. Syst. Softw. Eng.*, vol. 19, pp. 15–22, 2023, doi: 10.1007/s11334-022-00504-z.

[91] F. Semeraro, A. Griffiths, and A. Cangelosi, “Human–robot collaboration and machine learning: A systematic review of recent research,” *Robot. Comput.-*

Integr. Manuf., vol. 79, Art. no. 102432, Feb. 2023, doi: 10.1016/j.rcim.2022.102432.

[92] I.-J. Ding and J.-L. Su, "Designs of human–robot interaction using depth sensor-based hand gesture communication for smart material-handling robot operations," *Proc. Inst. Mech. Eng., Part B: J. Eng. Manuf.*, vol. 237, no. 3, pp. 392–413, 2022, doi: 10.1177/09544054221102247.

[93] H. Zhou, G. Yang, B. Wang, X. Li, R. Wang, X. Huang, H. Wu, and X. V. Wang, "An attention-based deep learning approach for inertial motion recognition and estimation in human–robot collaboration," *J. Manuf. Syst.*, vol. 67, pp. 97–110, Apr. 2023, doi: 10.1016/j.jmsy.2023.01.007

[94] M. Alatise and G. Hancke, "A review on challenges of autonomous mobile robot and sensor fusion methods," *IEEE Access*, early access, Feb. 2020, doi: 10.1109/ACCESS.2020.2975643.

[95] L. Ma, X. Yu, Y. Yang, Y. Hu, X. Zhang, H. Li, X. Ouyang, P. Zhu, R. Sun, and C.-P. Wong, "Highly sensitive flexible capacitive pressure sensor with a broad linear response range and finite element analysis of micro-array electrode," *J. Materiomics*, vol. 6, no. 2, pp. 321–329, Jun. 2020, doi: 10.1016/j.jmat.2019.12.008.

[96] W. Chen, Q. Yang, Q. Liu, Y. Zhang, L. He, Y. Xia, Z. Wang, Y. Huang, J. Chen, and C. Xia, "Study of a novel capacitive pressure sensor using spiral comb electrodes," arXiv:2407.08559, 2024.

[97] R. Likhite, A. Banerjee, A. Majumder, M. Karkhanis, H. Kim, and C. H. Mastrangelo, "Parametrically amplified low-power MEMS capacitive

humidity sensor," *Sensors*, vol. 19, no. 18, Art. no. 3954, 2019, doi: 10.3390/s19183954.

[98] L. Cha, S. Groß, S. Mao *et al.*, "Stretchable Capacitive and Resistive Strain Sensors: Accessible Manufacturing Using Direct Ink Writing," *arXiv preprint arXiv:2502.18363*, 2025.

[99] G. Stano, A. Di Nisio, A. M. Lanzolla, *et al.*, "Additive manufacturing for capacitive liquid level sensors," *Int. J. Adv. Manuf. Technol.*, vol. 123, pp. 2519–2529, 2022, doi: 10.1007/s00170-022-10344-7.

[100] D. Zhao, J. Ji, J.-S. Zhao, S. Y. Misyurin, and D. Martins, "Applications and design methodology of mobile robotic manipulators," *Proc. Inst. Mech. Eng., Part C: J. Mech. Eng. Sci.*, vol. 239, no. 18, pp. 7285–7306, 2025, doi: 10.1177/09544062251347212

[101] J. Cheng, O. Amft, G. Bahle, and P. Lukowicz, "Designing sensitive wearable capacitive sensors for activity recognition," *IEEE Sens. J.*, vol. 13, no. 10, pp. 3935–3947, Oct. 2013, doi: 10.1109/JSEN.2013.2259693..

[102] W. Shan, "Soft-matter capacitive sensor for measuring pressure and shear deformation in two directions," in *Proc. IEEE Int. Conf. Robot. Autom. (ICRA)*, 2013, doi: 10.1109/ICRA.2013.6631071.

[103] R. B. Mishra, N. El-Atab, A. M. Hussain, and M. M. Hussain, "Recent progress on flexible capacitive pressure sensors: From design and materials to applications," *Adv. Mater. Technol.*, 2021, Art. no. 2001023, doi: 10.1002/admt.202001023.

[104] H. N. Dac, D. N. Anh, T. V. Quoc, D. Q. Tham, K. H. Manh, and T. C. Duc, "Non-destructive thin film thickness measurement based on coplanar

capacitive sensor and printed circuit board platform," *IETE J. Res.*, vol. 70, no. 8, pp. 7014–7024, 2024, doi: 10.1080/03772063.2024.2315209.

[105] G. E. Thorncroft and J. F. Klausner, "A capacitance sensor for two-phase liquid film thickness measurements in a square duct," *J. Fluids Eng.*, vol. 119, no. 1, pp. 164–169, Mar. 1997, doi: 10.1115/1.2819103.

[106] P. Wang, E. Fan, and P. Wang, "Comparative analysis of image classification algorithms based on traditional machine learning and deep learning," *Pattern Recognit. Lett.*, vol. 141, pp. 61–67, Jan. 2021, doi: 10.1016/j.patrec.2020.07.042.

[107] T. Brito, J. Queiroz, L. Piardi, L. A. Fernandes, J. Lima, and P. Leitão, "A machine learning approach for collaborative robot smart manufacturing inspection for quality control systems," *Procedia Manuf.*, vol. 51, pp. 11–18, 2020, doi: 10.1016/j.promfg.2020.10.003.

[108] M. Moor, M. Sarkans, T. Kangru, T. Otto, and J. Riives, "AI functionalities in cobot-based manufacturing for performance improvement in quality control application," *J. Mach. Eng.*, vol. 24, no. 2, pp. 44–55, 2024, doi: 10.36897/jme/189169.

[109] J. Sun, C. Li, X.-J. Wu, V. Palade, and W. Fang, "An effective method of weld defect detection and classification based on machine vision," *IEEE Trans. Ind. Informat.*, vol. 15, no. 12, pp. 6322–6333, Dec. 2019, doi: 10.1109/TII.2019.2896357.

[110] Z. Ren, F. Fang, N. Yan, *et al.*, "State of the art in defect detection based on machine vision," *Int. J. Precis. Eng. Manuf.-Green Technol.*, vol. 9, pp. 661–691, 2022, doi: 10.1007/s40684-021-00343-6.

[111] X. Tao, H. Gao, Q. Wu, C. He, L. Zhang, and Y. Zhao, “Detection of defects in adhesive coating based on machine vision,” *IEEE Sens. J.*, vol. 24, no. 4, pp. 5172–5185, Feb. 2024, doi: 10.1109/JSEN.2023.3344124.

[112] H. Zhao, Y. Lv, J. Sha, R. Peng, Z. Chen, and G. Wang, “Research on detection method of coating defects based on machine vision,” in *Proc. IEEE Int. Conf. Artif. Intell. Comput. Appl. (ICAICA)*, pp. 519–524, Jun. 2021, doi: 10.1109/ICAICA52286.2021.9498238.

[113] P. ForouzeshFar, A. A. Safaei, F. Ghaderi, *et al.*, “Dental caries diagnosis from bitewing images using convolutional neural networks,” *BMC Oral Health*, vol. 24, Art. no. 211, 2024, doi: 10.1186/s12903-024-03973-9.

[114] W. Wahyuningsih, G. S. Nugraha, and R. Dwiyansaputra, “Classification of dental caries disease in tooth images using a comparison of EfficientNet-B0, MobileNetV2, ResNet-50, InceptionV3 architectures,” *J. Tek. Inform. (JUTIF)*, vol. 5, no. 4, pp. 177–185, 2024, doi: 10.52436/1.jutif.2024.5.4.2187.

[115] V. Sharma, D. Sharma, M.-L. Tsai, R. G. G. Ortiz, A. Yadav, P. Nagrota, C.-W. Chen, P.-P. Sun, and C.-D. Dong, “Insights into the recent advances of agro-industrial waste valorization for sustainable biogas production,” *Bioresour. Technol.*, vol. 390, Art. no. 129829, Dec. 2023, doi: 10.1016/j.biortech.2023.129829.

[116] M. Bouamar and M. Ladjal, “Evaluation of the performances of ANN and SVM techniques used in water quality classification,” in *Proc. IEEE Int. Conf. Electron. Circuits Syst. (ICECS)*, pp. 1047–1050, 2007, doi: 10.1109/ICECS.2007.4511173.

[117] H. Bhavsar and M. H. Panchal, “A review on support vector machine for data classification,” *Int. J. Adv. Res. Comput. Eng. Technol.*, vol. 1, no. 10, Dec. 2012.

[118] M. Galindo-Salcedo, A. Pertúz-Moreno, S. Guzmán-Castillo, Y. Gómez-Charris, and A. R. Romero-Conrado, “Smart manufacturing applications for inspection and quality assurance processes,” *Procedia Comput. Sci.*, vol. 198, pp. 536–541, 2022, doi: 10.1016/j.procs.2021.12.282.

[119] Z. Lončarević, S. Reberšek, S. Šela, J. Skvarč, A. Ude, and A. Gams, “Adaptive visual quality inspection based on defect prediction from production parameters,” *IEEE Access*, vol. 12, pp. 93899–93910, 2024, doi: 10.1109/ACCESS.2024.3424664.

[120] A. Papavasileiou, G. Michalos, and S. Makris, “Quality control in manufacturing – review and challenges on robotic applications,” *International Journal of Computer Integrated Manufacturing*, vol. 38, no. 1, pp. 79–115, 2025, doi: 10.1080/0951192X.2024.2314789.

[121] K. K. Kieselbach, M. Nöthen, and H. Heuer, “Development of a visual inspection system and the corresponding algorithm for the detection and subsequent classification of paint defects on car bodies in the automotive industry,” *J. Coat. Technol. Res.*, vol. 16, pp. 1033–1042, 2019, doi: 10.1007/s11998-018-00178-y.

[122] P. Visser, H. Terryn, and J. M. C. Mol, “Aerospace coatings,” in *Active Protective Coatings*, A. Hughes, J. Mol, M. Zheludkevich, and R. Buchheit, Eds., Springer Ser. Mater. Sci., vol. 233. Dordrecht, The Netherlands: Springer, 2016, doi: 10.1007/978-94-017-7540-3_12.

[123] M.-R. Pendar, F. Rodrigues, J. C. Páscoa, and R. Lima, “Review of coating and curing processes: Evaluation in automotive industry,” *Phys. Fluids*, vol. 34, no. 10, Art. no. 101301, Oct. 2022, doi: 10.1063/5.0109376.

[124] S. Sacher and J. G. Khinast, “An overview of pharmaceutical manufacturing for solid dosage forms,” in *Process Simulation and Data Modeling in Solid Oral Drug Development and Manufacture*, Methods in Pharmacology and Toxicology. New York, NY, USA: Springer, 2016, doi: 10.1007/978-1-4939-2996-2_10.

[125] A. N. Zaid, “A comprehensive review on pharmaceutical film coating: Past, present, and future,” *Drug Des. Devel. Ther.*, vol. 14, pp. 4613–4623, 2020, doi: 10.2147/DDDT.S277439.

[126] R. Accorsi, A. Tufano, A. Gallo, F. G. Galizia, G. Cocchi, M. Ronzoni, A. Abbate, and R. Manzini, “An application of collaborative robots in a food production facility,” *Procedia Manuf.*, vol. 38, pp. 341–348, 2019, doi: 10.1016/j.promfg.2020.01.044.

[127] S. Bakalis, D. Georgogis, D. Argyropoulos, and C. Emmanouilidis, “Food Industry 4.0: Opportunities for a digital future,” in *Food Engineering Innovations Across the Food Supply Chain*, 2022, pp. 357–368, doi: 10.1016/B978-0-12-821292-9.00011-X.

[128] J. Miranda, P. Ponce, A. Molina, and P. Wright, “Sensing, smart and sustainable technologies for Agri-Food 4.0,” *Comput. Ind.*, vol. 108, pp. 21–36, Jun. 2019, doi: 10.1016/j.compind.2019.02.002.

[129] V. Subramanian, “Predictive analytics in cold chain packaging for reducing spoilage using linear regression,” in *Proceedings of the IEEE International*

Conference on Electronics, Automation, and Modern Science and Technology (ICEAMST), 2025, doi: 10.1109/ICEAMST67459.2025.11335633.

[130] W. Grobbelaar, A. Verma, and V. Shukla, "Analyzing human robotic interaction in the food industry," *J. Phys.: Conf. Ser.*, vol. 1714, Art. no. 012032, 2021, doi: 10.1088/1742-6596/1714/1/012032.

[131] P. Tsarouchi, A. S. Matthaiakis, S. Makris, and G. Chryssolouris, "On a human–robot collaboration in an assembly cell," *Int. J. Comput. Integr. Manuf.*, vol. 30, no. 6, pp. 580–589, 2017, doi: 10.1080/0951192X.2016.1187297

[132] T. M. Barnes, D. Mijaljica, J. P. Townley, F. Spada, and I. P. Harrison, "Vehicles for drug delivery and cosmetic moisturizers: Review and comparison," *Pharmaceutics*, vol. 13, no. 12, Art. no. 2012, Nov. 2021, doi: 10.3390/pharmaceutics13122012..

[133] K. Al-Smadi, M. Ali, J. Zhu, A. Abdoh, K. Phan, and Y. Mohammed, "Advances in characterization of transdermal and topical products using texture analyzer systems," *AAPS PharmSciTech*, vol. 26, no. 5, Art. no. 157, 2025, doi: 10.1208/s12249-025-03148-X.

[134] M. Steiner-Browne, N. A. K. Aramouni, and R. Mouras, "Experimental design of a film flow cleaning rig equipped with in-line process analytical technology (PAT) tool for real-time monitoring," *Heliyon*, vol. 10, no. 15, Art. no. e34679, 2024, doi: 10.1016/j.heliyon.2024.e34679.

[135] G. Kokotinis, G. Michalos, Z. Arkouli, and S. Makris, "On the quantification of human–robot collaboration quality," *Int. J. Comput. Integr. Manuf.*, vol. 36, no. 10, pp. 1431–1448, 2023, doi: 10.1080/0951192X.2023.2189304.

[136] M. Faccio and Y. Cohen, “Intelligent cobot systems: human-cobot collaboration in manufacturing,” *J. Intell. Manuf.*, vol. 35, May 2023, doi: 10.1007/s10845-023-02142-z.

[137] S. Puttero, E. Verna, G. Genta, *et al.*, “Collaborative robots for quality control: An overview of recent studies and emerging trends,” *Journal of Intelligent Manufacturing*, 2025, doi: 10.1007/s10845-025-02600-w.

[138] A. Keshvarparast, D. Battini, O. Battaia, and A. Pirayesh, “Collaborative robots in manufacturing and assembly systems: literature review and future research agenda,” J. Intell. Manuf., vol. 35, no. 5, pp. 2065–2118, 2024, doi: 10.1007/s10845-023-02137-w.

[139] S. Wang and R. J. Jiao, “Smart in-process inspection in human–cyber–physical manufacturing systems: A research proposal on human–automation symbiosis and its prospects,” Machines, vol. 12, no. 12, 2024, Art. no. 873, doi: 10.3390/machines12120873.

[140] S. Niese and J. Quodbach, “Application of a chromatic confocal measurement system as new approach for in-line wet film thickness determination in continuous oral film manufacturing processes,” Int. J. Pharm., vol. 551, no. 1–2, pp. 203–211, Nov. 2018, doi: 10.1016/j.ijpharm.2018.09.028.

[141] A. Abdalla, M. Faraj, F. Samsuri, D. Rifai, K. Ali, and Y. Al-Douri, “Challenges in improving the performance of eddy current testing: Review,” *Meas. Control*, vol. 52, 2019, Art. no. 002029401880138, doi: 10.1177/0020294018801382.

[142] F. Vicentini, “Collaborative robotics: A survey,” *J. Mech. Des.*, vol. 143, no. 4, Art. no. 040802, 2021, doi: 10.1115/1.4046238.

[143] M. M. Rahman, F. Khatun, I. Jahan, R. Devnath, and M. A. A. Bhuiyan, “Cobotics: The evolving roles and prospects of next-generation collaborative robots in Industry 5.0,” *J. Robot.*, vol. 2024, Art. no. 2918089, 2024, doi: 10.1155/2024/2918089.

[144] B. de Moura, A. da Mata, M. Ferreira Martins, F. Sepulveda, and R. Ramos, “A novel methodology to measure the film thickness profile based on current stimulation for two-phase flow,” *Meas. Sci. Technol.*, vol. 32, 2021, doi: 10.1088/1361-6501/ac2437

[145] K. Su, Y.-C. Shen, and J. A. Zeitler, “Terahertz sensor for non-contact thickness and quality measurement of automobile paints of varying complexity,” *IEEE Trans. Terahertz Sci. Technol.*, vol. 4, no. 4, pp. 432–439, Jul. 2014, doi: 10.1109/TTHZ.2014.2325393.

[146] H. E. Farag, E. Toyserkani, and M. B. Khamesee, “Non-destructive testing using eddy current sensors for defect detection in additively manufactured titanium and stainless-steel parts,” *Sensors*, vol. 22, no. 14, Art. no. 5440, 2022, doi: 10.3390/s22145440.

[147] C. Urrea and J. Kern, “Recent advances and challenges in industrial robotics: A systematic review of technological trends and emerging applications,” *Processes*, vol. 13, no. 3, Art. no. 832, 2025, doi: 10.3390/pr13030832.

[148] S. Patil, V. Vasu, and K. V. S. Srinadh, “Advances and perspectives in collaborative robotics: A review of key technologies and emerging trends,” *Discover Mech. Eng.*, vol. 2, Art. no. 13, 2023, doi: 10.1007/s44245-023-00021-8.

[149] S. Heinlein, S. Mariani, J. Milewczyk *et al.*, “Improved thickness measurement on rough surfaces by using guided wave cut-off frequency,” *NDT & E International,* vol. 132, pp. 102713, 2022.

[150] X. Chen, J. He, and S. Wang, “Deep learning-driven pathology detection and analysis in historic masonry buildings of Suzhou,” *npj Herit. Sci.*, vol. 13, Art. no. 197, 2025, doi: 10.1038/s40494-025-01783-y.

[151] U. Hudomalj, E. Fallahi Sichani, L. Weiss, *et al.*, “In situ spatially resolved coating thickness measurements in thermal spraying,” *J. Therm. Spray Technol.*, vol. 33, pp. 806–818, 2024, doi: 10.1007/s11666-023-01656-5..

[152] T. Czimmermann, G. Ciuti, M. Milazzo, M. Chiurazzi, S. Roccella, C. M. Oddo, and P. Dario, “Visual-based defect detection and classification approaches for industrial applications—A survey,” *Sensors*, vol. 20, no. 5, Art. no. 1459, 2020, doi: 10.3390/s20051459.

[153] R. K. May, M. J. Evans, S. Zhong, L. F. Gladden, Y. Shen, and J. A. Zeitler, “Terahertz in-line sensor for direct coating thickness measurement of individual tablets during film coating in real-time,” *J. Pharm. Sci.*, vol. 100, no. 4, pp. 1535–1544, Apr. 2011, doi: 10.1002/jps.22356.

[154] N. Vieweg, N. Regner, K. Dutzi, *et al.*, “Online thickness measurements of acrylate based coatings on knitted polyester fabric using terahertz time domain spectroscopy,” *Journal of Industrial Textiles*, vol. 53, 2023, doi: 10.1177/15280837231207396.

[155] A. Karimi, Z. B. Harris, E. Heller *et al.*, “Measurement of Multilayer Coating Thickness on Interwoven Carbon-Fiber-Reinforced Polymers Using the Terahertz PHASR Scanner,” *arXiv preprint arXiv:2505.08172*, 2025.

[156] W. Cai, M. Bondy, B. Carlson, and M. Baylis, “Prediction of automotive body-in-white distortion in paint baking process,” *Manuf. Lett.*, vol. 41, suppl., pp. 270–280, Oct. 2024, doi: 10.1016/j.mfglet.2024.09.032.

[157] G. Le Lay and A. Daerr, “Controlling deposition and characterizing dynamics of thin liquid films with high temporal and spatial resolution,” *Phys. Fluids*, vol. 37, no. 6, Art. no. 062101, Jun. 2025, doi: 10.1063/5.0268672.

[158] N. Bai, Y. Xue, S. Chen, *et al.*, “A robotic sensory system with high spatiotemporal resolution for texture recognition,” *Nat. Commun.*, vol. 14, Art. no. 7121, 2023, doi: 10.1038/s41467-023-42722-4.

[159] D. Liu, W. Zhang, Y. Tang, Y. Jian, C. Gong, and F. Qiu, “Evaluation of the uniformity of protective coatings on concrete structure surfaces based on cluster analysis,” *Sensors*, vol. 21, no. 16, Art. no. 5652, Aug. 2021, doi: 10.3390/s21165652.

[160] C. Han, J. Lee, M. B. G. Jun, *et al.*, “Visual coating inspection framework via self-labeling and multi-stage deep learning strategies,” *J. Intell. Manuf.*, vol. 36, pp. 2461–2478, 2025, doi: 10.1007/s10845-024-02372-9.

[161] Z. Li, Y. Yan, X. Wang, *et al.*, “A survey of deep learning for industrial visual anomaly detection,” *Artif. Intell. Rev.*, vol. 58, Art. no. 279, 2025, doi: 10.1007/s10462-025-11287-7.

[162] Y. Hu, Y. Wang, K. Hu, and W. Li, “Adaptive obstacle avoidance in path planning of collaborative robots for dynamic manufacturing,” *J. Intell. Manuf.*, vol. 34, no. 2, pp. 789–807, Feb. 2023, doi: 10.1007/s10845-021-01825-9.

[163] M. Haseeb, H. I. Hussain, B. Ślusarczyk, and K. Jermsittiparsert, “Industry 4.0: A solution towards technology challenges of sustainable business

performance," *Social Sciences*, vol. 8, no. 5, Art. no. 154, 2019, doi: 10.3390/socsci8050154.

[164] M. Ingaldi and R. Ulewicz, "Problems with the implementation of Industry 4.0 in enterprises from the SME sector," *Sustainability*, vol. 12, no. 1, Art. no. 217, 2020, doi: 10.3390/su12010217.

[165] K.-Y. Shin and H.-C. Park, "Smart manufacturing systems engineering for designing smart product-quality monitoring system in the Industry 4.0," in *Proc. IEEE Int. Conf. Control, Autom. Comput. Sci. (ICCAS)*, pp. 1693–1698, Oct. 2019, doi: 10.23919/ICCAS47443.2019.8971667.

[166] L. Wang, S. Liu, H. Liu, and X. Wang, "Overview of human robot collaboration in manufacturing," in *Human Robot Collaboration in Manufacturing*, Cham, Switzerland: Springer, 2020, pp. 15–58, doi: 10.1007/978-3-030-46212-3_2

[167] D. V. Enrique, J. C. M. Druczkoski, T. M. Lima, and F. Charrua-Santos, "Advantages and difficulties of implementing Industry 4.0 technologies for labor flexibility," *Procedia Comput. Sci.*, vol. 181, pp. 347–352, 2021, doi: 10.1016/j.procs.2021.01.177.

[168] R. Arrais, C. Costa, P. Ribeiro, L. Rocha, M. Silva, and G. Veiga, "On the development of a collaborative robotic system for industrial coating cells," *Int. J. Adv. Manuf. Technol.*, vol. 115, pp. 1–19, Jul. 2021, doi: 10.1007/s00170-020-06167-z.

[169] R. Wu, F. Zhou, N. Li, H. Liu, N. Guo, and R. Wang, "Enhanced You Only Look Once X for surface defect detection of strip steel," *Front. Neurorobot.*, vol. 16, Art. no. 1042780, 2022, doi: 10.3389/fnbot.2022.1042780.

[170] S. Y. Lee, B. A. Tama, S. J. Moon, and S. Lee, “Steel surface defect diagnostics using deep convolutional neural network and class activation map,” *Appl. Sci.*, vol. 9, no. 24, Art. no. 5449, 2019, doi: 10.3390/app9245449.

[171] J. Wang, T. Chen, X. Xu, L. Zhao, D. Yuan, Y. Du, X. Guo, and N. Chen, “An improved YOLOv8 model for strip steel surface defect detection,” *Appl. Sci.*, vol. 15, no. 1, Art. no. 52, 2025, doi: 10.3390/app15010052.

[172] Y. Cai, Y. Gao, Y. Zhuang, S. Wu, F. Chen, Y. Jin, P. Zhu, L. Qin, and Y. Su, “Advances in measurement and simulation methods of thin liquid film corrosion,” *Materials*, vol. 18, no. 19, p. 4479, 2025, doi: 10.3390/ma18194479.

[173] B. Huang, J. Liu, Q. Zhang, K. Liu, X. Liu, and J. Wang, “Improved Faster R-CNN network for liquid bag foreign body detection,” *Processes*, vol. 11, no. 8, Art. no. 2364, 2023, doi: 10.3390/pr11082364.

[174] J. M. Davis, B. J. Fischer, and S. M. Troian, “A general approach to the linear stability of thin spreading films,” in *Interfacial Fluid Dynamics and Transport Processes*, R. Narayanan and D. Schwabe, Eds., Lecture Notes in Physics, vol. 628. Berlin, Heidelberg, Germany: Springer, 2003. doi: 10.1007/978-3-540-45095-5_5.

[175] Y. Hu, A. Gillespie, A. Padmanabha *et al.*, “RoboCAP: Robotic Classification and Precision Pouring of Diverse Liquids and Granular Media with Capacitive Sensing,” *arXiv preprint arXiv:2405.07423*, 2024.

[176] M. Javaid, A. Haleem, R. P. Singh, S. Rab, and R. Suman, “Significance of sensors for Industry 4.0: Roles, capabilities, and applications,” *Sens. Int.*, vol. 2, Art. no. 100110, 2021, doi: 10.1016/j.sintl.2021.100110.

[177] T. C. Callari, Y. Curzi, and N. Lohse, “Realising human-robot collaboration in manufacturing? A journey towards Industry 5.0 amid organisational paradoxical tensions,” *Technol. Forecast. Soc. Change*, vol. 219, Art. no. 124249, 2025, doi: 10.1016/j.techfore.2025.124249.

[178] K. He, X. Zhang, S. Ren, and J. Sun, “Deep residual learning for image recognition,” in *Proc. IEEE Conf. Comput. Vis. Pattern Recognit. (CVPR)*, Las Vegas, NV, USA, Jun. 2016, pp. 770–778, doi: 10.1109/CVPR.2016.90.

[179] S. Bianco, R. Cadène, L. Celona, and P. Napoletano, “Benchmark analysis of representative deep neural network architectures,” *IEEE Access*, vol. 6, pp. 64270–64277, 2018, doi: 10.1109/ACCESS.2018.2877890.

[180] D. R. Soumya, D. L. K. Reddy, A. Nagar, and A. K. Rajpoot, “Enhancing brain tumor diagnosis: Utilizing ResNet-101 on MRI images for detection,” in *Proc. 2nd Int. Conf. Vision Towards Emerging Trends Commun. Netw. Technol. (ViTECoN)*, Vellore, India, May 2023, pp. 1–5, doi: 10.1109/ViTECoN58111.2023.10157378.

[181] W. Xie, W. Lin, P. Li, H. Lai, Z. Wang, P. Liu, Y. Huang, Y. Liu, L. Tang, and G. Lyu, “Developing a deep learning model for predicting ovarian cancer in Ovarian-Adnexal Reporting and Data System Ultrasound (O-RADS US) category 4 lesions: A multicenter study,” *Journal of Cancer Research and Clinical Oncology*, vol. 150, no. 7, p. 346, Jul. 2024, doi: 10.1007/s00432-024-05872-6.

[182] A. Lamberti, W. Van Eesbeeck, and S. Nardone, “Non-destructive inspection of additively manufactured classified components in a nuclear installation,” *NDT*, vol. 2, no. 3, pp. 228–248, 2024, doi: 10.3390/ndt2030014.

[183] L. Chen, G. Bi, X. Yao, J. Su, C. Tan, W. Feng, M. Benakis, Y. Chew, and S. Moon, “In-situ process monitoring and adaptive quality enhancement in laser additive manufacturing: A critical review,” *J. Manuf. Syst.*, vol. 74, pp. 527–574, Jun. 2024, doi: 10.1016/j.jmsy.2024.04.013.

[184] E. Micro. "Distance Sensors," https://www.micro-epsilon.co.uk/distance-sensors/ . Accessed: Oct. 20, 2024.

[185] E. Terzic, J. Terzic, R. Nagarajah, and M. Alamgir, “Capacitive sensing technology,” in *A Neural Network Approach to Fluid Quantity Measurement in Dynamic Environments*, London, U.K.: Springer, 2012, pp. 11–37, doi: 10.1007/978-1-4471-4060-3_2.

[186] J. Rawlins, “Chapter 6: Capacitance,” in *Applied Science and Technology Handbook*, Oxford, U.K.: Newnes, 2000, doi: 10.1016/B978-075067173-6/50007-9.

[187] C.-Y. Lee and C.-W. Chang, “Dielectric constant enhancement with low dielectric loss growth in graphene oxide/mica/polypropylene composites,” *J. Compos. Sci.*, vol. 5, no. 2, Art. no. 52, 2021, doi: 10.3390/jcs5020052.

[188] P. Industrial. "Baker Film Applicators," https://industrialphysics.com/product/baker-film-applicators/. Accessed: Aug. 05,2024.

[189] D. C. Montgomery, E. A. Peck, and G. G. Vining, *Introduction to Linear Regression Analysis*, 6th ed. Hoboken, NJ, USA: Wiley, Feb. 2021.

[190] K. Przystupa, “Research on the durability and reliability of industrial layered coatings on metal substrate due to abrasive wear,” *Materials*, vol. 16, no. 5, p. 1779, 2023, doi: 10.3390/ma16051779.

[191] M. Friedrichs, Z. Peng, T. Grunwald, M. Rohwerder, B. Gault, and T. Bergs, "PtIr protective coating system for precision glass molding tools: Design, evaluation and mechanism of degradation," *Surf. Coat. Technol.*, vol. 385, Art. no. 125378, 2020, doi: 10.1016/j.surfcoat.2020.125378.

[192] S. J. Shetty, "Vision-based inspection system employing computer vision & neural networks for detection of fractures in manufactured components," *arXiv preprint arXiv:1901.08864*, 2019.

[193] A. Papavasileiou, G. Michalos, and S. Makris, "Quality control in manufacturing—review and challenges on robotic applications," *Int. J. Comput. Integr. Manuf.*, vol. 38, no. 1, pp. 79–115, 2025, doi: 10.1080/0951192X.2024.2314789.

[194] M. Mazzetto, M. Teixeira, É. O. Rodrigues *et al.*, "Deep learning models for visual inspection on automotive assembling line," *arXiv preprint arXiv:2007.01857*, 2020.

[195] M. Shadwani, S. Sachan, and P. Sachan, *Capacitive sensing and its applications*, 2018, doi: 10.13140/RG.2.2.15752.32001.

[196] Y. Yu, L. Ma, H. Ye, Y. Zheng, and Y. Ma, "Design of instantaneous liquid film thickness measurement system for conductive or non-conductive fluid with high viscosity," *AIP Adv.*, vol. 7, no. 6, Art. no. 065207, 2017, doi: 10.1063/1.4985721.

Appendix A Vision System Implementation

Capture Images for Calibration

```
import cv2
import os

# Create a directory to save the captured images
output_dir = 'calibration_images'
if not os.path.exists(output_dir):
    os.makedirs(output_dir)

# Initialize webcam
cap = cv2.VideoCapture(1)

# Check if the webcam is opened correctly
if not cap.isOpened():
    print("Error: Could not open video capture.")
    exit()

print("Press 'c' to capture an image and 'q' to quit.")
image_counter = 0

while True:
    # Capture frame-by-frame
    ret, frame = cap.read()

    if not ret:
        print("Error: Could not read frame.")
        break

    # Display the frame
    cv2.imshow('Chessboard Capture', frame)
```

```
    # Wait for key press
    key = cv2.waitKey(1) & 0xFF

    if key == ord('c'):
        # Save the captured image
        img_filename = os.path.join(output_dir, f'image_{image_counter:05d}.jpg')
        cv2.imwrite(img_filename, frame)
        print(f'Captured {img_filename}')
        image_counter += 1

    elif key == ord('q'):
        # Quit the loop
        break

# Release the capture and close windows
cap.release()
cv2.destroyAllWindows()
```

Camera Calibration

```
import cv2

import numpy as np

import glob


# Define the chessboard size and prepare object points

chessboard_size = (7, 6)  # Adjust this if your chessboard has a different size

objp = np.zeros((np.prod(chessboard_size), 3), np.float32)

objp[:, :2] = np.mgrid[0:chessboard_size[0], 0:chessboard_size[1]].T.reshape(-1, 2)
```

```
# Arrays to store object points and image points from all images
objpoints = []
imgpoints = []

# Load images
images = glob.glob('C:\\Users\\oqbaz\\Desktop\\image-python\\MEDAQLib-
  5.0.0.32858\\Snippets\\Python\\Calibration_images\\calibration_images\\*.jpg')

if not images:
print("No images found. Please check the path.")
else:
print(f"Found {len(images)} images.")

for fname in images:
print(f"Processing image: {fname}")
img = cv2.imread(fname)
if img is None:
print(f"Failed to load image {fname}")
continue

# Display the image to check quality and contents
cv2.imshow('Loaded Image', img)
cv2.waitKey(1000)  # Display each image for 1 second
```

```
gray = cv2.cvtColor(img, cv2.COLOR_BGR2GRAY)

# Find the chessboard corners
ret, corners = cv2.findChessboardCorners(gray, chessboard_size, None)

if ret:
objpoints.append(objp)
imgpoints.append(corners)
print(f"Chessboard corners found in image {fname}")

# Draw and display the corners
img = cv2.drawChessboardCorners(img, chessboard_size, corners, ret)
cv2.imshow('Chessboard Corners', img)
cv2.waitKey(500)
else:
print(f"Chessboard corners not found in image {fname}")

cv2.destroyAllWindows()

if not objpoints:
print("No chessboard corners were found in any image. Please ensure the images
  contain a visible chessboard.")
else:
# Calibrate the camera
```

```
ret, camera_matrix, dist_coeffs, rvecs, tvecs = cv2.calibrateCamera(
objpoints, imgpoints, gray.shape[::-1], None, None)

# Save the calibration result
np.savez('calibration_data.npz',
camera_matrix=camera_matrix,
dist_coeffs=dist_coeffs,
rvecs=rvecs,
tvecs=tvecs)

print("Camera calibrated successfully!")
print("Camera matrix:\n", camera_matrix)
print("Distortion coefficients:\n", dist_coeffs)
```

Capture images for training and validation processes

```
import cv2
import os

# Create a directory to save the captured images
output_dir = 'calibration_images'
if not os.path.exists(output_dir):
    os.makedirs(output_dir)

# Initialize webcam
cap = cv2.VideoCapture(1)
```

```
# Check if the webcam is opened correctly
if not cap.isOpened():
    print("Error: Could not open video capture.")
    exit()

print("Press 'c' to capture an image and 'q' to quit.")

image_counter = 0

while True:
    # Capture frame-by-frame
    ret, frame = cap.read()

    if not ret:
        print("Error: Could not read frame.")
        break

    # Display the frame
    cv2.imshow('Chessboard Capture', frame)

    # Wait for key press
    key = cv2.waitKey(1) & 0xFF

    if key == ord('c'):
        # Save the captured image
        img_filename = os.path.join(output_dir, f'image_{image_counter:05d}.jpg')
        cv2.imwrite(img_filename, frame)
        print(f'Captured {img_filename}')
        image_counter += 1
```

```
    elif key == ord('q'):
        # Quit the loop
        break

# Release the capture and close windows
cap.release()
cv2.destroyAllWindows()
```

Split Images

```
import os
import random
import shutil

# Set your dataset directories
train_original_dir = r'C:\Users\oqbaz\OneDrive - University of Strathclyde\Uqba Othman\Conference Paper-II\Last Data set\dataset\train_original'
val_original_dir = r'C:\Users\oqbaz\OneDrive - University of Strathclyde\Uqba Othman\Conference Paper-II\Last Data set\dataset\val_original'

# Set new directories for training and validation
train_dir = r'C:\Users\oqbaz\OneDrive - University of Strathclyde\Uqba Othman\Conference Paper-II\Last Data set\dataset\train'
val_dir = r'C:\Users\oqbaz\OneDrive - University of Strathclyde\Uqba Othman\Conference Paper-II\Last Data set\dataset\val'

# Ensure the output directories exist
os.makedirs(train_dir, exist_ok=True)
os.makedirs(val_dir, exist_ok=True)

# List of classes (folders)
```

```
classes = ['fault', 'nospread', 'perfect']

# Function to split and move images
def split_and_move_images(class_name):
    # Create directories for class in training and validation
    os.makedirs(os.path.join(train_dir, class_name), exist_ok=True)
    os.makedirs(os.path.join(val_dir, class_name), exist_ok=True)

    # List all images in original directory
    images = os.listdir(os.path.join(train_original_dir, class_name))
    random.shuffle(images)  # Shuffle the list of images

    # Calculate split indices
    split_index = int(0.7 * len(images))  # 70% for training, 30% for validation

    # Split into training and validation sets
    train_images = images[:split_index]
    val_images = images[split_index:]

    # Move images to appropriate directories
    for img in train_images:
        src = os.path.join(train_original_dir, class_name, img)
        dst = os.path.join(train_dir, class_name, img)
        shutil.copyfile(src, dst)

    for img in val_images:
        src = os.path.join(train_original_dir, class_name, img)
        dst = os.path.join(val_dir, class_name, img)
        shutil.copyfile(src, dst)
```

```
# Iterate over each class and split/move images
for class_name in classes:
    split_and_move_images(class_name)

print("Dataset splitting and moving completed successfully!")
```

Deploy Camera with trained Model

```
import cv2
import numpy as np
import torch
import torch
import torchvision.transforms as transforms
from PIL import Image
from torchvision.models import resnet18
from transfer_without_k_fold import TransferLearningModel  # Import your custom model class

# Camera calibration values (if applicable)
camera_matrix = np.array([[699.03176075, 0., 324.65701877],
                          [0., 701.86003627, 227.7140062],
                          [0., 0., 1.]])
dist_coeffs = np.array([0.0416326, 0.03007998, 0.00107624, -0.0068396, -0.51911224])

# Load the trained model
device = torch.device('cuda' if torch.cuda.is_available() else 'cpu')

# Instantiate your custom model (ensure it matches exactly with the model trained in your training script)
model = TransferLearningModel(num_classes=3)  # Assuming 3 classes, adjust as per your trained model
```

```
# Load the trained weights
model.load_state_dict(torch.load('resnet18_finetuned.pth', map_location=device))
model.eval()
model.to(device)

# Define preprocessing transform
transform = transforms.Compose([
    transforms.Resize((224, 224)),  # Ensure this matches with your training transform
    transforms.ToTensor(),
    transforms.Normalize(mean=[0.485, 0.456, 0.406], std=[0.229, 0.224, 0.225])
])

# Label names corresponding to the classes
label_names = ['Fault', 'No Spread', 'Perfect']  # Replace with your actual class names

# Initialize camera capture
cap = cv2.VideoCapture(1)  # 0 is for the default camera, adjust if needed

# Frame counter for unique file names
frame_counter = 0

while True:
    ret, frame = cap.read()
    if not ret:
        break

    # Undistort the image using the camera calibration values (if applicable)
    frame_undistorted = cv2.undistort(frame, camera_matrix, dist_coeffs)
```

```
# Convert frame from BGR to RGB (as expected by torchvision's transforms)
rgb_frame = cv2.cvtColor(frame_undistorted, cv2.COLOR_BGR2RGB)

# Convert to PIL image
pil_img = Image.fromarray(rgb_frame)

# Preprocess the frame
img = transform(pil_img)
img = img.unsqueeze(0).to(device)  # Add batch dimension and move to device

# Perform inference
with torch.no_grad():
    outputs = model(img)
    _, predicted = torch.max(outputs, 1)
    prediction = predicted.item()  # Assuming single image inference

# Display results with label names
label = label_names[prediction]
cv2.putText(frame_undistorted, f'Prediction: {label}', (50, 50),
            cv2.FONT_HERSHEY_SIMPLEX, 1, (0, 255, 0), 2)
cv2.imshow('Camera Feed', frame_undistorted)

key = cv2.waitKey(1) & 0xFF
if key == ord('q'):  # Press 'q' to exit
    break
elif key == ord('c'):  # Press 'c' to capture the current frame
    # Save the current frame as an image file
    cv2.imwrite(f'captured_frame_{frame_counter}.jpg', frame_undistorted)
```

```
        frame_counter += 1

# Release the camera and close all windows
cap.release()
cv2.destroyAllWindows()
```

Appendix B Sensing System Implementation

```
import cv2
import os

# Create a directory to save the captured images
output_dir = 'calibration_images'
if not os.path.exists(output_dir):
    os.makedirs(output_dir)

# Initialize webcam
cap = cv2.VideoCapture(1)

# Check if the webcam is opened correctly
if not cap.isOpened():
    print("Error: Could not open video capture.")
    exit()

print("Press 'c' to capture an image and 'q' to quit.")
image_counter = 0

while True:
    # Capture frame-by-frame
    ret, frame = cap.read()
```

```
    if not ret:
        print("Error: Could not read frame.")
        break

    # Display the frame
    cv2.imshow('Chessboard Capture', frame)

    # Wait for key press
    key = cv2.waitKey(1) & 0xFF

    if key == ord('c'):
        # Save the captured image
        img_filename = os.path.join(output_dir, f'image_{image_counter:05d}.jpg')
        cv2.imwrite(img_filename, frame)
        print(f'Captured {img_filename}')
        image_counter += 1

    elif key == ord('q'):
        # Quit the loop
        break

# Release the capture and close windows
cap.release()
cv2.destroyAllWindows()
```

Appendix C Inspection Assessment Results

Table C- 1 Assessment form of empty spreading stage.

Inspection Item	Details	Operator Input
Date	**Enter the date of the inspection.**	9-Oct-2024
Time	**Enter the time the inspection is performed.**	14.53
Operator Name	**Name of the operator performing the inspection.**	Uqba Othman
Liquid Type	**Specify the type of liquid being used in the coating/spreading process.**	Testing liquid from Unilever
Camera Inspection Results	**Indicate the surface quality based on camera assessment:** **☐ Full: Uniform coating** **☐ Fault: Defective area(s)** **☐ Empty: No coating applied**	Empty
Sensing Results	**Indicate whether the voltage readings are within the acceptable range for the required thickness. If 'No', specify waypoints with issues below.**	Yes
Waypoints with Issues	**Select the specific waypoints (as shown in Figure 6) where sensing results indicate issues.**	☐ (1) ☐ (2) ☐ (3) ☐ (4) ☐ (5) ☐ (6) ☐ (7) ☐ (8) ☐ (9)
Additional Notes	**Provide comments on issues or observations during the inspection.**	There was no issue configured out in this stage. As the estimated result was obtained. The operator intended to capture image and collect sensing readings while the spreading area is empty.

Table C- 2 Assessment form of the obtained results from sensing and vision systems for targeted thickness 15 microns spreading.

Inspection Item	**Details**	**Operator Input**
Date	**Enter the date of the inspection.**	9-Oct-2024
Time	**Enter the time the inspection is performed.**	15.10
Operator Name	**Name of the operator performing the inspection.**	Uqba Othman
Liquid Type	**Specify the type of liquid being used in the coating/spreading process.**	Testing liquid from Unilever
Camera Inspection Results	**Indicate the surface quality based on camera assessment:** **☐ Full: Uniform coating** **☐ Fault: Defective area(s)** **☐ Empty: No coating applied**	Full
Sensing Results	**Indicate whether the voltage readings are within the acceptable range for the required thickness. If 'No', specify waypoints with issues below.**	Yes
Waypoints with Issues	**Select the specific waypoints (as shown in Figure 6) where sensing results indicate issues.**	☐ (1) ☐ (2) ☐ (3) ☐ (4) ☐ (5) ☐ (6) ☐ (7) ☐ (8) ☐ (9)
Additional Notes	**Provide comments on issues or observations during the inspection.**	There was no issue configured out in this stage. As the estimated result was obtained. The operator intended to capture image and collect sensing readings while the spreading area is filled with targeted thickness 15 microns.

Table C- 3 Assessment form of the obtained results from sensing and vision systems for targeted thickness 30 microns spreading.

Inspection Item	**Details**	**Operator Input**
Date	**Enter the date of the inspection.**	9-Oct-2024
Time	**Enter the time the inspection is performed.**	15.30
Operator Name	**Name of the operator performing the inspection.**	Uqba Othman
Liquid Type	**Specify the type of liquid being used in the coating/spreading process.**	Testing liquid from Unilever
Camera Inspection Results	**Indicate the surface quality based on camera assessment:** **☐ Full: Uniform coating** **☐ Fault: Defective area(s)** **☐ Empty: No coating applied**	Full
Sensing Results	**Indicate whether the voltage readings are within the acceptable range for the required thickness. If 'No', specify waypoints with issues below.**	Yes
Waypoints with Issues	**Select the specific waypoints (as shown in Figure 6) where sensing results indicate issues.**	☐ (1) ☐ (2) ☐ (3) ☐ (4) ☐ (5) ☐ (6) ☐ (7) ☐ (8) ☐ (9)
Additional Notes	**Provide comments on issues or observations during the inspection.**	There was no issue configured out in this stage. As the estimated result was obtained. The operator intended to capture image and collect sensing readings while the spreading area is filled with targeted thickness 30 microns.

Table C- 4 Assessment form of the obtained results from sensing and vision systems for targeted thickness 60 microns spreading.

Inspection Item	**Details**	**Operator Input**
Date	**Enter the date of the inspection.**	9-Oct-2024
Time	**Enter the time the inspection is performed.**	15.50
Operator Name	**Name of the operator performing the inspection.**	Uqba Othman
Liquid Type	**Specify the type of liquid being used in the coating/spreading process.**	Testing liquid from Unilever
Camera Inspection Results	**Indicate the surface quality based on camera assessment:** ☐ **Full: Uniform coating** ☐ **Fault: Defective area(s)** ☐ **Empty: No coating applied**	Full
Sensing Results	**Indicate whether the voltage readings are within the acceptable range for the required thickness. If 'No', specify waypoints with issues below.**	Yes
Waypoints with Issues	**Select the specific waypoints (as shown in Figure 6) where sensing results indicate issues.**	☐ (1) ☐ (2) ☐ (3) ☐ (4) ☐ (5) ☐ (6) ☐ (7) ☐ (8) ☐ (9)
Additional Notes	**Provide comments on issues or observations during the inspection.**	There was no issue configured out in this stage. As the estimated result was obtained. The operator intended to capture image and collect sensing readings while the spreading area is filled with targeted thickness 60 microns.

Table C- 5 Assessment form of the obtained results from sensing and vision systems for targeted thickness 90 microns spreading.

Inspection Item	**Details**	**Operator Input**
Date	**Enter the date of the inspection.**	9-Oct-2024
Time	**Enter the time the inspection is performed.**	16.10
Operator Name	**Name of the operator performing the inspection.**	Uqba Othman
Liquid Type	**Specify the type of liquid being used in the coating/spreading process.**	Testing liquid from Unilever
Camera Inspection Results	**Indicate the surface quality based on camera assessment:** **☐ Full: Uniform coating** **☐ Fault: Defective area(s)** **☐ Empty: No coating applied**	Full
Sensing Results	**Indicate whether the voltage readings are within the acceptable range for the required thickness. If 'No', specify waypoints with issues below.**	Yes
Waypoints with Issues	**Select the specific waypoints (as shown in Figure 6) where sensing results indicate issues.**	☐ (1) ☐ (2) ☐ (3) ☐ (4) ☐ (5) ☐ (6) ☐ (7) ☐ (8) ☐ (9)
Additional Notes	**Provide comments on issues or observations during the inspection.**	There was no issue configured out in this stage. As the estimated result was obtained. The operator intended to capture image and collect sensing readings while the spreading area is filled with targeted thickness 90 microns.

Table C- 6 Assessment form of testing fault spreading

Inspection Item	Details	Operator Input
Date	**Enter the date of the inspection.**	9-Oct-2024
Time	**Enter the time the inspection is performed.**	16.30
Operator Name	**Name of the operator performing the inspection.**	Uqba Othman
Liquid Type	**Specify the type of liquid being used in the coating/spreading process.**	Testing liquid from Unilever
Camera Inspection Results	**Indicate the surface quality based on camera assessment:** **☐ Full: Uniform coating** **☐ Fault: Defective area(s)** **☐ Empty: No coating applied**	Fault
Sensing Results	**Indicate whether the voltage readings are within the acceptable range for the required thickness. If 'No', specify waypoints with issues below.**	No
Waypoints with Issues	**Select the specific waypoints (as shown in Figure 6) where sensing results indicate issues.**	☐ (2) ☐ (3) ☐ (4) ☐ (5) ☐ (8) ☐ (9)
Additional Notes	**Provide comments on issues or observations during the inspection.**	In this test, the operator observed technical fault in the spreading stage. The liquid was not covering all areas uniformly as collected data from sensing and vision confirmed this claim. For thickness prediction, voltage readings from P1, P6 and P7 show that the targeted thickness is 30 microns. At P1, the voltage reading is 5.32V The predicted thickness is 26.99

		microns. At P6, the voltage reading is 5.35V The predicted thickness is 30.15 microns. At P7, the voltage reading is 5.41V The predicted thickness is 36.47 microns. Further setup check is required. Check if the spreader bar is clean!